10. LOWER IMBRIAN SERIES

FIGURE 10.1 (overleaf).—Units of the Imbrian System where first recognized (compare figs. 1.6, 2.1). View centers on massive, rugged Montes Apenninus, part of the Imbrium-basin rim. Imbrium-basin ejecta grades from coarsely hummocky forms on Apennine flank to smoother drumlinlike or whaleback forms near crater Ukert (near bottom; 23 km, 8° N., 1.5° E., probably Lower Imbrian). Archimedes (at top; 83 km, 30° N., 4° W.), which is superposed on rugged Montes Archimedes and plains of the Apennine Bench (Hackman, 1966), is flooded by mare basalt. Massive slumping from Montes Apenninus is indicated by parallel structure and outlines of ridges northwest of Apennine front. Type area of top of Imbrian System is in bay of Mare Imbrium between the Apennine Bench and crater Eratosthenes (truncated by left edge of photograph). Orbiter 4 frame M–102.

10. LOWER IMBRIAN SERIES

CONTENTS

INTRODUCTION

The extensively exposed and relatively well sampled Lower Imbrian Series is the key to the ages and origins of most materials of the lunar terrae. Deposits of the Lower Imbrian Orientale and Imbrium basins constitute the Moon's most extensive laterally continuous stratigraphic horizons (pl. 8). The Imbrium basin dominates the surface visible from Earth and was the first basin to be treated stratigraphically (see chaps. 2, 4; fig. 10.1). Deposits of the Orientale basin dominate the terrae on both sides of long 90 W. and serve as models for other basin materials, as previous discussions have made clear. Thus, the Lower Imbrian Series dominates a large part of the lunar surface, despite the small number of events that emplaced its rock units (pl. 8). Both groups of basin deposits make excellent stratigraphic markers for dividing the lunar stratigraphic column (table 7.1) because of their great extent and clear expression.

Because of their early discovery and prominence, the Imbrium-basin deposits attracted more sampling missions than did any other class of terra units. The curtailed Apollo 13 and the successful Apollo 14 flights were sent to a point on the Fra Mauro Formation, the most distinctive Imbrium-basin unit. Exploration of the Imbrium rim at Montes Apenninus was the main objective of the Apollo 15 mission. The Cayley and Descartes Formations, though considered to be volcanic when selected as targets for the Apollo 16 landing (see chap. 2), are Lower Imbrian photogeologic units emplaced by impact and may also contain Imbrium-basin material.

In terms of total volume of returned material, however, rocks emplaced during the Early Imbrian Epoch are less well represented than Nectarian and pre-Nectarian materials. Apollos 14 and 15 together returned much less terra material than did Apollo 17. Arguably, the abundant Apollo 16 collection may include more material processed in the Nectarian than in the Imbrian Period (see chap. 9). Effects of igneous crustal processes active in pre-Nectarian time have profoundly affected all sample collections (see chap. 8).

The problem of determining which compositions and textures of the Apollo 14, 15, and 16 samples were created during the Early Imbrian events that emplaced them and which were created earlier occupies considerable space in this chapter. The first half of the chapter is devoted to the Imbrium basin and to the samples returned from its deposits by the Apollo 14 and 15 missions. I develop the viewpoint that the Apollo 14 materials owe their properties to their emplacement in the Fra Mauro Formation, as originally proposed but not currently so widely believed. A similar analysis for the more controversial Cayley and Descartes Formations sampled by Apollo 16 is less conclusive. Resolution of the remaining questions about the Apollo 14 through 16 rocks would significantly aid in dating large areas on the absolute and relative time scales and in correlating compositions with sources in the crust. Nonsampled Lower Imbrian units, including the Orientale basin that already has been thoroughly described, are given less attention here.

DEFINITION

Deposits of the Imbrium basin and the radial system of grooves called "Imbrian(um) sculpture" have long served as the main reference for dividing materials into Imbrian and pre-Imbrian on the nearside (see chap. 7; Gilbert, 1893; Shoemaker and Hackman, 1962). In August 1967, photography of the Orientale basin at the end of the Lunar Orbiter 4 mission added a major stratigraphic horizon to the Imbrian System as it had previously been defined. Superpositional relations (fig. 10.2), morphologic freshness (figs. 4.4, 10.3), and size-frequency distributions (fig. 10.4) all indicate that Orientale is younger than Imbrium. Orientale is older than the nearby mare surface, which would have been swamped by the basin ejecta if it predated Orientale (figs. 10.3, 10.5). The Orientale deposits constitute excellent stratigraphic markers because of their vigorous topographic expression and clear relations with other units over a wide area (pls. 3, 8). They probably would have been used as a stratigraphic datum to define a major time-stratigraphic boundary, had they been in a better position for study during the telescopic phase of the geologic-mapping program. This key horizon has, in fact, been used on some geologic maps to divide informal lower and upper series of the Imbrian System (for example, McCauley, 1973).

The two series of the Imbrian System are here defined formally. The *Lower Imbrian Series* includes all materials from the bottom of the Fra Mauro Formation to the top of the Hevelius Formation (fig. 7.1). The type area of the base of the Lower Imbrian Series is the type area of the Fra Mauro Formation, lat 0°–2° S., long 16°–17.5° W. (figs. 10.1, 10.19; Wilhelms, 1970b). The type area of the top of the series is the type area of the Hevelius Formation, near lat 2° N., long 68° W. (fig. 4.4*H*; McCauley, 1967a). A reference area for the top of the series is bounded by lat 2° S.–2° N., long 75°–80° W. (fig. 10.3). The *Upper Imbrian Series* includes all materials above the top of the Hevelius Formation—that is, younger than the Orientale basin—to the top of the Imbrian System as defined in chapter 11. The *Early Imbrian Epoch* thus began at the moment of the Imbrium impact and ended when the Hevelius Formation came to rest. The *Late Imbrian Epoch* began when the Hevelius came to rest and ended when the mare materials that define the top of the Imbrian System solidified.

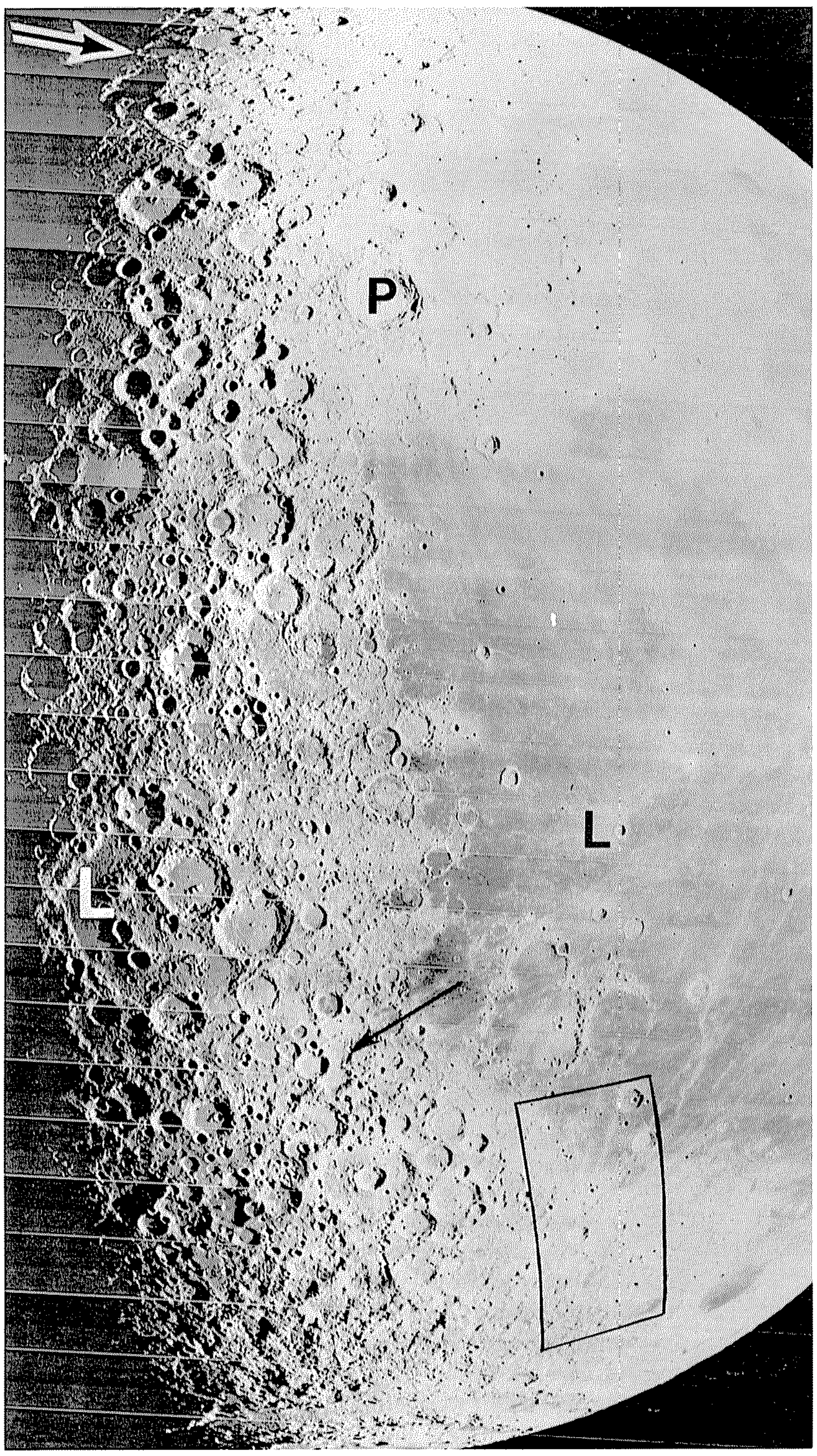

FIGURE 10.2.—Superpositions of secondary craters of the Orientale basin on those of the Imbrium basin.

A. Regional view of northwest nearside limb, including north pole (black-and-white arrow). Orientale basin is at bottom. Black arrow parallels Imbrium sculpture (northeast-southwest) and marks superposition indicated in *B*. White L, pre-Nectarian Lorentz basin (360 km, 34° N., 97° W.); P, Eratosthenian crater Pythagoras (130 km, 64° N., 63° W.); black L, Copernican crater Lichtenberg (20 km, 32° N., 68° W.), embayed by Copernican mare basalt (see chap. 13). Numerous craters with uplifted floors are near terra-mare boundary (see chap. 6). Area of figure 10.3 is outlined. Orbiter 4 frame M–189.

INTERIOR AND NEAR-RIM IMBRIUM-BASIN DEPOSITS

Introduction

Imbrium is the Moon's largest well-preserved basin (table 4.1) but is not entirely understood. Its basaltic fill, Mare Imbrium, obscures an area larger than the entire Orientale topographic basin (table 6.1). Interior deposits and large parts of interior rings are visible only at the Apennine Bench (figs. 1.6, 2.1, 4.3*AA*, 10.6). Concentric mare ridges help somewhat in locating buried rings (Hartmann and Kuiper, 1962; Brennan, 1976). The southwest, west, and northwest sectors of the topographic rim are also buried by basalt flows,

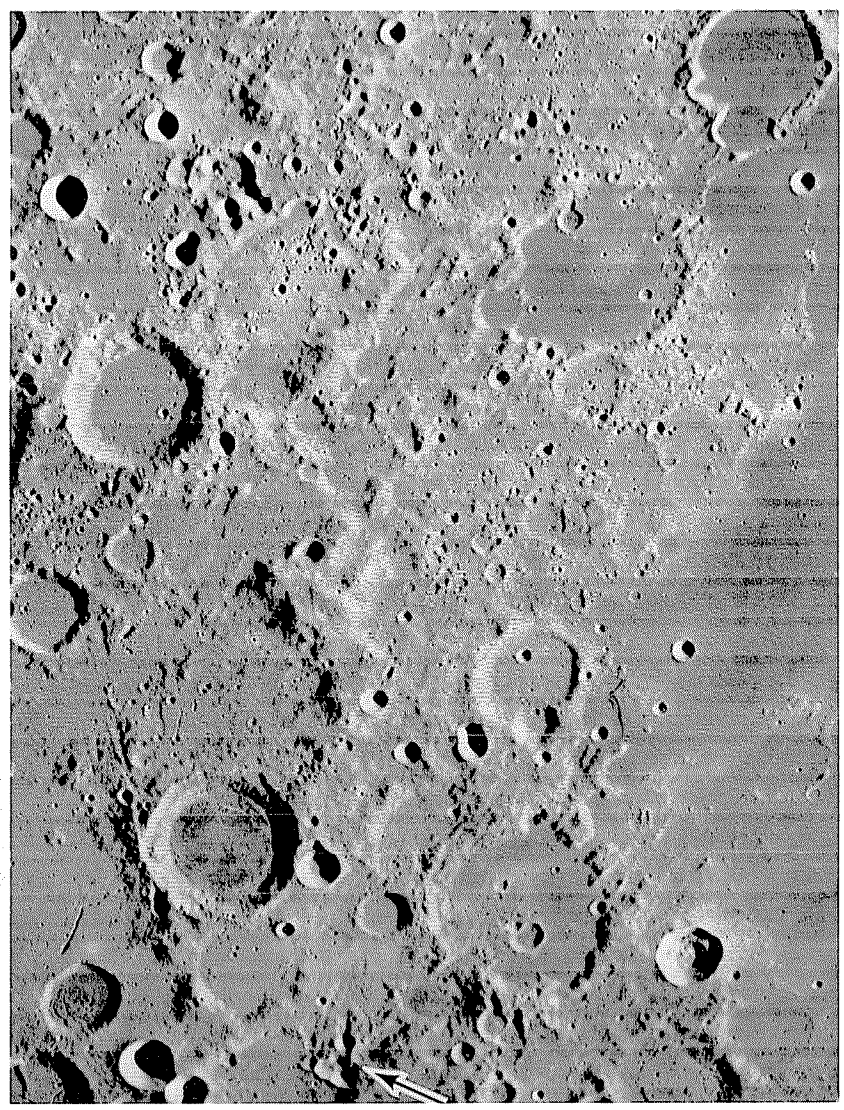

B. Detailed view of Orientale-secondary craters, showing herringbone-patterned ejecta interrupting Imbrium-radial chains (arrow at bottom). Orbiter 4 frame H–189.

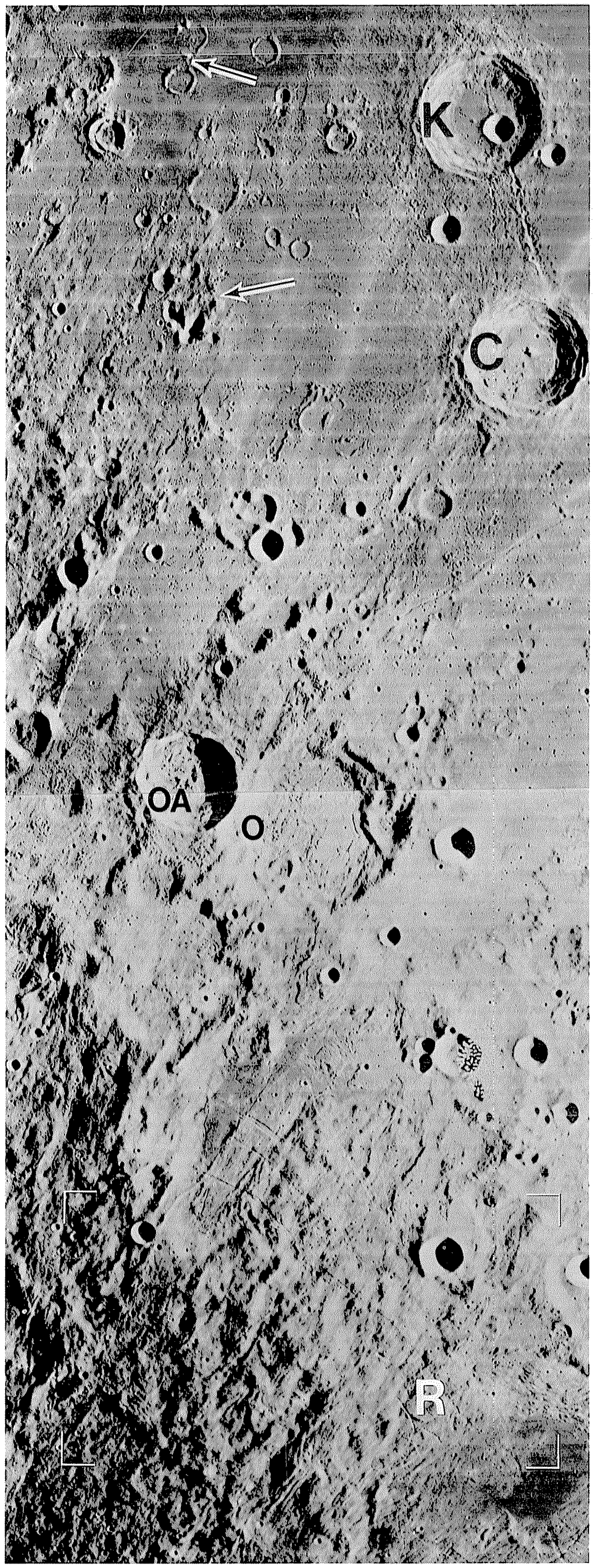

FIGURE 10.3.—Orientale-secondary craters and plains deposits, partly flooded by mare basalt (arrows); old mare unit is at lower arrow (see fig. 10.2*A* for location). Reference area for typical exposure of inner facies of the Hevelius Formation (2° N.–2° S., 75–80° W.) is enclosed by corner markers. Secondary craters of Krafft (K; 51 km, 17° N., 73° W.) and Cardanus (C; 50 km) are superposed on Orientale deposits and old mare, but are flooded on west by younger mare; similar ages and sizes of these two craters suggest twin impacts (see chap. 3). Ejecta of Copernican crater Olbers A (OA; 43 km, 8° N., 78° W.) is superposed on Orientale deposits and partly covered by small patch of very young mare. Olbers (O; 75 km, probably Nectarian) and Riccioli (R; 146 km, probably pre-Nectarian) are buried by Orientale deposits. Orbiter 4 frame H–174.

pyroclastic materials, and deposits of such large craters as Iridum (figs. 3.8, 5.12). The connections between rings in the north and northeast are partly buried (pl. 8). Therefore, the identity not only of the boundary of excavation but even of the topographic rim is uncertain in the half of the basin periphery from the southwest to the northeast sectors. In the east and south, Montes Apenninus and Carpatus (figs. 10.6, 10.7) constitute the topographic rim and, in my opinion, the excavation boundary (see chap. 4). These ranges are equivalent to Montes Cordillera in position and morphology (Wilhelms and McCauley, 1971; M'Gonigle and Schleicher, 1972; Brennan, 1976) and in origin (Baldwin, 1974a; Wilhelms and others, 1977; Hodges and Wilhelms, 1978).

The best exposures of Imbrium-basin materials are on Montes Apenninus, in large tracts southeast of that range, and north of Mare Frigoris. This section describes the Imbrium materials from the inside out and interprets them by comparison with their Orientale equivalents.

Apennine Bench Formation—Apollo 15 samples

Hackman (1964, 1966) named the level or wavy materials between Montes Archimedes and Montes Apenninus the "Apennine Bench Formation" (figs. 2.1, 6.10, 10.1, 10.7). Page (1970) extended this name to other, similar plains inside the Imbrium-basin rim that underlie deposits of Imbrian craters and the mare (figs. 2.4, 10.8). Overlap of

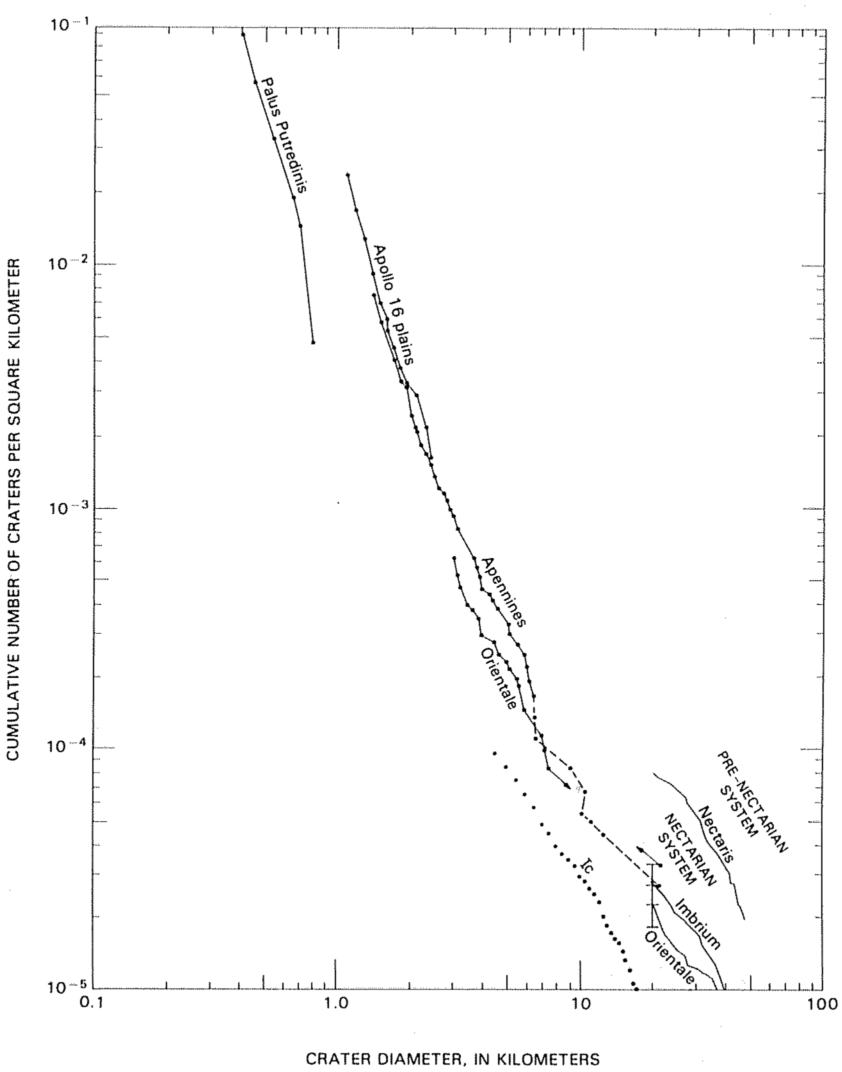

FIGURE 10.4.—Cumulative size-frequency distributions of craters superposed on major Imbrian units. Counts of craters larger than 20 km in diameter on deposits of the Imbrium and Orientale basins are from this study; Nectarian and pre-Nectarian fields are added for comparison (figs. 8.6, 9.22). Other curves are plotted from data of Neukum and others (1975a); data points for the Apennines are from two counts by Neukum and others (1975a), which have a common point at 3 km. Curve for Imbrian craters (Ic) is from Wilhelms and others (1978).

the Apennine Bench Formation on the rugged Imbrium-basin topography shows that the plains are at least slightly younger than the basin (figs. 10.7, 10.8).

As for other terra-plains deposits, interpretations of origin have shifted back and forth between volcanic and impact. E.M. Shoemaker and R.J. Hackman (oral commun., 1963) proposed that the Apennine Bench Formation consists of Imbrium-basin ejecta or impact melt. The impact-melt interpretation is supported by position inside the basin and by morphologies indicating subsidence of a fluidlike material (fig. 10.7; Wilhelms, 1980). The Apennine Bench Formation and the Maunder Formation of Orientale are similar in these respects (table 4.3). Volcanic interpretations, which are also consistent with the fluidlike appearance, were favored in the era when lunar light-colored plains in general were commonly thought to be volcanic (Hackman, 1966; Wilhelms, 1970b; Carr and others, 1971; Wilhelms and McCauley, 1971).

A volcanic origin is supported by discovery among the Apollo 15 samples of fragments of possible terra-type volcanic rock. The Apennine Bench Formation probably underlies the mare basalt in the region of the landing site (figs. 10.7, 10.8; Carr and others, 1971), although the formation is not exposed within range of the astronaut traverses (fig. 10.9). The distribution of KREEP-rich fragments in the regolith (Basu and McKay, 1979) is consistent with derivation from beneath the mare (Spudis, 1978b). Their Th-rich medium-K KREEP chemistry matches the composition detected by the orbiting gamma-ray spectrometer over Apennine Bench exposures west of the landing site (Spudis, 1978a; Hawke and Head, 1978b; Metzger and others, 1979; Clark and Hawke, 1981). Because the fragments have igneous textures and no meteoritic siderophile elements, many investigators have concluded that they are true endogenic igneous rocks (fig. 10.10; Irving, 1975, 1977; Dowty and others, 1976; Ryder, 1976; Meyer, 1977; Basaltic Volcanism Study Project, 1981, p. 274–278). A further argument for a volcanic origin is that the samples were probably derived from a source more radioactive than any now present beneath the landing site (as shown by the Apollo 15 heat-flow experiment; Langseth and others, 1976); an Imbrium melt sheet would incorporate material similar to the present subbasin material (Spudis, 1978a). An episode of KREEP volcanism in the Early Imbrian Epoch is indicated, possibly triggered by the Imbrium impact (Spudis, 1978a).

The volcanic interpretation is still not universally accepted. Taylor (1982, p. 214–216) pointed out that the absence of siderophiles and fragments does not prove an igneous origin and suggested that Montes Apenninus are as rich in KREEP as is the Apennine Bench. Some interpretations of the orbital data, however, favor a higher Th content for the bench (Metzger and others, 1979).

Three geochronologic methods have yielded ages for the medium-K KREEP-rich samples 15382 and 15386 averaging 3.85 aeons (table 10.1). This average age probably dates the emplacement of the KREEP-rich basalt and constrains the age of the Imbrium basin to 3.85 aeons or older, regardless of whether the KREEP-rich liquids were melted by impact or endogenic heat.

Montes Apenninus massifs—Apollo 15 samples

Steep rugged massifs that are among the Moon's highest mountains form the crest of Montes Apenninus; they probably were uplifted structurally and overlain by ejecta (figs. 10.1, 10.7, 10.8, 10.11; Carr and others, 1971; Wilhelms, 1980). Large slump masses lie as far as 60 km northwest of embayments in the mountains, which were evidently the sources of the slumps (figs. 6.10, 10.7, 10.8; Wilhelms and others, 1977; Wilhelms, 1980). Parts of the Apennine Bench Formation overlie some of these slumps (Spudis, 1978a; Wilhelms, 1980). Most investigators currently believe that Montes Apenninus are an exterior scarp of an Imbrium basin smaller than its topographic rim. Others, including me (see section in chap. 4 entitled "Origin of Rings"), regard an origin as the excavation boundary as much more likely because the Apennines are a massive elevated range of mountains, the largest on the lunar nearside, and because they mark a sharp discontinuity in the textures of basin deposits (figs. 10.1, 10.6, 10.7).

The identity of the boundary of excavation in other sectors is less clear. The Apennines and Montes Carpatus, another obvious part of the topographic-basin rim, define a circle 1,200 km in diameter with Montes Alpes and an oval 1,500 km long with the north shore of Mare Frigoris (pl. 3; figs. 4.3*AA*, 10.6). The Apenninus-Carpatus ring apparently divides in Montes Caucasus (figs. 10.6, 10.12). The southern Caucasus continue as Montes Alpes, and the northern Caucasus as the Frigoris shore (Wilhelms and McCauley, 1971). In the interpretation given in chapter 4, the large oval bounds the Imbrium cavity. The hypothesis that the outer parts of large basins are differentially excavated may explain the divergence; the Frigoris sector was excavated to a larger diameter than was the Carpatus sector, which was blocked by the Serenitatis rim. Lineations in the northern Caucasus (figs. 10.6, 10.12) point to an impact point at the center of the Carpatus-Alpes circle at lat 33° N., long 18° W. (table 4.1).

The origin of Montes Archimedes, the rugged elevation south of the crater Archimedes, is ambiguous (fig. 10.1). It lies at the same distance from the center as does Montes Alpes (pl. 3; Wilhelms and McCauley, 1971) but also resembles the slumps derived from the Apennine scarp. Thus, it may be either part of an Imbrium-basin ring or a slump.

One of the major objectives of the Apollo 15 mission in July 1971 was to collect samples of Montes Apenninus. According to impact models based on simple craters (see chap. 3), this basin-rim material might have come from deep within the Moon. Primitive materials or, at least, pre-Imbrian materials might have been uplifted and exposed

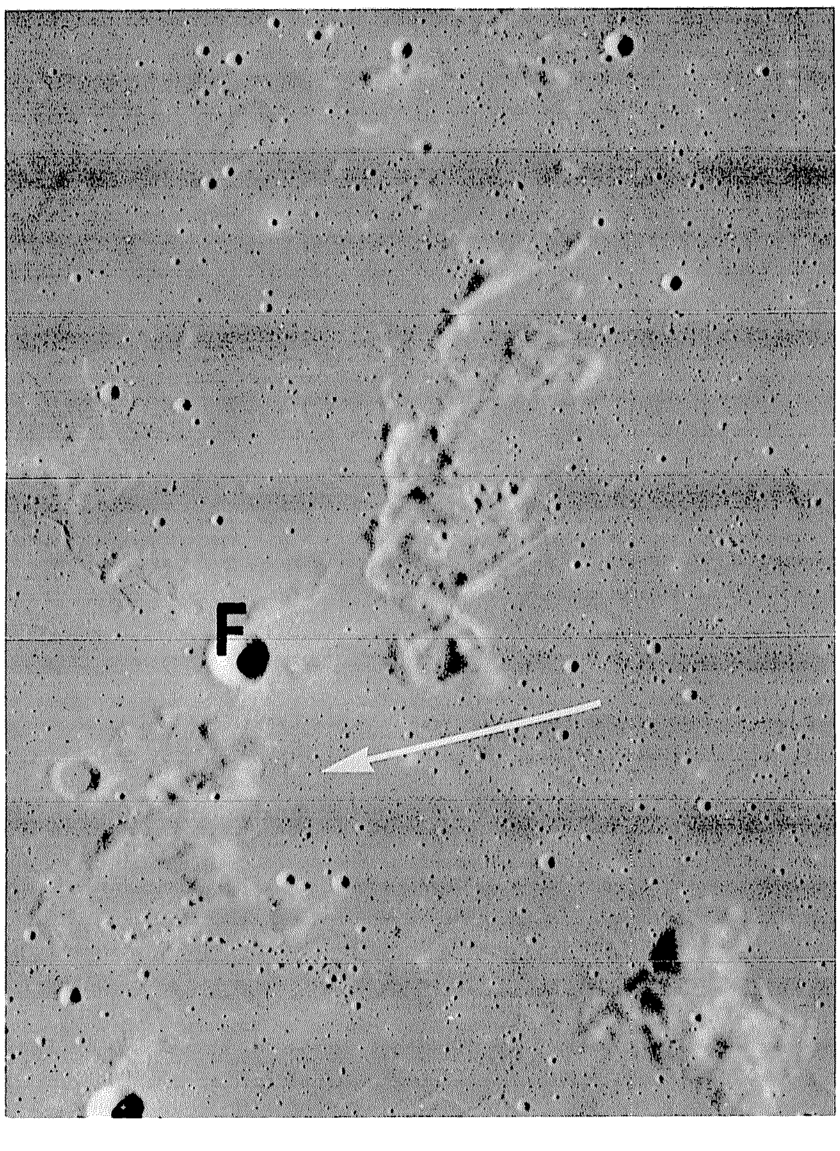

FIGURE 10.5.—Partly buried crater group (above arrow) in Oceanus Procellarum (2° S., 40.5° W.), identified as secondary to Orientale basin by ejecta orientation subradial to Orientale (centered 1,700 km to west in direction of arrow) and subequal size (about 5 km; compare crater F, Flamsteed FB, 5 km). Orbiter 4 frame H–143.

FIGURE 10.6.—Imbrium basin, bounded by Montes Alpes (Al), Caucasus (white C), and Apenninus (Ap). Imbrium-radial crater chains (black-and-white arrows) north of Mare Frigoris (F) are superposed on deposits of Nectarian Humboldtianum basin (H; 61° N., 84° E.; Lucchitta, 1978) and on many craters, including pre-Nectarian W. Bond (W; 158 km) and Barrow (B; 93 km; compare fig. 10.15). Humboldtianum deposits cover probable Nectarian craters Nansen (N; 122 km, 81° N., 95° E.) and Schwarzschild (S; 235 km, 71° N., 120° E.), and are overlain by Nectarian crater Endymion (E; 125 km, 54° N., 57° E.), Lower Imbrian crater Compton (black C; 162 km, 56° N., 105° E.; compare fig. 9.4), and Copernican crater Hayn (87 km, north of H). Fewer small prebasin craters are visible near both basins than along upper left edge of photograph. White arrow, north pole. Orbiter 4 frame M–116.

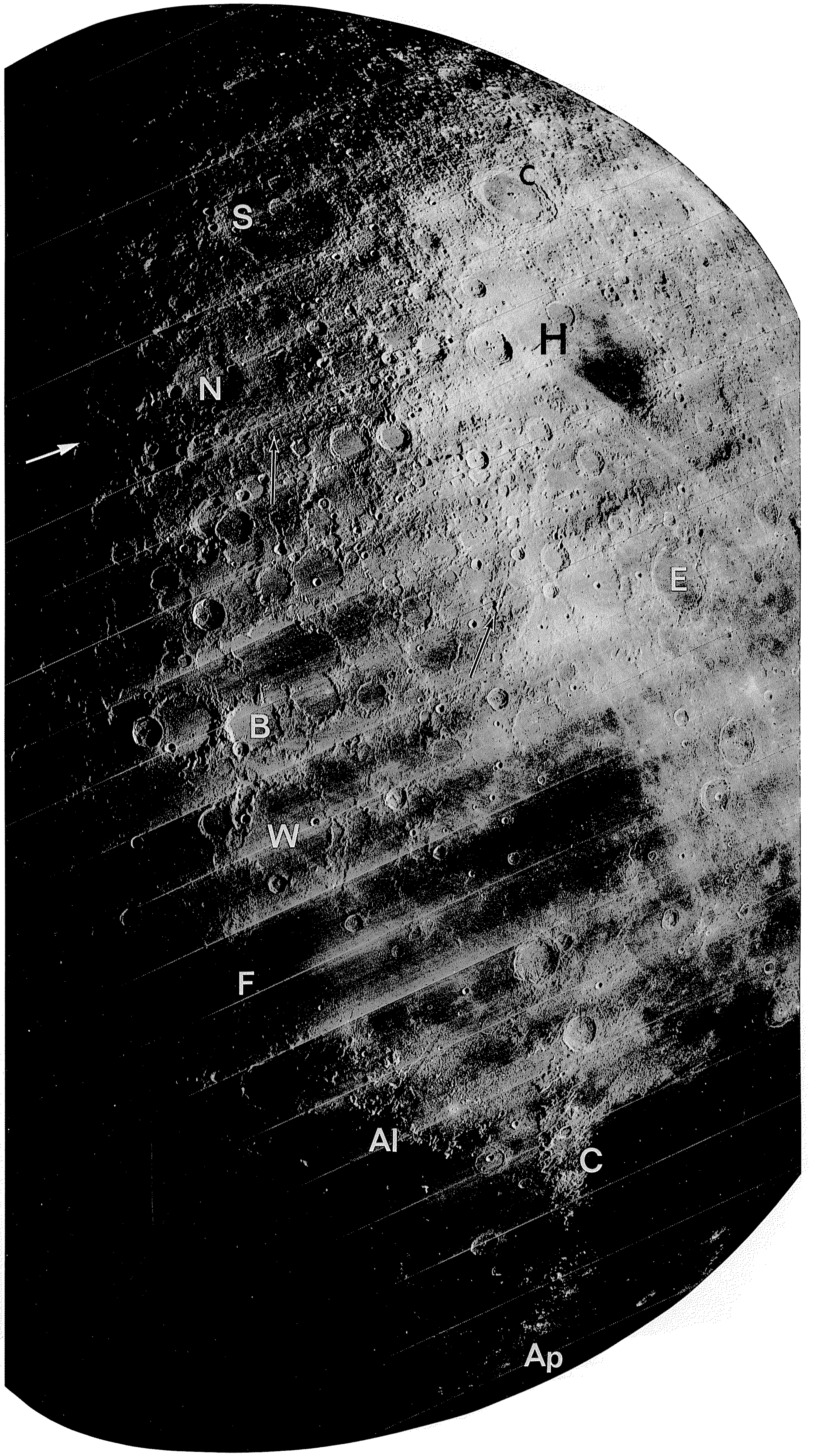
S
H
N
E
B
W
F
Al
C
Ap

TABLE 10.1.—*Absolute ages of Imbrium-basin materials*

[Stations: Apollo 14 (see fig. 10.21): Traverse EVA 1 was within 150 m of the Lunar Module (LM); stations C1, C', and C2 are on the rim flank of Cone Crater along traverse EVA 2; F, 400 m east of LM on EVA 2; G, 250 m east of LM on EVA 2. Apollo 15 (see fig. 10.9): Station 7 is at Spur Crater along the front of Montes Apenninus.
Rock types: CMR, crystalline melt rock of uncertain origin (volcanic basalt or clast-poor or -rich impact-melt rock); CPM, clast-poor impact-melt rock; FMB, Fra Mauro breccia (clast-rich impact-melt rock); xln, crystalline. Lithologic descriptions in much of the geochronologic literature are inadequate for categorizing samples further; for example, the term "basalt" is commonly used for impact-melt rocks (see chap. 8).
Ages calculated using International Union of Geological Sciences (IUGS) radioactive-decay constants (Steiger and Jäger, 1977), except those determined by Husain and others (1972) (see headnote, table 9.1). Most Ar-Ar ages are ^{40}Ar-^{39}Ar plateau ages. Age determinations with error ranges of ±0.10 aeon or greater and those obviously outside the likely range (for example, those of Upper Imbrian mare-basalt grains) are omitted.
References: AD74, Alexander and Davis (1974); AK74, Alexander and Kahl (1974); C72, Compston and others (1972); CL79, Carlson and Lugmair (1979); H72, Husain and others (1972); K72, Kirsten and others (1972); M72, Murthy and others (1972); M74, Mark and others (1974); M79, McKay and others (1979); N74, Nyquist and others (1974); N75, Nyquist and others (1975); PW71, Papanastassiou and Wasserburg (1971b); PW76, Papanastassiou and Wasserburg (1976); S73, Stettler and others (1973); T71, Turner and others (1971); T72, Turner and others (1972); T73, Turner and others (1973; summarized in Turner, 1977); WP71, Wasserburg and Papanastassiou (1971); Y72, York and others (1972)]

Sample	Station	Rock type	Age	Method	Reference
		Apollo 14 young group			
14001,7,3	EVA 1	2-4 mm CMR	3.81±0.03	Rb-Sr	PW71
			3.84±0.04	Ar-Ar	T71
14066	F	510-g FMB			
,21,1.02		Whole rock	3.84±0.03	Ar-Ar	AD74
,21,1.01		Xln matrix	3.86±0.03	Ar-Ar	AD74
,21,2.04,2		White xln clast[1]	3.88±0.03	Ar-Ar	AD74
,21,2.01		Breccia clast[1]	3.90±0.02	Ar-Ar	AD74
14073	G	10-g CPM (plagioclase separates).	3.80±0.04	Rb-Sr	PW71
			3.82±0.05	Ar-Ar	T72
14150	G	4-10-mm fines			
,7,3		CPM	3.82±0.02	Rb-Sr	M79
,7,2		CPM	3.83±0.01	Rb-Sr	M79
14161	EVA 1	2-4-mm fines			
,34,2		CMR	3.80±0.08	Ar-Ar	K72
,34,6		CPM	3.84±0.04	Ar-Ar	K72
,34,5		CMR[1]	3.87±0.08	Ar-Ar	K72
,34,4		CMR[1]	3.90±0.06	Ar-Ar	K72
14167	EVA 1	2-4-mm fines			
,6,1		CMR	3.79±0.03	Ar-Ar	H72
,6,7		CMR	3.82±0.03	Ar-Ar	H72
,6,3		CMR	3.83±0.05	Ar-Ar	H72
,8,1		CMR[1]	3.88±0.04	Ar-Ar	T71
,9		CMR[1]	3.91-3.95	Ar-Ar	Y72
14257,12,1	EVA 1	2-4-mm fine	3.87±0.06	Ar-Ar	H72
14270,1-7	EVA 1	26-g FMB	3.83±0.05	Ar-Ar	AK74
14276	EVA 1	13-g CPM	3.80±0.04	Rb-Sr	WP71
14303,13,R5,1	EVA 1	Clast from 898-g FMB	3.85±0.04	Ar-Ar	K72
14310	G	3.4-kg CPM	3.78±0.03	Ar-Ar	H72
			3.79±0.04	Rb-Sr	PW71
			3.81±0.05	Ar-Ar	T72
			3.82±0.06	Ar-Ar	S73
			3.83±0.04	Ar-Ar	T71
			3.85±0.04	Rb-Sr	C72
			3.85±0.05	Ar-Ar	Y72
			3.85±0.06	Rb-Sr	M72
			3.86±0.03	Rb-Sr	M74
		Apollo 14 old group (pre-Imbrian)			
14053	C2	High-Al basalt	3.88-3.92	See table 9.5.	
14072	C'	do	3.91-3.98	Do	
14321	C1	do	3.85-3.96	Do	
		Apollo 15 group			
15382	7	KREEP-basalt fragment	3.82±0.02	Rb-Sr	PW76
			3.84±0.05	Ar-Ar	S73
			3.85±0.05	Ar-Ar	T73
15386	7	do	3.85±0.08	Sm-Nd	CL79
			3.86±0.04	Rb-Sr	N75
15434,73	7	do.?	3.83±0.04	Rb-Sr	N74
15455	7	Impact melt of breccia matrix.	3.86±0.04	Ar-Ar	AK74

[1]Probably older than the Fra Mauro Formation.

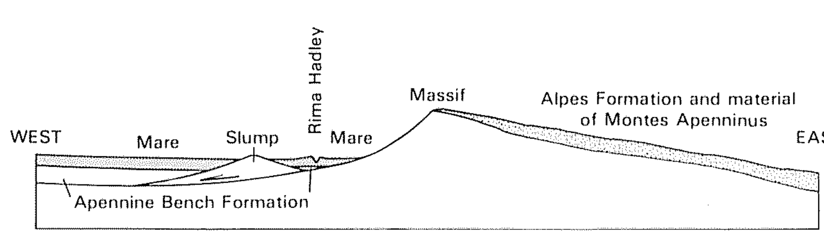

FIGURE 10.8.—Diagrammatic geologic cross section of region of Apollo 15 landing site, based on figure 10.7. Indicated history: (1) uplift of massifs and ejection of the Alpes Formation and "material of Montes Apenninus," (2) slumping of large blocks from Apennine front, (3) emplacement of the Apennine Bench Formation (either impact melt or volcanic basalt), and (4) emplacement of mare basalt.

FIGURE 10.7.—Region of Apollo 15 landing site (arrow). Mare basalt of Palus Putredinis (PP) is overlain by secondary craters and rays of Autolycus, centered north of area. Sinuous rille is Rima Hadley. Iab, Apennine Bench Formation; s, slumps from Apennine front; C, Conon (22 km; compare fig. 10.15). Stereoscopic pair of Apollo 15 frames M–413 (right) and M–415 (left).

in the Imbrium-basin massifs. Materials of the Serenitatis basin are likely to be included because that basin's west rim is cut off by the Apennines and thus lay in the target area of the Imbrium impact (pl. 3; fig. 9.30; Wilhelms and McCauley, 1971; Spudis and Head, 1977).

Fewer samples than expected were obtained from the massifs. Most that were collected are small and of uncertain geologic context because outcrops are covered by thick colluvium (fig. 10.11). The largest samples are two "black and white rocks" (15445, 15455), totaling 1.17 kg in mass and representing a 1-m boulder sampled at station 7 (figs. 10.9, 10.13; Swann and others, 1972). Dark, aphanitic impact-melt rock of low-K KREEP composition encloses light-colored clasts of mafic ANT rock (Reid and others, 1977; Ryder and Bower, 1977). The ANT rock was crushed or fragmented in one or several episodes (James, 1977). Some of the clasts are composed of ancient, apparently "pristine" noritic and troctolitic rock (table 8.4; Nyquist and others, 1979b). The impact-melt rock is similar in composition to impact-melt rock from the Taurus-Littrow massifs of the Serenitatis basin, though richer in Mg (Taylor, S.R., and others, 1973). This similarity may support the photogeologic observation that Serenitatis material was part of the Imbrium-basin impact target. Alternatively, it may indicate that low-K KREEP is a common crustal constituent (Ryder and Wood, 1977).

The lithologic similarity to the Serenitatis melt-rich deposit has led to suggestions that the black-and-white rocks are part of a melt-rich deposit of the Imbrium basin (Ryder and Bower, 1977; Ryder and Wood, 1977). The ^{40}Ar-^{39}Ar gas-retention age of 3.86 ± 0.04 aeons (table 10.1; Alexander and Kahl, 1974) probably dates the assembly of the breccia deposit and, therefore, the Imbrium impact.

FIGURE 10.9.—Area of Apollo 15 astronaut traverses. Numbered circles are sampling stations. Prepared by U.S. Defense Mapping Agency; base from Apollo 15 frames P–9370 and P–9377.

Material of Montes Apenninus

Four textural types of Imbrium-basin ejecta lie on the southeast Apennine flank (fig. 10.14; table 4.3). One type has been given the informal name "material of Montes Apenninus" (Wilhelms and McCauley, 1971), not to be confused with the massif material. This unit is characterized by closely spaced imbricate slivers concentric with the Apennine crest (figs. 10.1, 10.7, 10.14). Its position near the Apennine crest and the coherent morphology of the blocks are consistent either with structural deformation along the excavation rim or with low-velocity lofting or pushing of late ejecta over the rim (Wilhelms, 1980). The unit resembles the concentric ejecta facies of the Orientale basin in morphology, relative position, and areal extent (figs. 4.4*E*, *F*; Wilhelms, 1980).

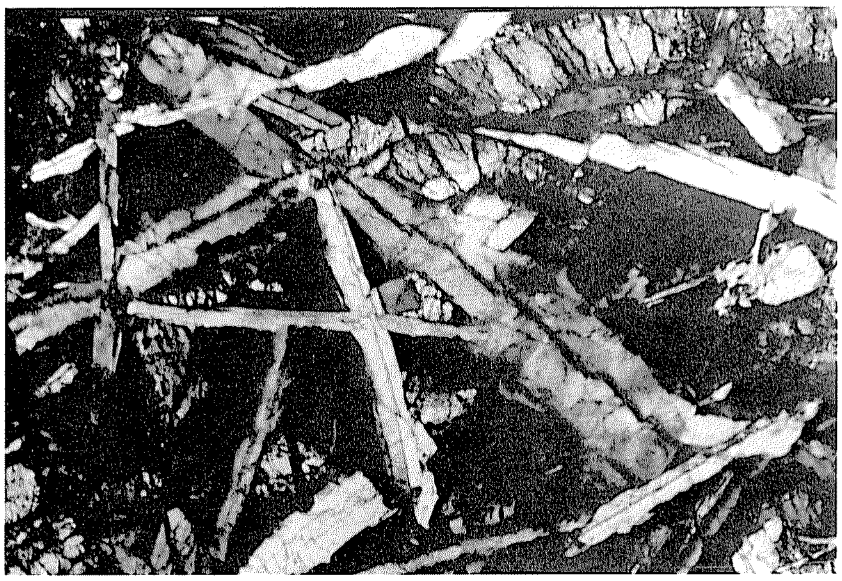

FIGURE 10.10.—Thin section of crystalline, probably volcanic KREEP-rich sample 15386,8, showing basaltic intersertal to subophitic texture (Dowty and others, 1976). Fragment lacks clastic inclusions and meteoritic siderophile elements (Irving, 1975, 1977; Dowty and others, 1976). Crossed polarizers; field of view, about 2 mm.

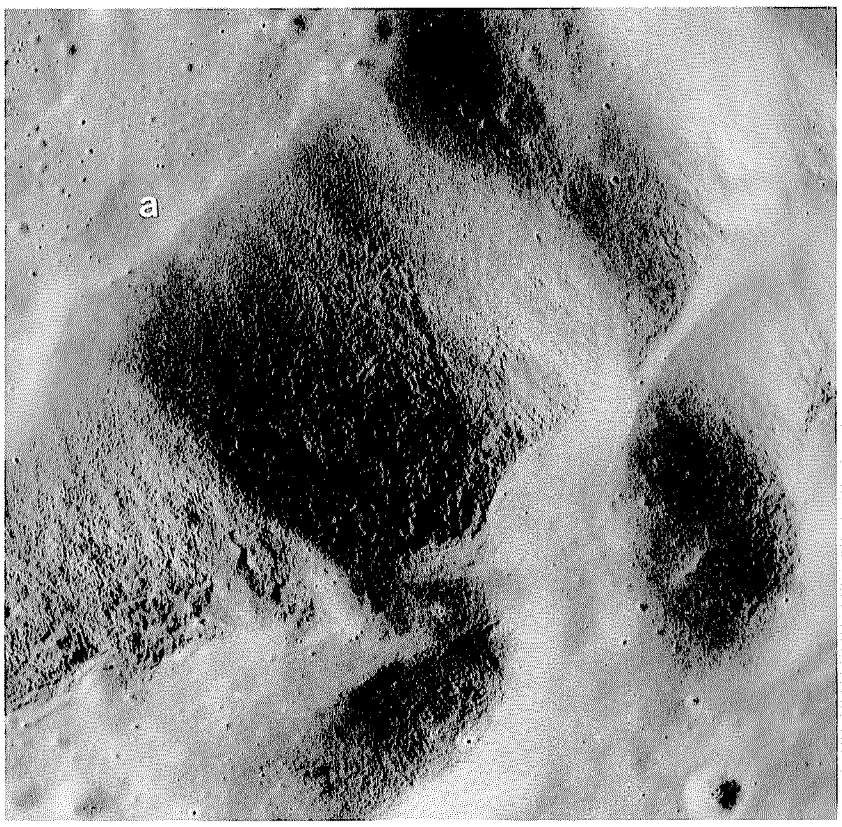

FIGURE 10.11.—Part of Montes Apenninus, showing paucity of outcrops and blocks on slope, and colluvial apron at base (a). Apollo 15 frame P–9804.

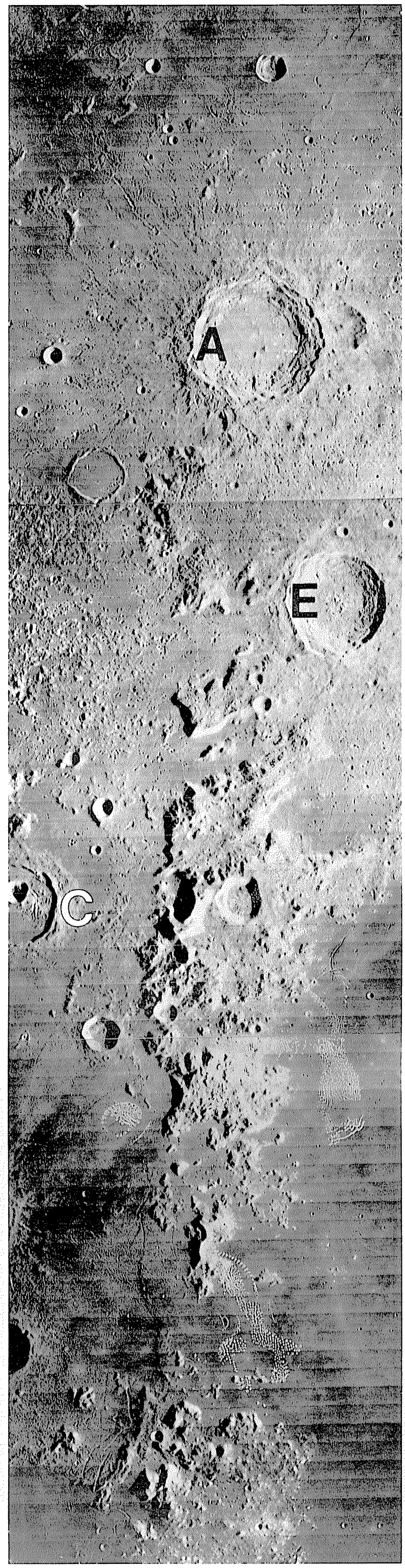

FIGURE 10.12.—Montes Caucasus, showing lineations oblique to trend of mountains and radial to center of Imbrium basin. Hummocky Alpes Formation is above crater Cassini (C; 57 km, 40° N., 5° E., probably Lower Imbrian) and west of Eudoxus (E; 67, 44° N., 16° E., probably Copernican), and in part of Montes Apenninus at bottom. A, Aristoteles (87 km, 50° N., 17° E., probably Eratosthenian). Orbiter 4 frame H–103.

Alpes Formation

Another, more extensive hummocky Imbrium-basin deposit is the Alpes Formation (Page, 1970). In contrast with the material of Montes Apenninus, the Alpes Formation consists of randomly oriented knobs and larger tracts of smoother material (figs. 10.1, 10.12, 10.14–10.16). This morphology closely resembles that of the Montes Rook Formation of Orientale (figs. 4.4*B*, *E*). The two units are also similar in spatial relation to massifs that are considered to be parts of major rings (Montes Alpes and the outer Montes Rook ring), which lie inside the topographic rims of their respective basins. The Alpes Formation, however, extends even farther from the Imbrium rim—as far as 600 km in the east—than does the Montes Rook Formation from Montes Cordillera (pl. 8; fig. 4.8). Both units were probably emplaced as low-velocity, late-stage ejecta from the inner parts of the basins. The Alpes Formation is the more extensive because the Imbrium basin is larger than Orientale.

Fissured plains

A third type of material on the Apennine flank forms level or wavy pools resting in depressions in the other units (fig. 10.14; Wilhelms, 1980). Some of these pools, as well as smooth veneers on rougher material, are cut by fissures of the types that suggest shrinkage of a formerly molten material (see chap. 3). This Apennine material is thus likely to be impact-melt rock like that occupying comparable positions on the flanks of craters and the Orientale basin (fig. 4.4*B*).

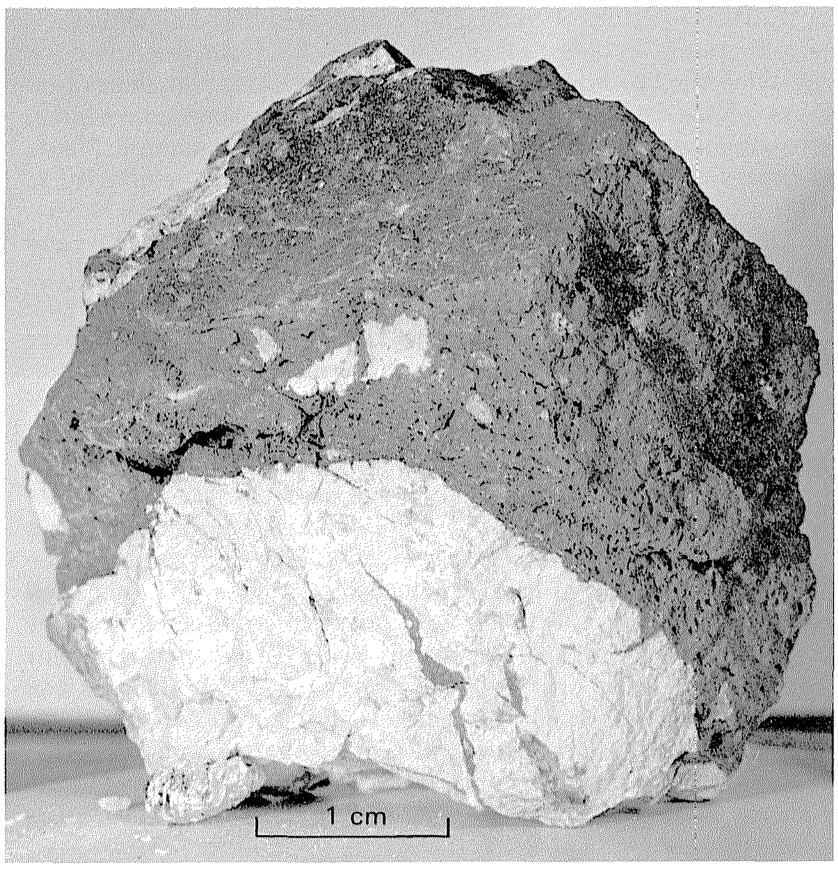

FIGURE 10.13.—"Black-and-white" breccia sample 15455 from rim of Spur Crater, station 7, Apollo 15 landing site. Black component is impact melt, probably formed by Imbrium impact (Ryder and Bower, 1977). White component is pre-Nectarian anorthositic norite (table 8.4).
A. Hand specimen after arrival from the Moon.

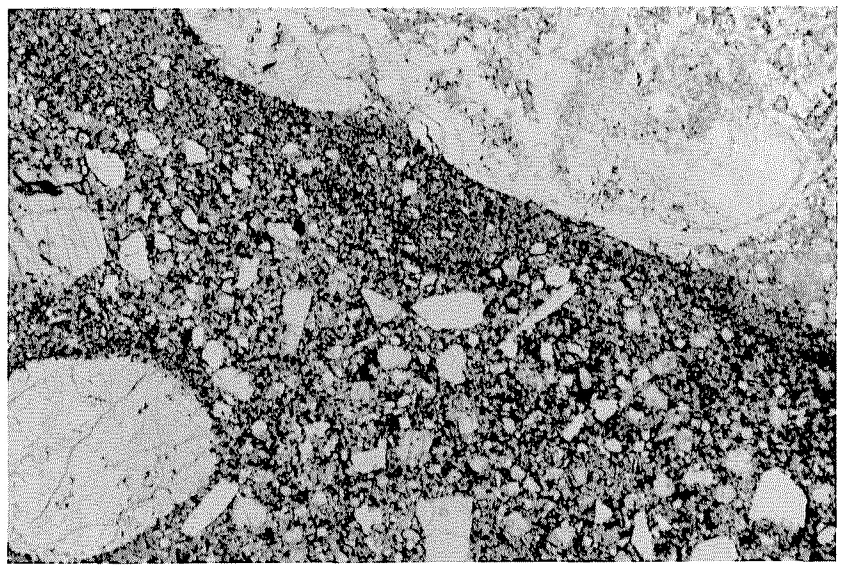

B. Thin section of 15455,29, showing chaotically distributed ANT clasts in melt matrix. Plane-polarized light; field of view, about 1 mm.

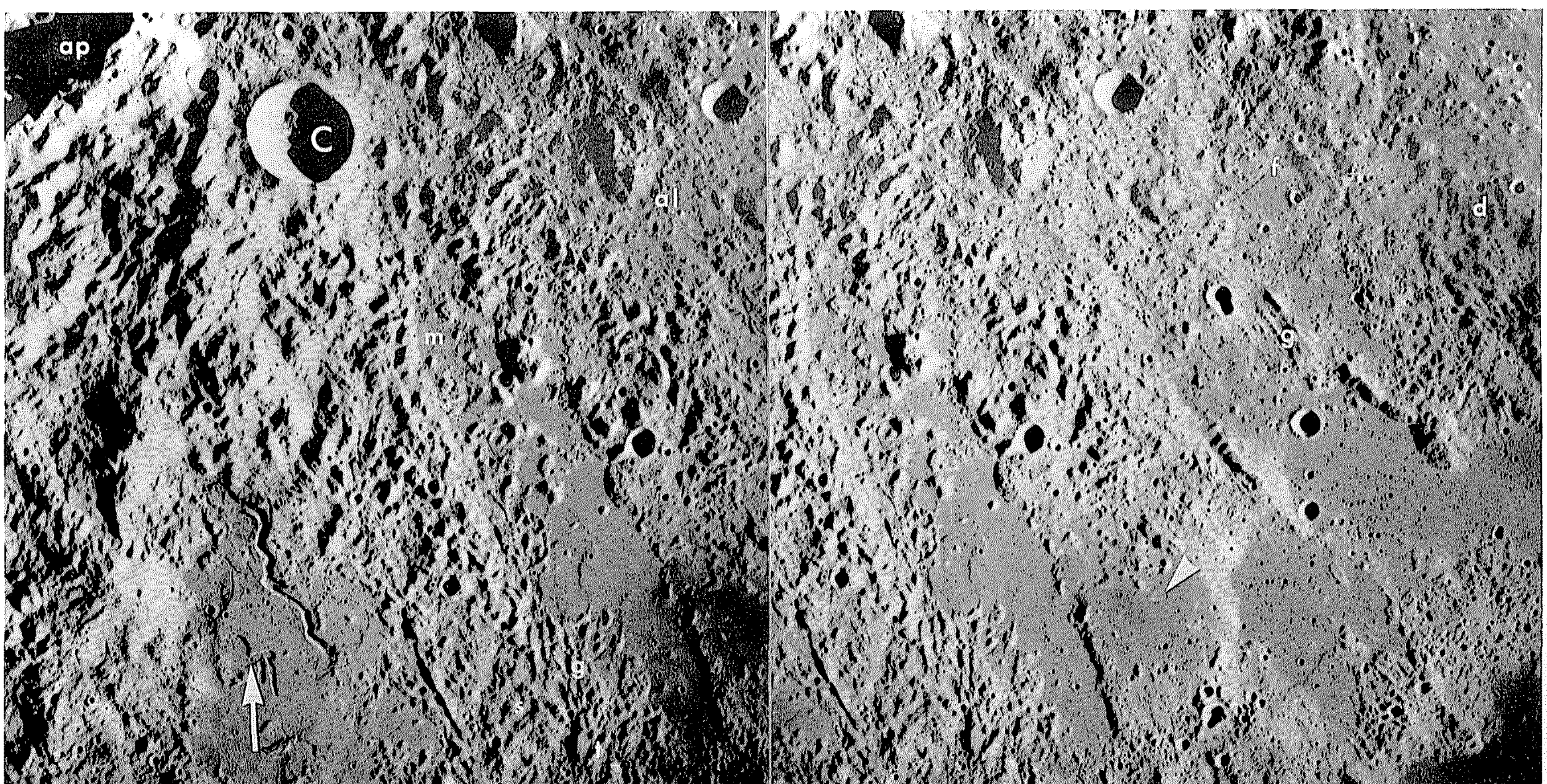

FIGURE 10.14.—Types of Imbrium ejecta on flank of Montes Apenninus. ap, northwest-facing Apennine scarp. Concentric "material of Montes Apenninus" is closest to scarp; farther out are knobby Alpes Formation (al), radially grooved terrain (g), smooth terrain (s), transverse fissures (f), and level ponds of probable impact melt (m). Arrows, irregular craters in mare, including "D caldera" (arrowhead in right frame; chap. 5; compare fig. 5.10*D*); d, dark-mantling material. C, fresh crater Conon (22 km; compare fig. 10.7). Stereoscopic pair of Apollo 17 frames M–1821 (right) and M–1823 (left). From Wilhelms (1980, fig. 13).

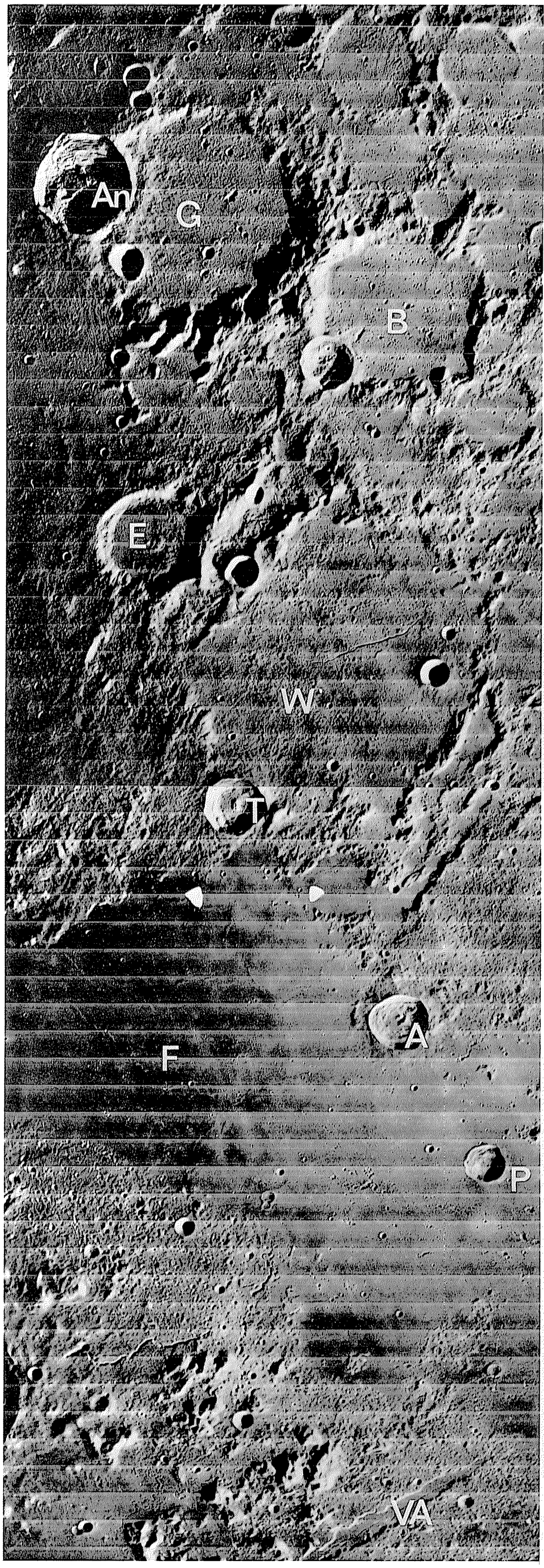

FRA MAURO FORMATION

Regional relations

A fourth unit on the Apennine flank, better developed farther out, is the Fra Mauro Formation (figs. 10.15–10.20; Eggleton, 1964, 1965; Wilhelms, 1970b). The Fra Mauro Formation extends 600 to 800 km from the rim of Imbrium in all exposed sectors (pls. 3, 8), and grades outward from coarsely hummocky to smooth and wavy (figs. 10.1, 10.14–10.16). The Fra Mauro Formation obliterates almost all prebasin craters to distances of 350 to 600 km from the Apennine crest. Thus, the Imbrium-basin deposits resemble exterior deposits of craters, whose continuous radial facies also extend beyond a coarse-textured zone out to 1.0 to 1.5 radii from the crater rim (chap. 3; Moore and others, 1974; Oberbeck and others, 1974). This similarity to craters was the chief basis for concluding that the Fra Mauro Formation is primary ejecta from the Imbrium basin (Shoemaker and Hackman, 1962).

The Fra Mauro Formation also resembles the Hevelius Formation of Orientale (fig. 4.4), except that the Fra Mauro includes more equidimensional hummocks and fewer distinct ridges. The continuous facies of the Hevelius extends 300 to 600 km from the rim of Montes Cordillera, 465 km in radius, which is the probable boundary of excavation of Orientale (see chap. 4). These similarities in morphology and extent relative to the diameters of the sources indicate that the Fra Mauro, Hevelius, and crater deposits form a related class of impact deposits. The inner and much of the outer facies of the Hevelius Formation include thick deposits that appear to have flowed along the surface (fig. 4.4), and the evident thickness and blockage by obstacles indicate that the Fra Mauro is also a major ground-flow deposit (Morris and Wilhelms, 1967; Wilhelms, 1980). Grooves and ridges indicative of the flow are also present (figs. 10.15–10.17, 10.19, 10.20). Small hills that have been interpreted as volcanic (fig. 10.17; Wilhelms, 1968; Wilhelms and McCauley, 1971) may, instead, be "deceleration dunes" formed like those of the transverse facies of the Hevelius Formation (figs. 4.4*G*, *H*).

Setting of the Apollo 14 landing site

The Apollo 14 landing site (figs. 10.18–10.21; lat 3.7° S., long 17.5° W.) was selected to obtain samples of primary ejecta from the Imbrium basin (Eggleton and Offield, 1970). Ridges and grooves radial to Imbrium and typical of the Fra Mauro Formation characterize the area around the landing site and most of the northern part of the north-south-elongate terra on which it is located (figs. 10.19, 10.20). The site is 550 km south of Montes Carpatus, which constitutes the south topographic rim of Imbrium and the boundary of the excavation cavity (fig. 10.18). Taking the Imbrium impact point as lat 33° N., long 18° W., the excavation cavity has a radius of about 540 km in this sector. Secondary craters are buried near the landing site (fig. 10.20; Eggleton and Offield, 1970) and are invisible farther north. Despite appearances that suggest dominance by primary ejecta at one-radius distances, the currently most hotly debated issue about the Apollo 14 rocks is the proportion of primary ejecta to nonbasin material in the sample collection.

Sample provenance

The samples returned by Apollo 14 were collected on two traverses outside the Lunar Module (LM) in February 1971 (fig. 10.21; Swann and others, 1971, 1977; Sutton and others, 1972). The first

FIGURE 10.15.—Several facies of Imbrium ejecta and an extensive stratigraphic section of older and younger units. Knobby, nonlineated Alpes Formation (bottom) is transected by Vallis Alpes (VA). All pre-Imbrian craters north of Mare Frigoris (F; compare fig. 10.6) are transected by Imbrium sculpture and filled by Lower Imbrian plains deposits. W. Bond (W; 158 km, 65° N., 4° E.) is also filled by hummocky and braided Fra Mauro Formation. W. Bond, Barrow (B; 93 km), and Goldschmidt (G; 120 km) are probably pre-Nectarian. Epigenes (E; 55 km) has a higher wall, despite its smaller size, and so it is probably Nectarian (not covered earlier by Humboldtianum deposits). Protagoras (P; 22 km) and Timaeus (T; 33 km) are not affected by Imbrium basin but are peripherally flooded by Imbrian mare basalt, and so they are Imbrian; Protagoras is degraded, possibly Lower Imbrian; Timaeus is fresh, Upper Imbrian. Archytas (A; 32 km) is fresh and superposed on mare, and so is probably Eratosthenian. Anaxagoras (An; 51 km, compare fig. 3.34) is very fresh and bright-rayed (see W. Bond floor), and so it is Copernican. Orbiter 4 frame H–116.

traverse (extravehicular activity [EVA]), west of the landing site, was relatively short but resulted in the collection of many fragments from the regolith and some large rocks. Most of the hand specimens of coherent rocks were collected on the second EVA, whose main goal was the ejecta of Cone Crater, 1.1 km northwest of the landing site (figs. 10.21–10.24). Cone is a Copernican crater, 25 million years old (table 13.2), 370 m across, and at least 75 m deep (Swann and others, 1977, pls. 1, 2). Interpretation of the rocks' ultimate provenance depends on whether Cone Crater sampled the Fra Mauro Formation, the underlying bedrock, or only the regolith built on the Fra Mauro Formation. Estimates of regolith thickness at the landing site range from 5–12 m, predicted from observations of small craters (Eggleton and Offield, 1970), through 8.5 m, inferred from seismic-refraction measurements (Cooper and others, 1974), to about 35 m, estimated theoretically on the basis of superposed craters (Moore and others, 1980b, p. 13–14). Because Cone Crater lies on a ridge crest, the regolith that it penetrated is unlikely to be thicker than even the largest of these values. Thus, Cone Crater probably penetrated the regolith and excavated the bedrock unit, which is identified as a 19- to 76-m-thick layer with a seismic velocity of 299 m/s (fig. 10.23; Kovach and Watkins, 1972; Chao, 1973).

Interpretations of what bedrock material the Cone impact excavated from beneath the regolith depend partly on interpretations of the ridge. The ridge is 50 to 100 m high (Sutton and others, 1972; Swann and others, 1977, pls. 1, 2). Hawke and Head (1977b) proposed that it is underlain by a large pre-Imbrian crater, in which case Cone might have excavated some of the crater material. Eggleton and Offield (1970), however, interpreted the ridge as one of the group that is characteristic of the Fra Mauro Formation and estimated a Fra Mauro thickness of 100 to 200 m on the basis of the ridge relief. In this interpretation, Cone probably did not penetrate beneath the Fra Mauro Formation. Even if the ridge is underlain by a pre-Imbrian crater, a substantial thickness of the Fra Mauro must overlie it (fig. 10.23; Chao, 1973). Because the bulk of a crater's ejecta comes from the upper part of the target material (Stöffler and others, 1974), the hand specimens of coherent rock from Cone's ejecta are likely to consist of Fra Mauro bedrock (Swann and others, 1977). Many of the smaller fragments could have been derived from regolith that overlay the Fra Mauro before the Cone impact; these fragments would also consist mostly of Fra Mauro material, recycled by impacts. However, they probably would also include bits of pre-Imbrian material dug from beneath the Fra Mauro Formation by craters older and larger than Cone (Head and Hawke, 1975; Swann and others, 1977, p. 28).

Samples important for interpreting and dating the Fra Mauro Formation were also collected, on both EVA's, from relatively smooth terrain near the LM and at stations A, B, E, F, and G (fig. 10.21). Before the mission, this smooth unit was interpreted alternatively as a facies of the Fra Mauro Formation or as a superposed volcanic deposit (Eggleton and Offield, 1970). It is clearly not volcanic and appears to be sufficiently similar in composition and lithology to the Cone Crater material as to be thought part of the Fra Mauro Formation (Swann and others, 1977). However, the relations among the parts of the landing-site region are somewhat unclear because of limited data gathered in the field.

Petrology

The coherent rocks from the Cone Crater ejecta exhibit flow banding, large-scale stratification, and strong thermal effects, features that suggested to early analysts an origin in a vigorously

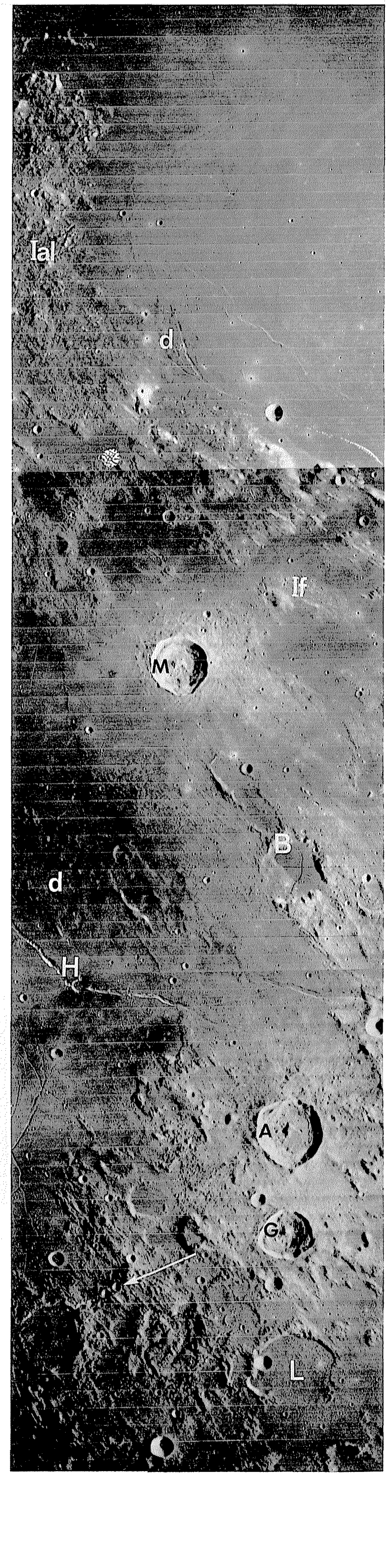

FIGURE 10.16.—Outward gradation of Imbrium deposits. H, Rima Hyginus (compare figs. 5.10*E*, 6.16*A*). Knobby ejecta (Alpes Formation, Ial) grades to smoother Fra Mauro Formation (If) in and near Montes Haemus. Surface flow of Imbrium ejecta apparently was deflected by Imbrium-secondary chain Boscovich (B; Boscovich Formation was interpreted as volcanic by Morris and Wilhelms, 1967). Terrain south of Hyginus, consisting of pre-Imbrian craters (for example, Lade [L; 56 km]; compare fig. 10.17), is scored by Imbrium lineations and is mapped either as pre-Imbrian lineated terrain (Wilhelms and McCauley, 1971) or as part of Imbrium zone (this volume). Arrow, possible Orientale-basin secondary chains; Orientale is centered 3,100 km to west in direction of arrow. d, dark-mantling deposits near Sulpicius Gallus (compare fig. 1.7) and north of Rima Hyginus. Fresh craters include Manilius (M; 39 km, 14.5° N., 9° E., probably latest Imbrian), Agrippa (A; 44 km, younger than mare and probably Eratosthenian), and Godin (G; 35 km, younger, more sparsely cratered, brighter, and with a higher reading in thermal infrared than Agrippa; probably Copernican). Overlaps with figures 10.1, 10.35, and 10.38. Orbiter 4 frame H-97.

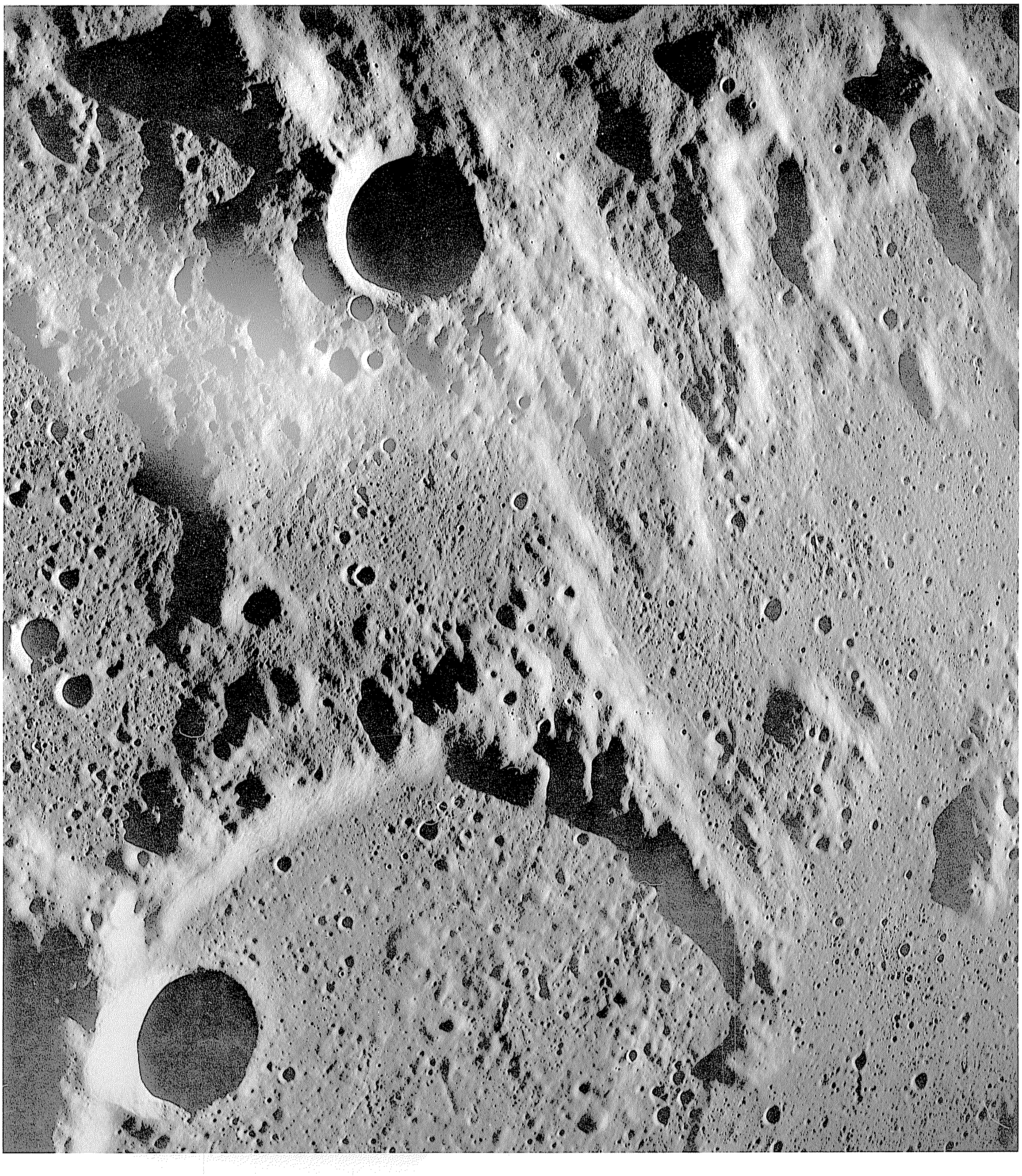

FIGURE 10.17.—Lineated terrain at top (north) is Fra Mauro Formation, probably superposed on Imbrium-secondary chains. Crater Lade (bottom; 56 km, 1° S., 10° E.) is filled with hummocky deposit, probably consisting of Fra Mauro material that flowed over rim and decelerated. Apollo 11 frame H–4552.

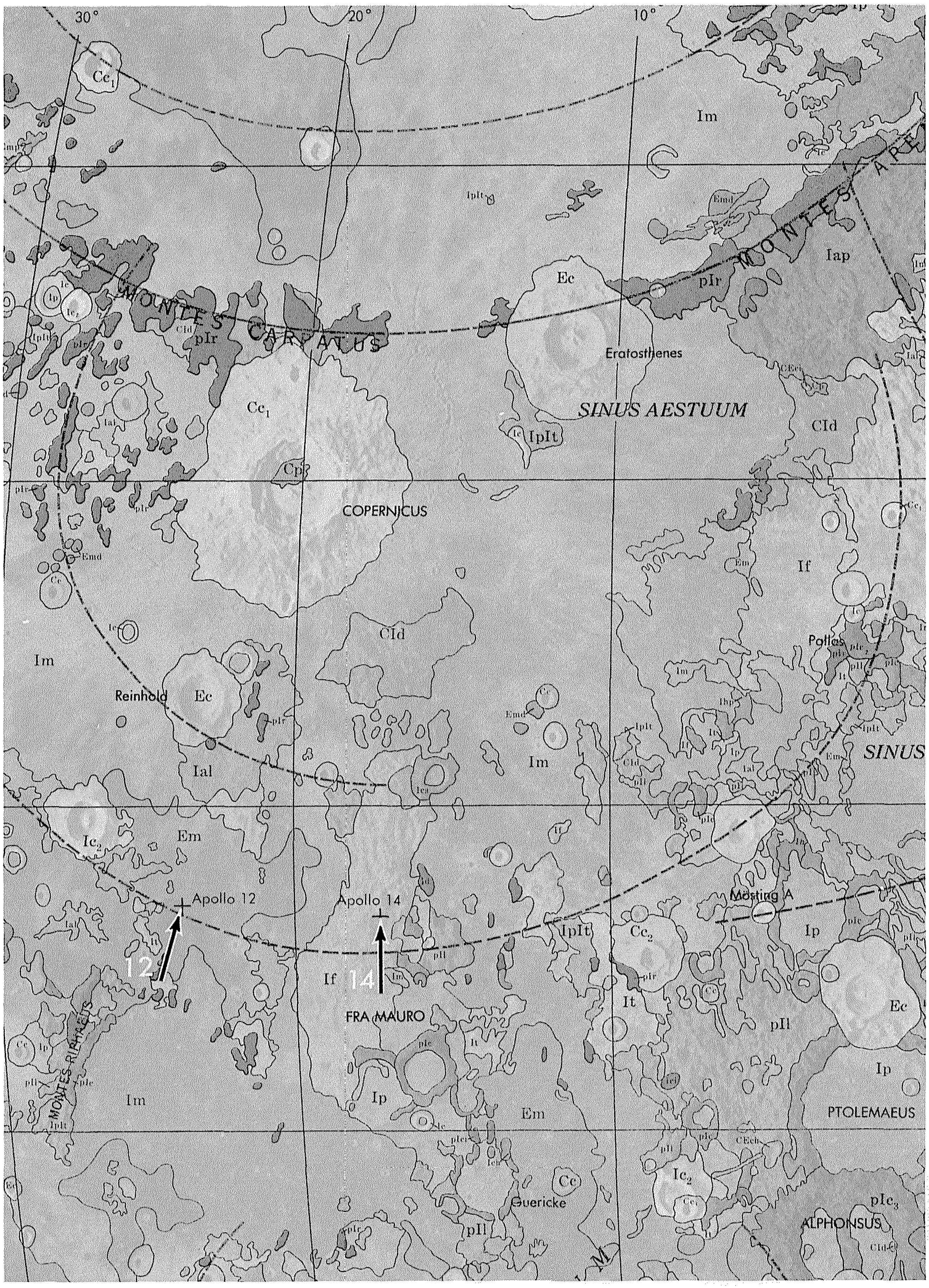

FIGURE 10.18.—Part of geologic map of lunar nearside (Wilhelms and McCauley, 1971), including Apollo 12 and 14 landing sites (arrows). If, Fra Mauro Formation; Em, Eratosthenian mare material (Apollo 12; see chap. 12). Montes Carpatus, 550 km north of Apollo 14 landing site, constitutes south rim of Imbrium basin. Ring passing near landing sites is part of Insularum basin in one interpretation, but may be ring of Procellarum basin (see chap. 8; pls. 3–7).

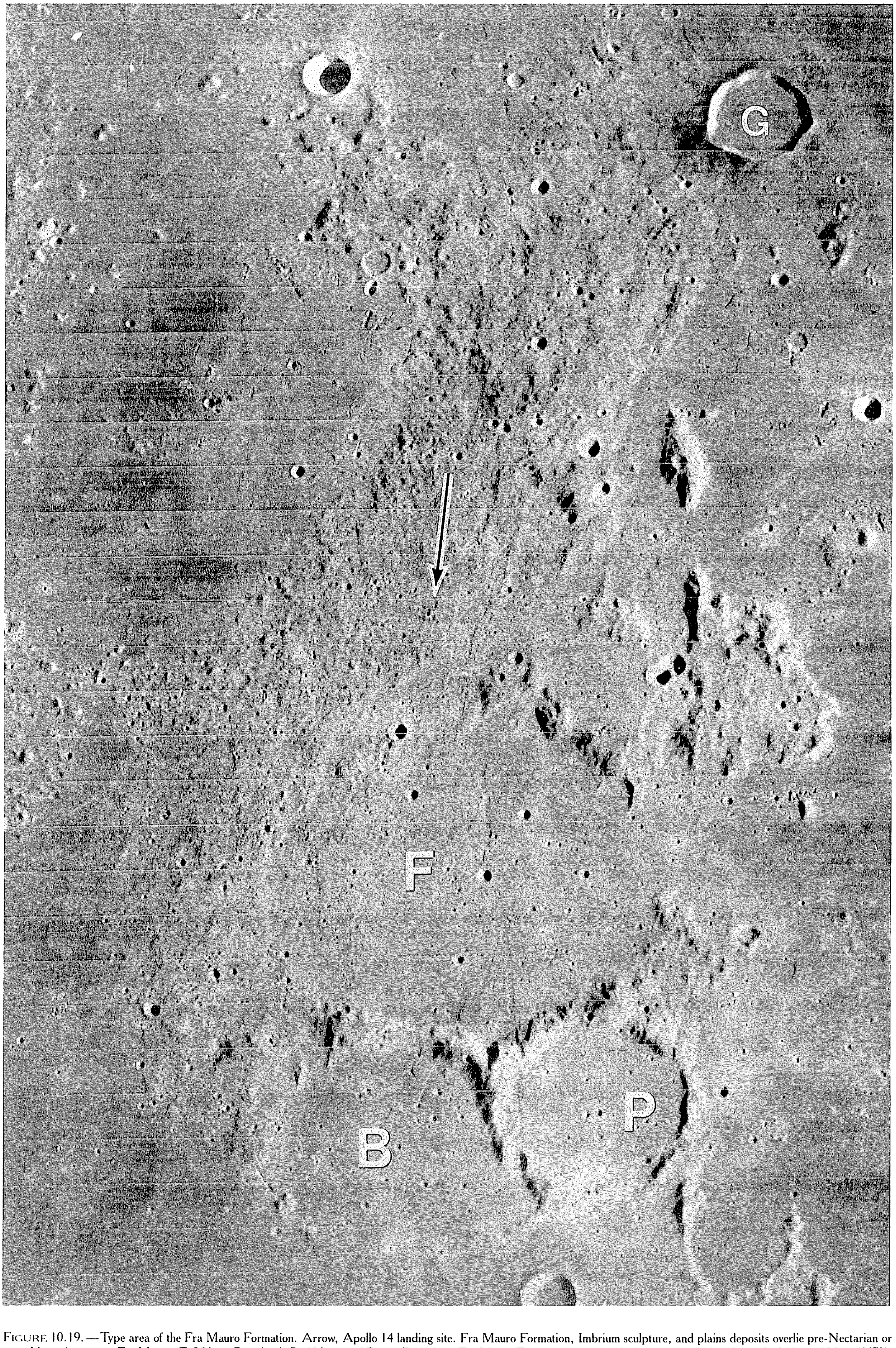

FIGURE 10.19.—Type area of the Fra Mauro Formation. Arrow, Apollo 14 landing site. Fra Mauro Formation, Imbrium sculpture, and plains deposits overlie pre-Nectarian or Nectarian craters Fra Mauro (F; 95 km), Bonpland (B; 60 km), and Parry (P; 48 km); Fra Mauro Formation is overlain by Imbrian crater Gambart (G; 25 km, 1° N., 15° W.). Orbiter 4 frame H–113.

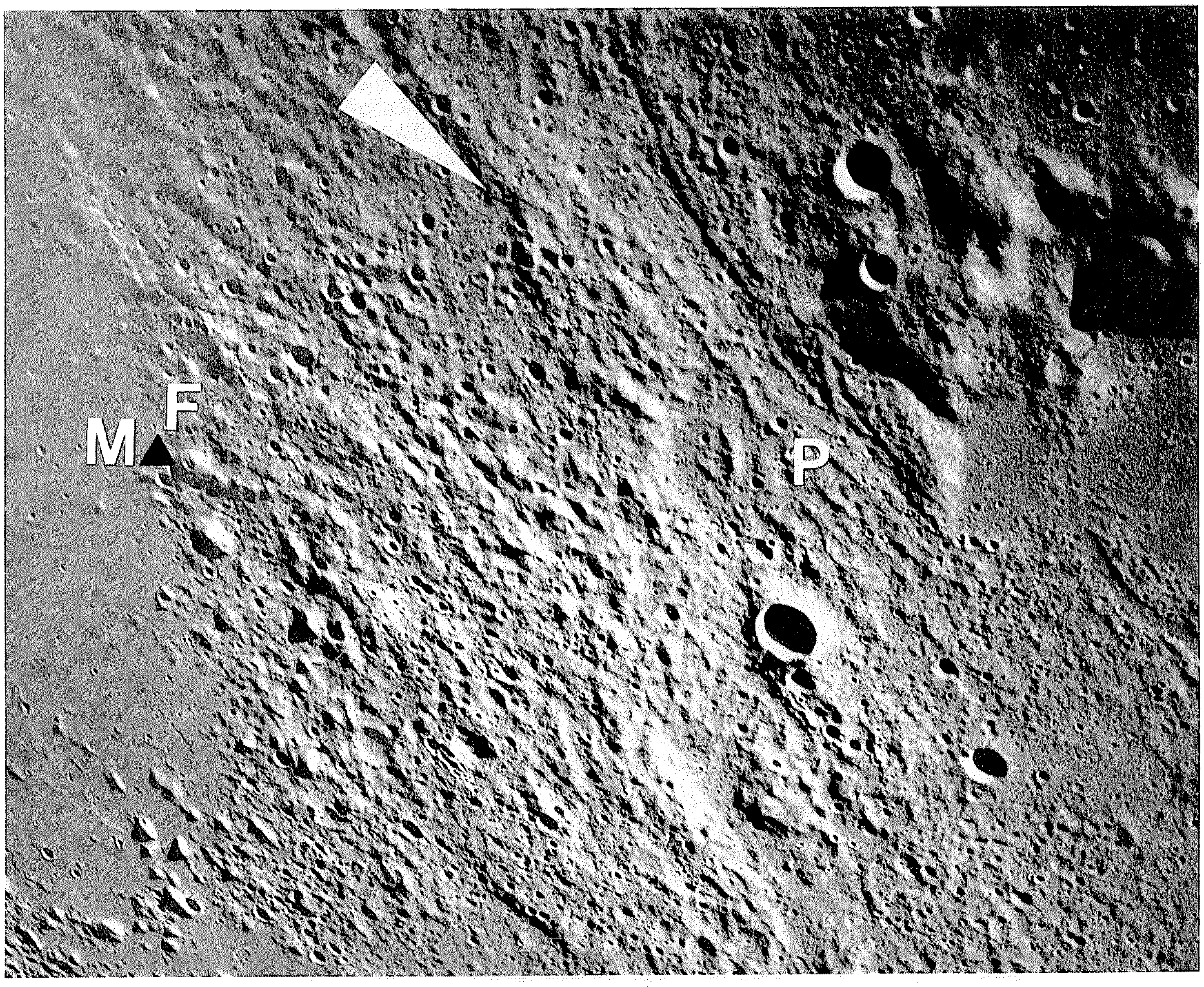

FIGURE 10.20.—Vicinity of Apollo 14 landing site, including Fra Mauro Formation (F) in sharp contact with mare material (M) at triangle. The Fra Mauro Formation is strongly lineated radially to Imbrium basin (compare fig. 10.19). Cone Crater is barely visible at tip of arrow. P, buried pre-Imbrian crater. Apollo 12 frame H–7597.

FIGURE 10.21.—Apollo 14 astronaut traverses. Pennant, landing point; ALSEP, geophysical instruments; lettered and numbered circles, sampling stations. Numerical scale refers to original map. Airbrush drawing by U.S. Geological Survey, published by U.S. Defense Mapping Agency for NASA.

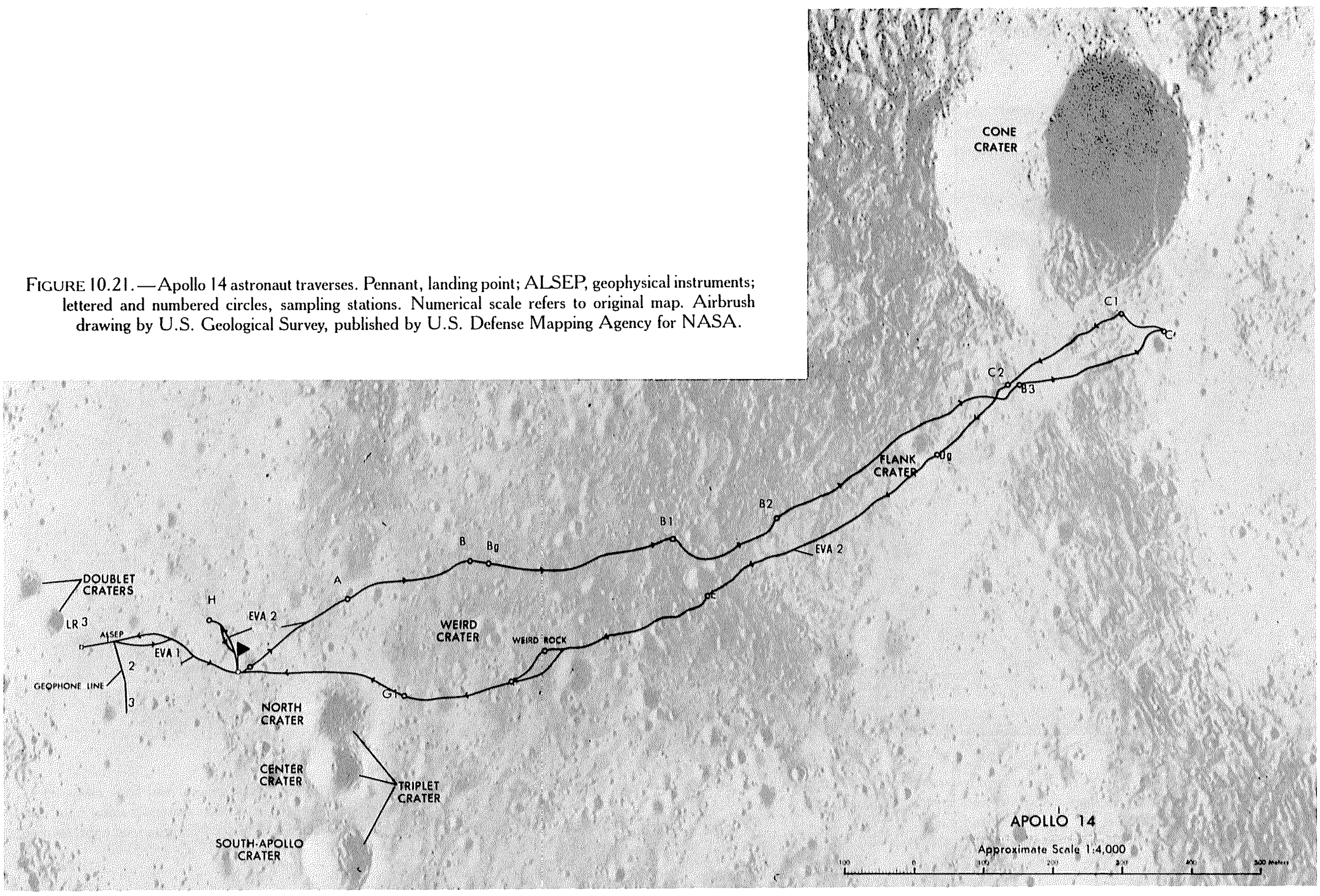

emplaced, hot ejecta blanket (fig. 10.22; Engelhardt and others, 1972; Quaide and Wrigley, 1972; Wilshire and Jackson, 1972). Heat-induced textures were first interpreted as the products of metamorphism or annealing (Quaide and Wrigley, 1972; Warner, 1972; Wilshire and Jackson, 1972) but are now widely considered to be the result of crystallization of impact melts (Engelhardt and others, 1972; Ryder and Bower, 1976; Lofgren, 1977). The impact-melt rock is crystalline-matrix breccia that grades from clast-free (fig. 2.8) to heavily laden with fragments (fig. 10.24). The most common types of this gradational series consist of more than 15 percent clasts in gray, coherent,

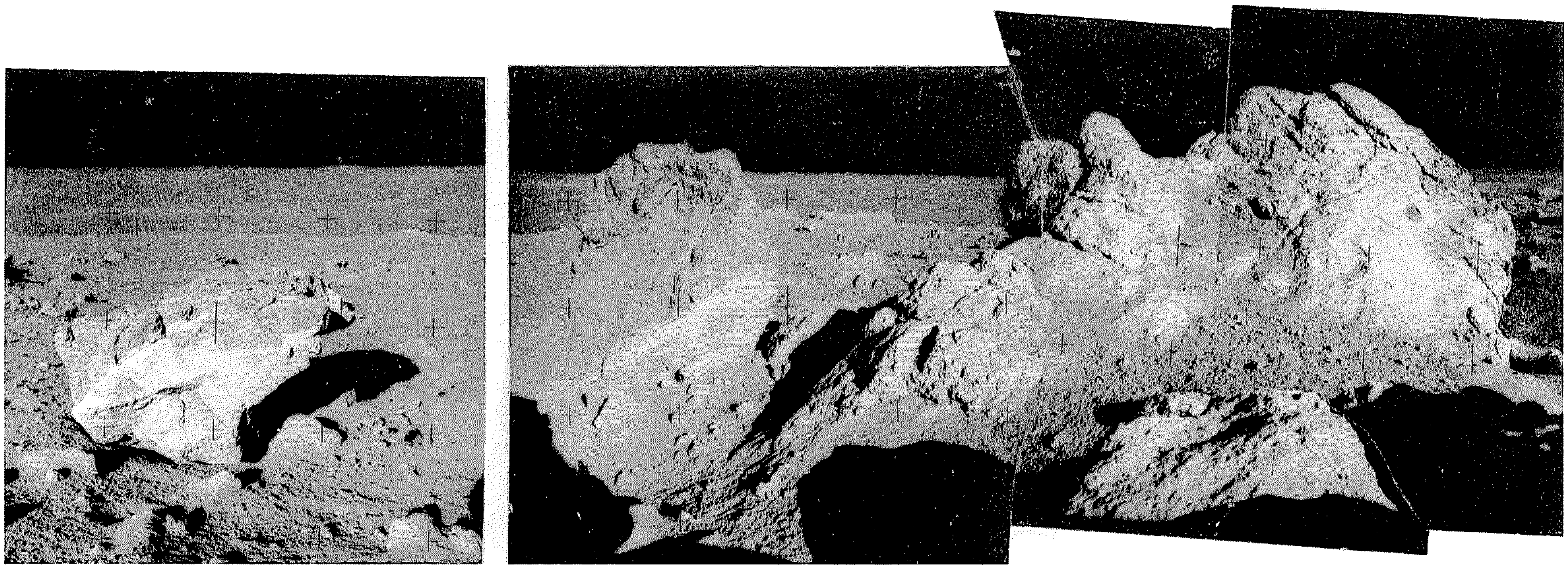

FIGURE 10.22.—Large boulders near rim of Cone Crater, containing light and dark materials. From Swann and others (1977, fig. 44).

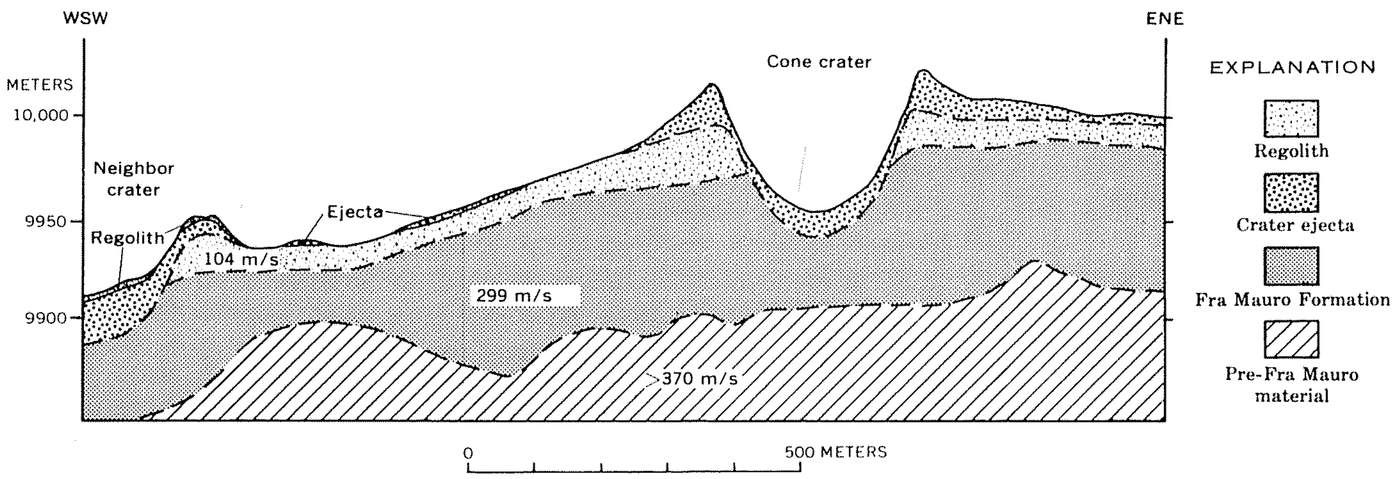

FIGURE 10.23.—Schematic geologic cross section of Apollo 14 landing site (from Chao, 1973). Section is drawn just north of landing site in west to Cone Crater in east. Thicknesses of geologic units are based mostly on active-seismic data (Kovach and Watkins, 1972). Compressional-wave velocities of some units are indicated. Elevations in vertical scale are based on reference elevation chosen to correspond to mean radius of Moon, 1,738 km.

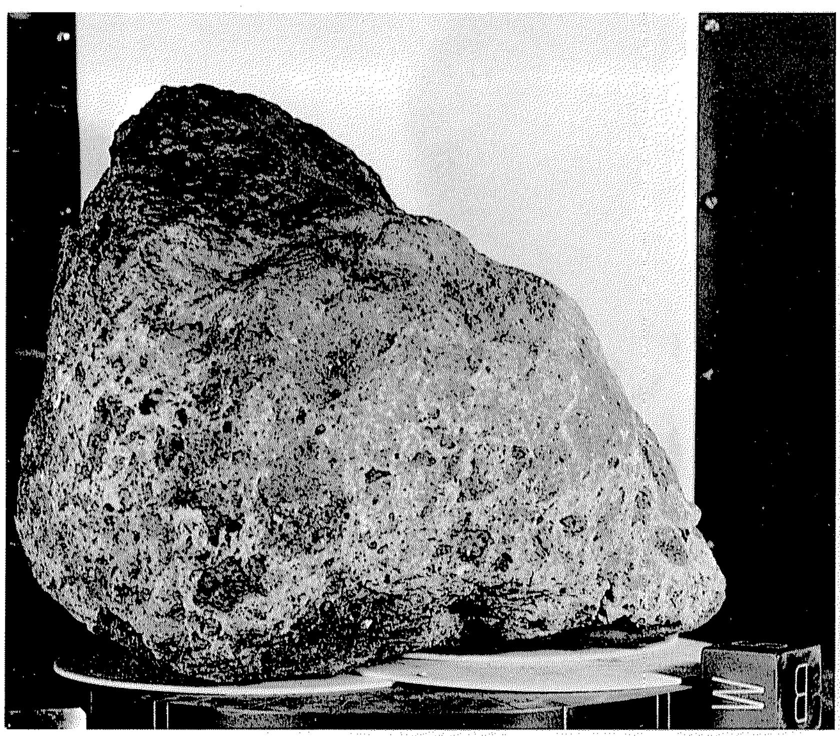

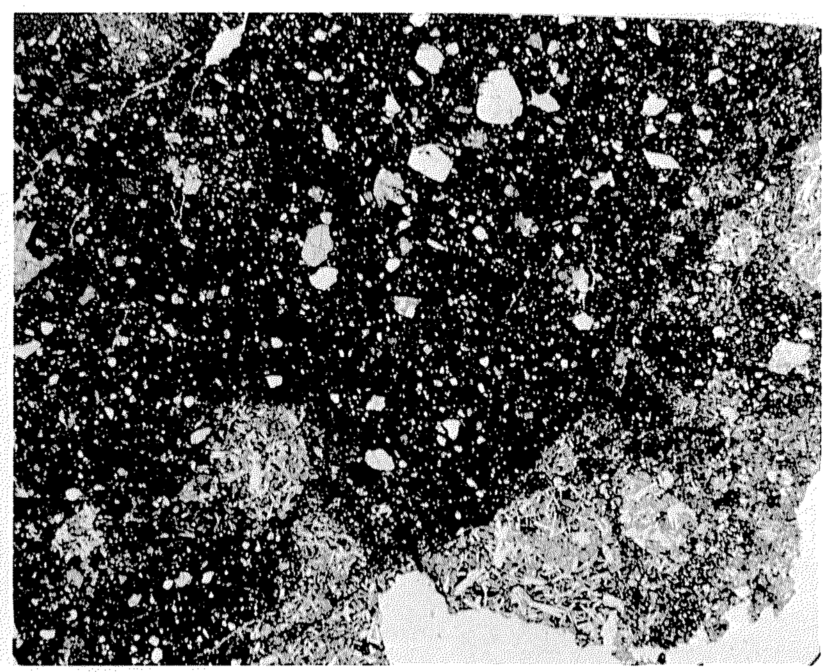

FIGURE 10.24.—Large (8.9 kg) Fra Mauro breccia sample 14321, "Big Bertha," from rim of Cone Crater, Apollo 14 landing site: a polymict breccia displaying multiple episodes of brecciation (Duncan and others, 1975; Grieve and others, 1975).
A. Entire hand specimen, showing complex relations of clasts and matrix.

B. Thin section of sample 14321,197, showing abundant mineral and lithic clasts set in dark, fine-grained matrix. Light-colored, coarsely crystalline materials along right and bottom edges are clasts of high-Al mare basalt (table 9.5). Nonpolarized light; field of view, about 1.5 cm.

melt-derived matrices (Chao and others, 1972; Engelhardt and others, 1972; Wilshire and Jackson, 1972; Chao, 1973; Simonds and others, 1977). These clast-laden breccia samples were collected from both Cone Crater and the smooth terrain; because they characterize the landing-site region, they have been termed *Fra Mauro breccias* (Chao and others, 1972). Light-colored friable breccia samples ("white rocks") are also common but are probably clasts previously included in the crystalline-matrix breccia (Chao and others, 1972). Samples of almost fragment-free impact melt (Green and others, 1972; Taylor and others, 1972; James, 1973; McKay and others, 1978, 1979) were collected from the regolith on the smooth terrain; the largest are samples 14073, 14276, and 14310 (fig. 2.8). At one time, these samples were widely considered to be volcanic (see chap. 8).

The samples are typically rich in KREEP. Most of the crystalline-matrix breccia seems to be relatively uniform in composition; 12 of the 16 samples analyzed by Simonds and others (1977) cluster together on a plot of MgO content versus Al_2O_3 content as does "vitric matrix" breccia, consisting of consolidated regolith fragments; not further discussed here). Clast-free rock samples 14276 and 14310 contain less MgO and more Al_2O_3 than the cluster. McKay and others (1979) found that the chemical and isotopic differences among the KREEP-rich impact-melt samples are consistent with an origin in a single melt sheet.

Emplacement process

A debate about emplacement mechanism persists even among those who agree that most samples are from the Fra Mauro Formation and that the Fra Mauro is somehow related to the Imbrium basin (fig. 10.25). One view is that the rocks that compose the Fra Mauro are parts of the primary ejecta of the basin (Eggleton and Offield, 1970; Chao and others, 1972; Dence and Plant, 1972; Engelhardt and others, 1972; Quaide and Wrigley, 1972; Wilshire and Jackson, 1972; Chao, 1973). That is, they were parts of the target material that traveled at least 550 km to their site of deposition (hypothesis b, fig. 10.25). This view is consistent with the generally uniform composition of the Fra Mauro breccia samples. Either thorough mixing of target materials or derivation from a compositionally uniform source, such as a KREEP-rich crustal layer or a KREEP-basalt section in the Procellarum basin, could have produced this uniformity. The primary-impact mechanism also allows for variations in composition and shock grades because of the general disorder of the basin-forming process. The differing compositions and shock grades of the friable, light-colored materials and the Fra Mauro breccia are readily comprehended in this model as the results of formation in different parts of the shock-engulfed target zone, followed by mixing during ejection or emplacement (Engelhardt and others, 1972). That is, some of the already heterogeneous bedrock-breccia, regolith, and volcanic deposits in the target zone were little altered by the Imbrium impact, whereas others were more highly shocked, melted, and homogenized.

The opposing view is that the crystalline-matrix breccia originated at or near the deposition site (Oberbeck and others, 1974; Morrison and Oberbeck, 1975; Head and Hawke, 1975; Oberbeck, 1975; Stöffler and others, 1976; Hawke and Head, 1977b, 1978a, b; Simonds and others, 1977). The proponents of this "local" hypothesis are troubled by the diversity of textures and compositions of the breccia samples and by the great distance of the Apollo 14 landing site from the Imbrium basin. They believe that the terrestrial analogs (Chao and others, 1972; Dence and Plant, 1972; Simonds and others, 1977) show that the abundant melt found in the breccia deposits could not have been transported so far. In the local-derivation models, the Fra Mauro Formation (and analogous deposits of Orientale and smaller craters) consists of mixtures of the primary ejecta with material derived from the local terrane by secondary impacts (hypothesis a, fig. 10.25). The radial ridges of the Fra Mauro that are interpreted as flows of primary ejecta in the first model are considered in the local-derivation model to be analogous to the herringbone texture visible among secondary craters of Copernicus-type craters (fig. 3.4), or to surges of debris that continued to flow outward after their generation by secondary impacts. Such coalesced debris flows may have erased the original secondary-ejecta pattern. On the basis of the upper equation in figure 10.26, Morrison and Oberbeck (1975) calculated that only 15 to 20 percent of the Fra Mauro Formation at the Apollo 14 landing site should consist of primary ejecta. Head and Hawke (1975) pointed out craters and basins whose melted and fragmental deposits are reasonable sources of the local materials. They considered the KREEP-rich compositions to have been derived from volcanic extrusions in the vicinity of the landing site (Hawke and Head, 1978b). They stated that mineralogically recorded shock pressures in the narrow range 20–30 GPa should be of Imbrium-basin origin and that less highly shocked and, possibly, more highly shocked material should be of local origin (Hawke and Head, 1978a).

Both the primary-ejecta model and the secondary-impact, local-material model probably contain some truth. Great diversity in shock grade and other lithologic attributes is surely possible at a given point in the ejecta deposit of a large impact. On the other hand, the pervasiveness of secondary impacts at great ranges from basins cannot be denied, and incorporation of the impacted local material is to be expected The issue is thus one of proportion. I believe that primary ejecta is the dominant component and that the proponents of secondary emplacement of the entire Fra Mauro Formation have overstated their case, for several reasons (Wilhelms and others, 1980):

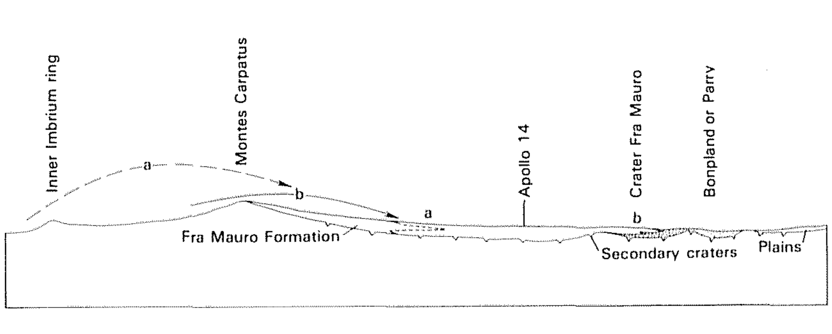

FIGURE 10.25.—Geologic cross section illustrating secondary-ejecta (a) and primary-ejecta (b) hypotheses for emplacement of the Fra Mauro Formation, drawn along north-south line in figure 10.18. In most secondary-ejecta models, Imbrium cavity is bounded by an inner ring, ejection trajectories are steep (dashed arc), and transition between primary and secondary deposits is close to rim (dashed sawteeth beneath right-hand letter a). In primary-ejecta model preferred here, basin rim is at Montes Carpatus, ejection trajectories are shallow (solid arc), and transition from primary to secondary deposits occurs south of Apollo 14 landing site (solid sawteeth beneath right-hand letter b). Secondary craters form in both models (diagrammatically indicated by notches in substrate): in hypothesis a, their ejecta forms sampled part of the Fra Mauro Formation; in hypothesis b, they are deeply buried by primary ejecta at Apollo 14 landing site.

$$- - - - \quad \mu = 46.4 \left[\frac{\sin 2\theta}{2 \tan \frac{R}{60.6}} + \sin^2\theta \right]^{-1} D^{-0.401} \cos^{1.134}\theta$$

$$—— \quad \mu = 30.5 \left[\frac{\sin 2\theta}{2 \tan \frac{R}{60.6}} + \sin^2\theta \right]^{-1} D^{-0.60} \cos^{1.20}\theta$$

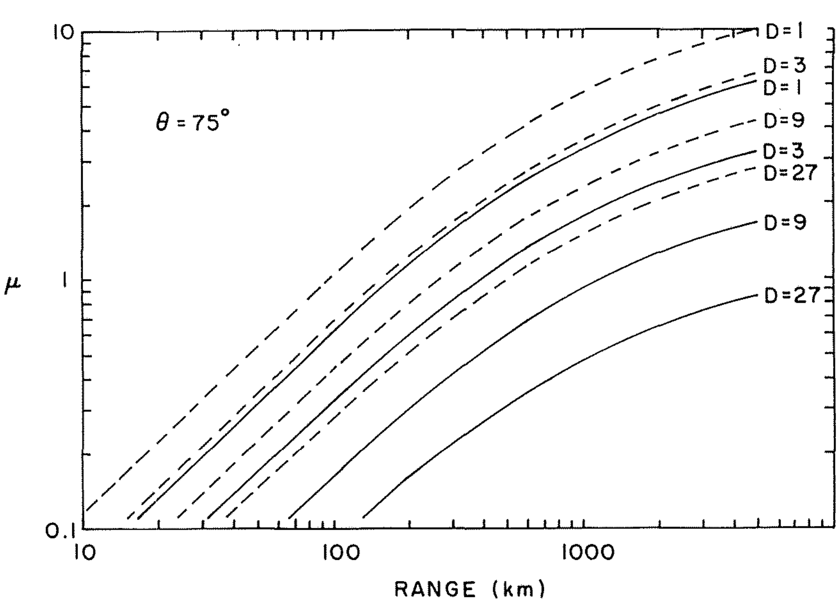

FIGURE 10.26.—Mass ratio of primary versus local material as a function of range from source of incoming ejecta. Dashed lines are based on upper equation, which assumes scaling of $D = KE^{-3.4}$ (Oberbeck and others, 1975); solid lines are based on lower equation, which assumes scaling of $D = KE^{-3.6}$ (H.J. Moore, written commun., 1980). μ, ratio of mass ejected from secondary crater to mass of ejecta projectile that created crater; θ, angle of impact (equal to angle of ejection), measured from local surface normal; D, diameter of secondary crater (in kilometers); R, range or distance along Moon's surface from point of ejection within primary crater or basin to secondary crater (in kilometers). Courtesy of H.J. Moore.

1. The topography of the landing-site region is dominated by ridges formed by flow of a thick deposit that has obscured the secondary craters. This flow originated either at the basin rim or at secondary-impact sites much closer to the basin than its present resting place. Either circumstance would change the "range" input in the equation (fig. 10.26).
2. The equation in figure 10.26 is model-dependent in other ways. The assumed ejection angle, size of the Imbrium basin, point of derivation within the basin, size of secondary craters (which are difficult to see and measure near the landing site), and diameter-energy scaling laws are all questionable. An apparently small change in the exponent of the energy in the scaling relation from -3.4 to -3.6 changes the equation to the lower form in figure 10.26 and greatly affects the results of calculations. Moreover, the equation is based on single-body impacts (Morrison and Oberbeck, 1975, p. 2527), whereas most basin ejecta at great ranges is likely to be comminuted (Schultz and Mendell, 1978). Many small low-density fragments impacting over an extended time at low velocities will build up a deposit of their own material rather than excavate local materials greater than their mass (Chao and others, 1975; Morgan and others, 1977, p. 672).
3. Photogeologic relations indicate the presence of abundant melt in basin-ejecta deposits. (a) Material ponded in depressions in the inner Orientale and Imbrium ejecta displays "mud crack" patterns of fine fissures, probably resulting from shrinkage of a coherent material (figs. 4.4*E*, 10.14; Moore and others, 1974). These fissured ponds resemble the external impact-melt pools of large craters, which increase in abundance and distance from the rim with increasing crater size and occur as far as two crater radii from some rims (chap. 3; Howard and Wilshire, 1975; Hawke and Head, 1977a). (b) Crater ejecta is coated by additional melt in the form of veneers that are gradational with the ponded melt (fig. 3.36; Howard, 1975; Howard and Wilshire, 1975; Hawke and Head, 1977a). (c) Large tongues of nontextured material apparently have segregated from the radially lineate Hevelius Formation and have formed distant lobes (fig. 4.4*D*). The lobate, commonly leveed morphology of these segregates suggests emplacement as viscous fluids, for which melt is a reasonable, though not exclusive, explanation (Eggleton and Schaber, 1972; Moore and others, 1974). Finally, (d) pools in the floors of many secondary craters appear to have once been molten, an appearance suggesting considerable ranges for ejected melt (figs. 3.9*A*, 4.4*C*; Moore and others, 1974; Schultz and Mendenhall, 1979).
4. Scaling laws suggest that large, basin-forming impacts generate more melt than small, crater-size impacts on either the Moon or the Earth (chap. 3; Rehfuss, 1974; O'Keefe and Ahrens, 1977; Lange and Ahrens, 1979; Melosh, 1980, p. 77). An increase in the ratio of projectile mass to crater size is predicted with increasing magnitude of impact (Baldwin, 1963, chap. 8; O'Keefe and Ahrens, 1975; Gaffney, 1978). The impact energy of large bodies is coupled into the target longer, so that the shock energy is distributed over a larger volume of rock. In contrast, small fast bodies strike and rapidly release their kinetic energy into small, intensely heated volumes of rock. The result is that large impacts generate larger volumes of less highly heated melt than do small impacts. As a corollary, melt of the large impacts would presumably be less thoroughly homogenized than that of small impacts.
5. Finally, the target may have been hot already, so that any impact would create more melt than would an impact into a cold target (Wood, 1975d, p. 515). Evidence of heat at crustal depths is contained in the coarse grain size of Apollonian metamorphic rocks (Stewart, 1975) and the textures of granulitic impactites, ascribed to accumulated heat from hot ejecta blankets (Warner and others, 1977). Radiogenic heat may have melted KREEP-rich magmas before (see chap. 9) and after (Apennine Bench Formation) the Imbrium impact, and liquid magma may even have been ejected (Schultz and Mendenhall, 1979).

These points are offered not as proof of a primary-ejecta origin but as reasonable alternatives to the local-origin models currently widely accepted. The data of Simonds and others (1976b, 1977) also seem to be consistent with a primary-ejecta origin, although those authors favored the local-origin model. Simonds and others (1976a, b) suggested that the Fra Mauro crystalline-matrix breccia formed as superheated impact melt plus cold fragmental debris and that the differences in clast content are solely responsible for the textural differences. As discussed above, the compositional data (Simonds and others, 1977; McKay and others, 1979) also seem to be more consistent with a limited range of source compositions than with the diverse "local" target cited by many authors. The main support for the local-derivation model seems to be (1) terrestrial-analog craters whose ejecta has not been identified (Canadian-shield craters), and (2) the upper equation in figure 10.26 (Morrison and Oberbeck, 1975), which is highly model-dependent and is qualitatively contradicted by the absence of conspicuous Imbrium-secondary craters in the appropriate uprange positions to have been the sources of the Fra Mauro Formation.

Absolute age

Two age clusters have been identified in the returned samples by both the ^{40}Ar-^{39}Ar (Turner, 1977) and Rb-Sr (Papanastassiou and Wasserburg, 1971b) methods, which agree well for these rocks (table 10.1). The younger cluster was obtained mainly for some clast-poor impact-melt rock samples (14073, 14276, 14310), for a few samples of Fra Mauro breccia, and for small fragments from mixed regolith samples. The measured ages of the clast-free rocks average 3.82 aeons; of the clast-free fragments, 3.83 aeons; and of other melt-rock samples of uncertain origin, including some that may belong to the older cluster, 3.84 aeons (table 10.1). If the dated samples are of Imbrium-basin impact-melt rock, as I believe, the basin formed 3.82 to 3.84 aeons ago, with an uncertainty of only a few tens of millions of years. However, the uncertain field relations between samples from the smooth terrain and from Cone Crater do not preclude the possibility that some samples are derived from melts of a post-Imbrium crater.

The best dated older group of Apollo 14 samples (extremes and stated analytical errors larger than 0.1 aeon eliminated) yields ages of 3.87 to 3.96 aeons (tables 9.5, 10.1). All three large samples (14053, 14072, and clasts of 14321) came from the Cone Crater flank, and all are of high-Al mare basalt (fig. 10.24; table 9.5; Grieve and others, 1975; Ridley, 1975; Taylor, 1975; Simonds and others, 1977; Ryder and Spudis, 1980). They differ further from the younger group in their lower initial Sr-isotope ratios (Papanastassiou and Wasserburg, 1971b). Although error bars overlap, these rocks form a distinct age group from the younger rocks. Clasts of breccia sample 14066 and some fragments from regolith samples 14161 and 14167, all collected within 400 m of the LM, may also belong to the older cluster (lithologies uncertain; listed with the younger group in table 10.1). The older clasts and regolith fragments appear to be fragments of pre-Imbrian rock, including volcanic basalt, incorporated into the Imbrium-ejecta breccia before its emplacement near the future landing site (chap. 9; Mark and others, 1975; Wetherill, 1977b). This basalt-in-breccia relation is consistent with either the primary- or the secondary-ejecta model; beds of basalt could have existed before the Imbrium impact either in the Imbrium target area (Wilshire and Jackson, 1972) or in the vicinity of the Apollo 14 landing site (Hawke and Head, 1978b). In either model, the age of the Imbrium basin is constrained as equal to (Compston and others, 1972) or less than (Wetherill, 1977b) 3.87 aeons.

Conclusions

The following working hypotheses (fig. 10.25) are consistent with all data from the samples known to me and with Moon-wide relations. (1) The crystalline-matrix clast-laden Fra Mauro breccia excavated from Cone Crater is sufficiently uniform structurally and compositionally to indicate derivation from a single major rock unit. (2) That unit is part of the photogeologically observable ridgy unit, the Fra Mauro Formation, which is composed mostly of primary ejecta of the Imbrium basin. (3) Part of the target material of the Imbrium impact consisted of mare basalt. (4) Ages of basalt clasts in the Fra Mauro breccia deposits constrain the age of the formation to 3.87 aeons or younger. (5) Ages of clast-poor impact-melt rocks in other parts of the landing-site region constrain the age of the formation to 3.82 aeons or older. (6) These results are consistent with the Apollo 15 ages (table 10.1). (7) The likely time of the Imbrium-basin impact is narrowed to 3.845 ± 0.03 aeons ago by these combined results.

IMBRIUM-BASIN SECONDARY CRATERS

Like the Hevelius Formation at Orientale, the Fra Mauro Formation grades outward from a thick and continuous coarsely textured blanket, through plains deposits, to a wide zone of secondary craters. Southeast of the Imbrium basin, the transition from plains to secondaries occurs about at Sinus Medii, 450 to 750 km from the Apenninus crest or 1,150 to 1,450 km from the basin center (figs. 10.16, 10.27, 10.28). Due south, the Fra Mauro Formation and mare materials have mostly buried the secondary craters, some of whose rims protrude around the margins of the Fra Mauro peninsula (fig. 10.19). In the north, this transition is also poorly defined because so many rugged linear chains of the Vallis Bouvard type (fig. 4.4*D*) are visible through the Fra Mauro continuous ejecta (figs. 10.6, 10.15). The transition is estimated to occur about 300 to 400 km north of Mare Frigoris or 1,000 to 1,100 km from the basin center (pl. 3). In all observed sectors, the transition occurs farther from the basin than for Orientale, as expected for a topographically larger basin.

The most striking characteristic of the zone of secondary craters is the "Imbrium sculpture" (figs. 10.15, 10.27–10.29). Most of this sculpture, once thought to be fault-controlled (see chap. 6), is now thought to consist of chains of elliptical secondary-impact craters (compare figs. 10.27, 10.29). Although some of the finer outer sculpture seems to have formed by surface flow (fig. 10.17), as in the Fra Mauro closer to the basin and in the Hevelius Formation, the origins of individual grooves and ridges cannot be determined so readily as around Orientale (Wilhelms, 1980).

Abundant secondary-impact craters appear beyond the groovelike chains at distances of about 1,700 km from the basin center (figs. 10.30, 10.31). Like the sculpture, the more nearly circular secondaries were once considered to be volcanic or primary-impact craters. One basis for this interpretation was the morphologic diversity within a given cluster (figs. 10.28, 10.29). However, individual satellitic craters of Orientale and of large craters also differ from one another (figs. 3.9, 4.4). Good photographs show that a range in morphologies from very sharp to almost obliterated results from differential burial of a coeval cluster by deposits that flowed from nearer the basin (figs. 4.4*G*, *H*; Oberbeck, 1975; Wilhelms, 1976; Wilhelms and

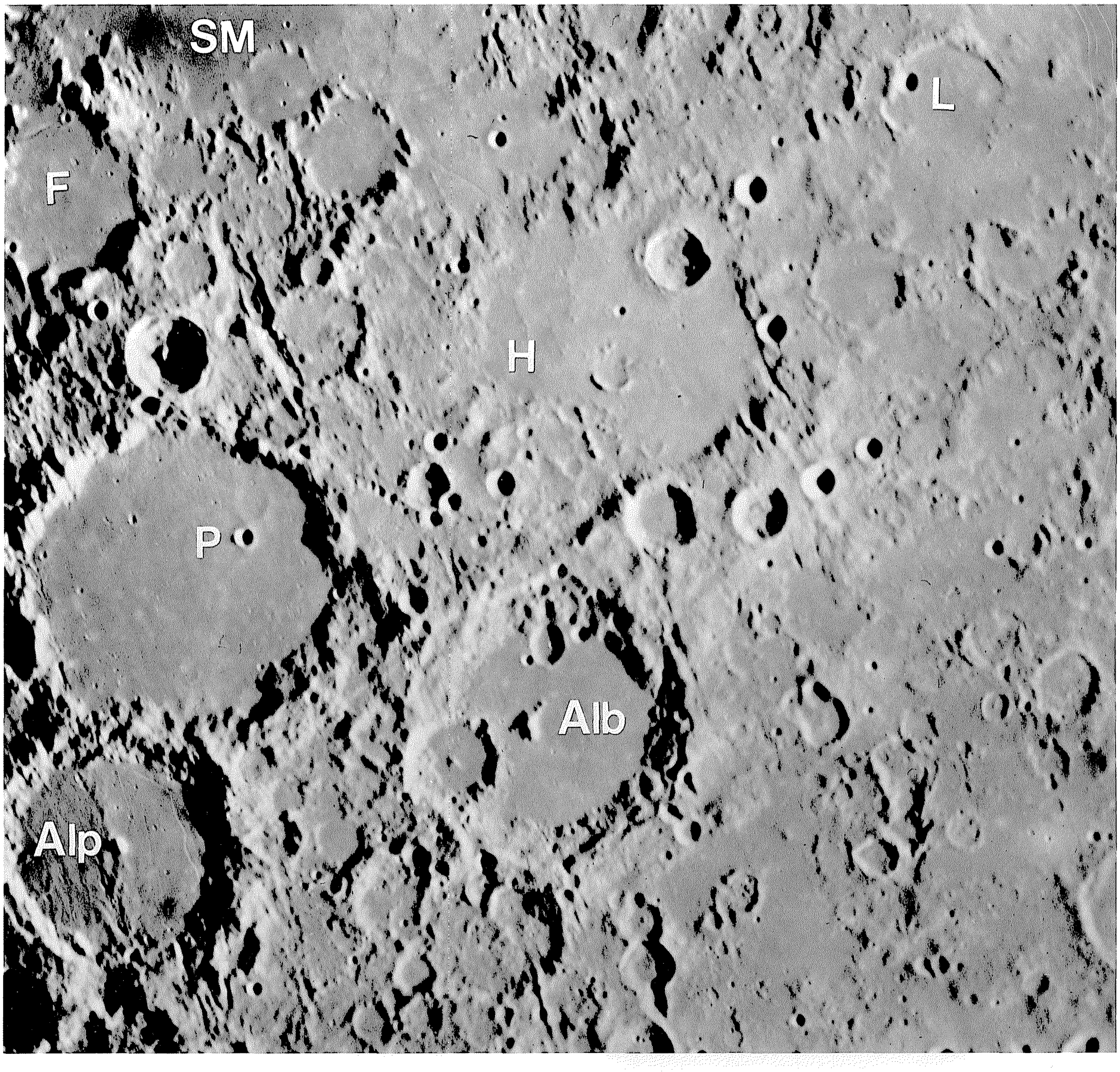

FIGURE 10.27.—Imbrium sculpture in south-central nearside highlands south of Sinus Medii (SM). Craters cut by sculpture include Lade (L; compare figs. 10.16, 10.17), Flammarion (F; 75 km), Hipparchus (H; 151 km), Ptolemaeus (P; 153 km), Albategnius (Alb; 136 km, compare figs. 10.29, 10.36), and Alphonsus (Alp; 119 km). Planar fill apparently transects sculpture. Subcircular secondary craters of Imbrium are visible below latitude of Ptolemaeus. Catalina Observatory photograph No. 1907.

others, 1978, p. 3749). The septa between craters and "domes" superposed on their intersections (figs. 3.9*B*, 4.4*C*, 10.29–10.31), which were once cited as evidence of volcanism, resemble forms created in similar positions by the interaction of ejecta in laboratory experiments (fig. 3.7). Only the gross form of the domes and intercrater ridges is observed in most of the Imbrium-secondary field. Study of Orientale analogs and the laboratory experiments were required before the secondary-impact origin of these domes and ridges could be supported.

An Imbrium-basin origin of furrows or pits outside the main concentration of secondaries (figs. 10.32, 10.33) is also likely. A large tract west of Mare Humorum (fig. 9.24*A*), which contains more rugged, hilly topographic elements than most terrain at the same distance from Imbrium (2,000 km from the basin center), was interpreted as Humorum-basin ejecta (Titley, 1967) (part of the Vitello Formation) or as volcanic (McCauley, 1973; Wilshire, 1973). Secondary-impact origin emerged as a reasonable alternative during mapping of the whole circum-Imbrium zone. This tract is well within the reach of Imbrium ejecta projectiles and contains numerous soft-appearing, north-northeast-trending Imbrium-radial gougelike depressions as long as 30 km. It also adjoins, and is faintly gradational with, pitted terrain related to Orientale (fig. 4.4*H*). The tract is likely to be a composite unit consisting of Humorum ejecta scoured by Imbrium-basin secondaries and then mantled by thin Orientale ejecta; it is included in the Imbrium-related zone on plates 3 and 8. A somewhat similar terrane, previously thought to be volcanic (Wilhelms, 1972a; Olson and Wilhelms, 1974), is superposed on the south Crisium-basin rim flank, including the vicinity of the Luna 20 landing site (figs. 10.33, 11.16). Imbrium-secondary origin is suggested by radiality of the bands of pits and furrows.

Imbrium-basin effects persist farther outward. The first clustered craters that were identified as secondary to the basin (Scott, 1972b) occur near the craters Riccius and Maurolycus, 1,900 km from Montes Apenninus or 2,600 km from the basin center (fig. 3.10*D*). Scattered secondary craters of Imbrium occur beyond 3,000 km from the basin center and, possibly, in all parts of the lunar terrae. Probable secondaries have been identified at least 3,300 km from the center

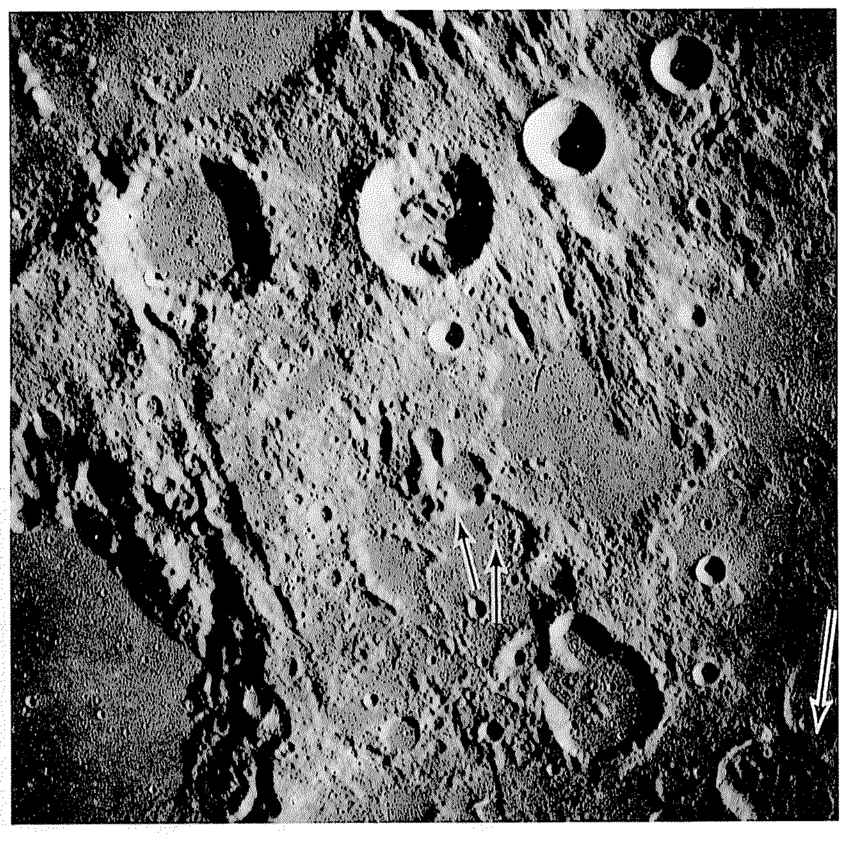

FIGURE 10.29.—Terrain east of crater Albategnius (truncated by left edge of photograph; compare figs. 10.27, 10.28). Imbrium sculpture is generally linear but consists of elliptical craters. Domelike intersections of craters and other small hills (arrows) were created by multiple secondary impacts (see chap. 3; compare fig. 3.9*B*), not volcanism. Apollo 16 frame M–392.

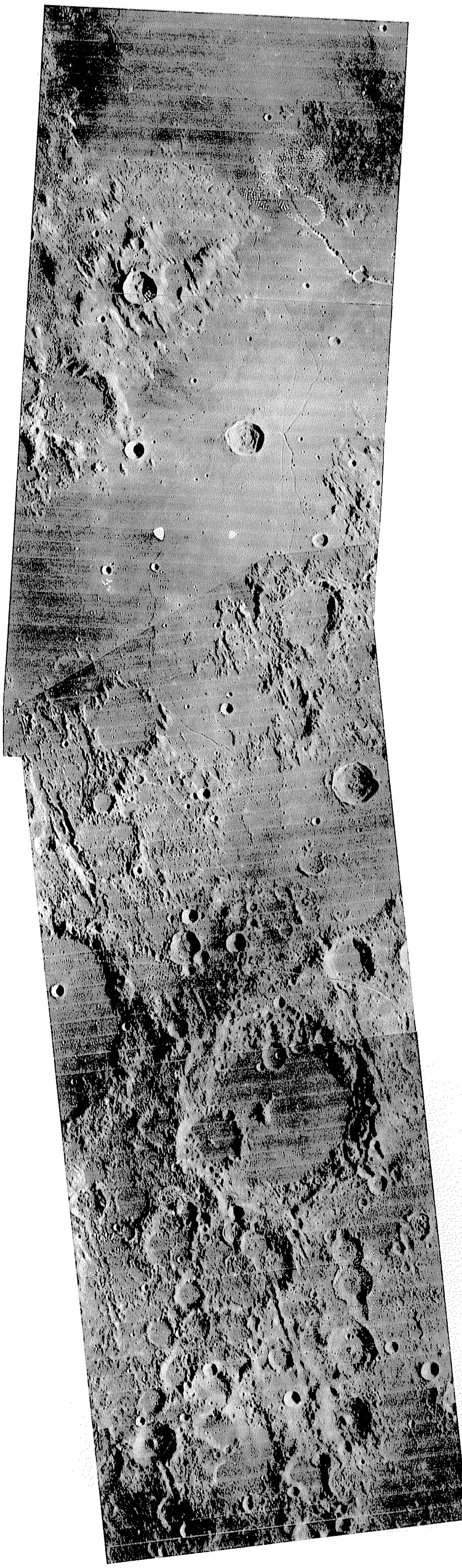

FIGURE 10.28.—Strip from Mare Vaporum (top) southward to lat 23.5 S., showing transition from smooth, continuous Fra Mauro deposits (compare fig. 10.16) to highly diverse secondary craters below latitude of Ptolemaeus and Albategnius (compare figs. 10.27, 10.36). Mosaic of Orbiter 4 frames H–101 (bottom) and H–102 (top); overlaps figures 7.7 and 10.16.

on the southeast nearside (fig. 9.2; Stuart-Alexander, 1971; Wilhelms and others, 1978, 1979). Linear chains on the farside are so closely radial to the basin as to indicate Imbrium origin (fig. 8.13; Wilhelms and El-Baz, 1977).

Finally, peculiar grooves at the antipode of Imbrium on the farside (figs. 10.32, 10.33; Stuart-Alexander, 1978) have been ascribed to convergence of Imbrium-basin ejecta (Moore and others, 1974) or to convergence of seismic waves from the Imbrium impact shock (Schultz and Gault, 1975a, b). Similar terrain north of Mare Marginis antipodal to Orientale was noted in chapter 4 (fig. 4.7). All grooved terrain may, in fact, be related to basins (fig. 10.33). The Serenitatis and Crisium antipodes are similarly grooved (fig. 9.21*A*; Hood and others, 1979). Strangely, all four of these antipodal grooved regions are also characterized by anomalous concentrations of bright swirls and by high remanent magnetism as observed from orbit (Hood and others, 1979). The cause-and-effect relations of these peculiar coincidences of old topography (the grooves), very young features superposed on maria and lacking intrinsic relief (the swirls), and magnetism have yet to be determined. Hood and others (1979) tentatively suggested that the basin impact magnetized the antipodal terrain, either by secondary impact or seismicity, so as to deflect the solar wind during the rest of geologic time and permit the maintenance of high albedo in the otherwise-fragile swirls.

LIGHT-PLAINS MATERIALS

Around both the Orientale and Imbrium basins, light-colored plains are concentrated in the transition zones between the continuous deposits and the secondary craters (figs. 4.4, 10.34, 10.35). The clearly visible Orientale relations and the fact that the samples of presumably typical plains material returned by Apollo 16 were emplaced by impact have combined to shift interpretations from a volcanic to an impact origin for terra plains in general (see chaps. 2, 4). The superposition of plains on the "Imbrium sculpture" (figs. 10.27, 10.35, 10.36), which was once considered prime evidence for a volcanic origin (Howard and Masursky, 1968; Milton, 1968a; Wilhelms, 1968, 1970b), has been shown to be consistent with impact emplacement on the basis of similar relations at Orientale. Plains occupying depressions thousands of kilometers from Imbrium may also be of impact and not volcanic origin because they generally occur downrange from secondary-crater clusters (fig. 4.6). Although the appearance and crater densities of many plains remain equally consistent with volcanic and impact origins (Neukum and others, 1975a; Neukum, 1977), and although volcanic substrates may underlie the surficial ejecta in some plains (chap. 9; Eggleton and Marshall, 1962; Schultz and Spudis, 1979), impacts evidently formed most of the visible plains.

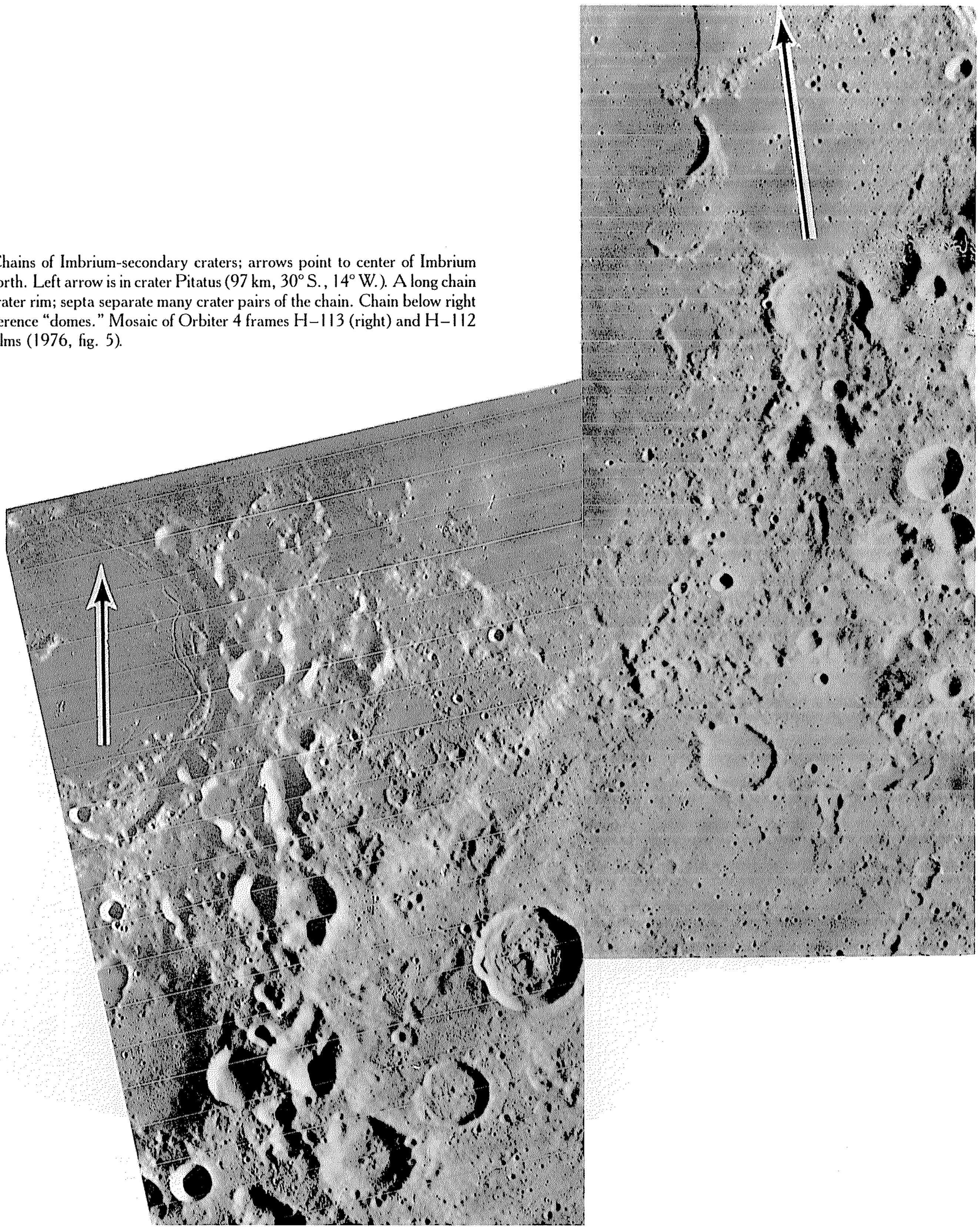

FIGURE 10.30.—Chains of Imbrium-secondary craters; arrows point to center of Imbrium basin, 2,000 km north. Left arrow is in crater Pitatus (97 km, 30° S., 14° W.). A long chain is superposed on crater rim; septa separate many crater pairs of the chain. Chain below right arrow shows interference "domes." Mosaic of Orbiter 4 frames H–113 (right) and H–112 (left). From Wilhelms (1976, fig. 5).

More patches of well-defined plains are Early Imbrian than of any other single age. Burial of the Apennine Bench Formation inside the Imbrium-basin rim by the deposits of the craters Archimedes and Cassini suggests an Early Imbrian age for this plains unit, and the radiometric dates point to an earliest Early Imbrian age. An earliest Early Imbrian age is suggested for the plains north of Mare Frigoris (fig. 10.15) by textural gradation with the Fra Mauro Formation, crater size-frequency values (figs. 7.15, 10.37), and visual inspection of crater densities. The partly planar Maunder Formation inside the Orientale basin almost certainly consists of impact melt contemporaneous with that basin (see chap. 4) and thus is latest Early Imbrian.

D_L values of 1,000 to 1,200 m have been identified with the plains north of Frigoris and, therefore, with the Imbrium basin (fig. 7.15; Boyce and others, 1974; Moore and others, 1980b). Similar values, however, have also been obtained for other plains (Boyce and others, 1974) that are clearly older than the basin (figs. 7.15, 8.11, 9.26, 9.28; Neukum, 1977; Wilhelms and El-Baz, 1977; Stuart-Alexander, 1978; Lucchitta, 1978). The inability of D_L values to discriminate among old deposits (fig. 7.15) may be due to several factors: (1) Such material properties as low cohesion of thick regoliths, and (2) the large sizes of superposed craters obviously present (fig. 9.26). For these large craters, (a) the production function may be less than the -2 cumulative assumed in D_L models (Soderblom, 1970; Soderblom and Lebofsky, 1972), and (b) initial crater shapes and wall slopes may differ from those of the small craters measured during D_L determinations. Stratigraphic relations and size-frequency counts are preferred here to D_L measurements as indicators of terra-plains age.

The relative age of the Cayley Formation is important to interpretations of the returned materials. On Lunar Orbiter 4 photographs, the Cayley generally seems to have flatter surfaces and fewer, sharper craters than the earliest Early Imbrian plains north of Mare Frigoris that are clearly contemporaneous with the Imbrium basin. (The Cayley seems to be less planar at higher resolution [fig. 10.38] and on the surface as seen by the astronauts.) D_L values of 475 to 640 m (fig. 7.15; Soderblom and Boyce, 1972; Boyce and others, 1974), some crater-density studies (fig. 10.37; Boyce and others, 1974; Neukum and others, 1975b), and visual inspection also suggest a clear temporal hiatus between the plains north of Mare Frigoris and the latest Early Imbrian plains at Orientale. The Cayley and circum-Orientale plains look alike on Lunar Orbiter 4 photographs. Some crater counts and D_L measurements also show them to be contemporaneous with each other and with the Hevelius and Maunder Formations (Soderblom and Boyce, 1972; Boyce and others, 1974). Therefore, an Orientale age has been suggested for the Cayley plains in the central nearside. Suggested mechanisms for creating Orientale-age surfaces on plains that are spatially related to Imbrium include mantling of older, Imbrium-basin-age (and Nectarian) plains by far-thrown Orientale ejecta (Hodges and others, 1973; Chao and others, 1975) and degradation induced by seismic waves from the Orientale impact (Schultz and Gault, 1975a). Either mechanism could theoretically have rejuvenated the cratered surface on the older material.

A dissenting view, based on different evaluations of the same data, is that the Cayley Formation is contemporaneous with the Imbrium basin. Other crater counts (fig. 10.37; Neukum and others, 1975a, b; Neukum, 1977), the inability of D_L determinations to date old plains, the plains' concentration around Imbrium, and the improbability that Orientale ejecta was sufficiently thick to cover all Cayley patches lead me to support this interpretation.

CAYLEY AND DESCARTES FORMATIONS

Introduction

The problem of determining whether the materials composing a geologic unit of impact origin were formed before or during the unit's emplacement is especially acute for the two units sampled by Apollo 16. Chapter 9 showed that the distribution and absolute ages of many Apollo 16 samples, particularly those from the Descartes Formation, are consistent with a Nectaris-basin origin. The overall mountainous topography of the Descartes could also be an expression of the Nectaris ejecta. As discussed in the previous section, however, the distribution and planar morphology of the Cayley Formation originated in the Imbrian Period. The paucity of overlying primary-impact craters and the topographic sharpness of the furrows (fig. 9.9) suggest that at least the surficial part of the Descartes Formation is also of Imbrian age. Because few lunar terra surfaces are shaped without addition of material, the presence of some Imbrian material in the Descartes is expected.

This section discusses the events in the units' histories that might have taken place during the Imbrian Period. Three possible ramifications of an Imbrium-basin origin are explored first: that the

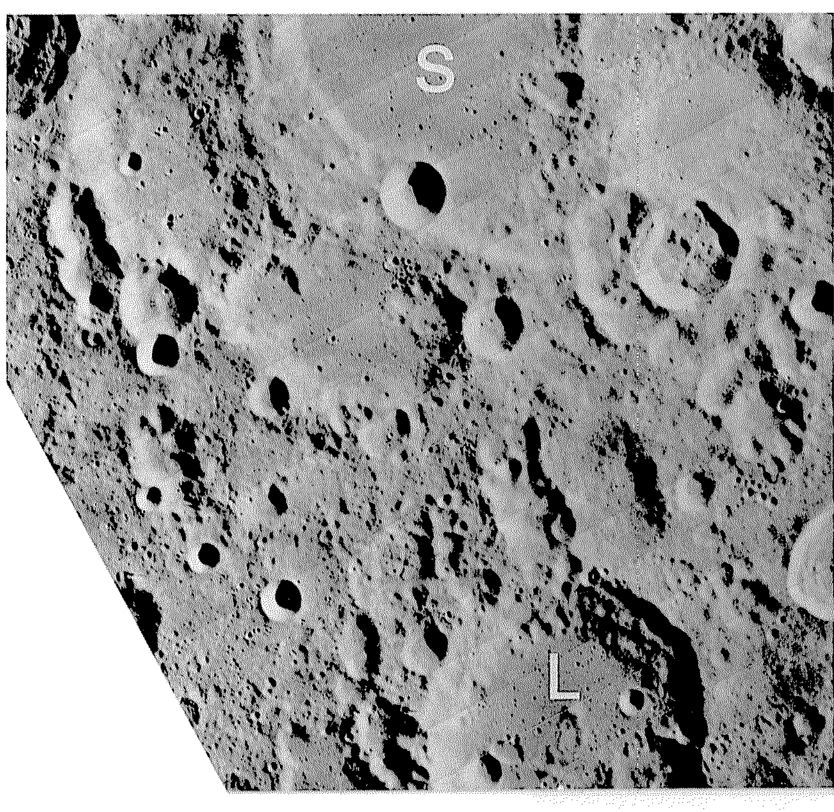

FIGURE 10.31.—Short chains of Imbrium secondary craters near craters Stöfler (S; 126 km) and Licetus (L; 75 km, 47° S., 7° E.), 2,600 km from center of Imbrium basin. Orbiter 4 frame H–107.

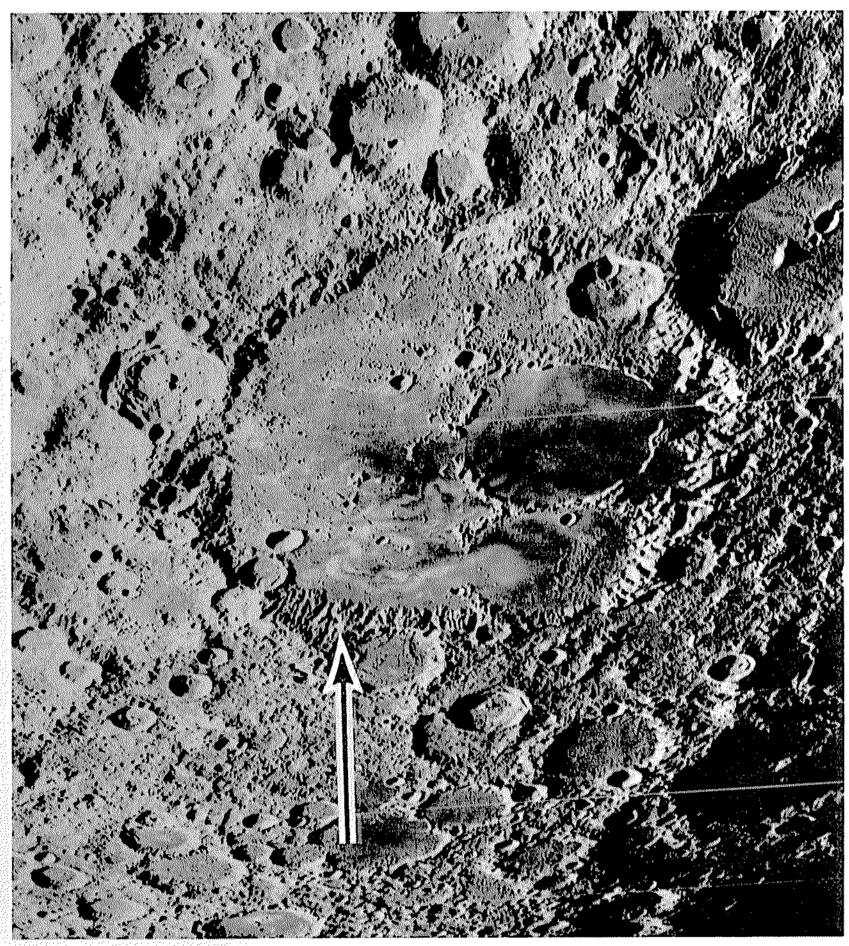

FIGURE 10.32.—Approximate antipode of Imbrium basin (arrow; 38° S., 160° E.). Grooves score rims of old craters in vicinity of antipode (Stuart-Alexander, 1978). Bright swirls above arrow are in Mare Ingenii. Figure-8 crater at right edge is Van de Graaff (234 km long, probably Nectarian). Orbiter 2 frame M–75.

units consist (1) mostly of Imbrium-basin ejecta, (2) mostly of Nectaris-basin ejecta reworked during the Imbrian Period, or (3) of basin ejecta of different provenance (fig. 10.39). Then follows a consideration of "local" origins as (1) reworked pre-Imbrian crater materials or (2) post-Imbrian materials—origins that I consider subordinate in importance to a basin origin at the Apollo 16 landing site.

Imbrium-basin origin

Spatial distribution, relative age, and comparison with the Orientale-basin geology, as already discussed, suggest that the agent which created the planar surface of the Cayley Formation was the Imbrium impact. Similarly, the furrows of the Descartes Formation

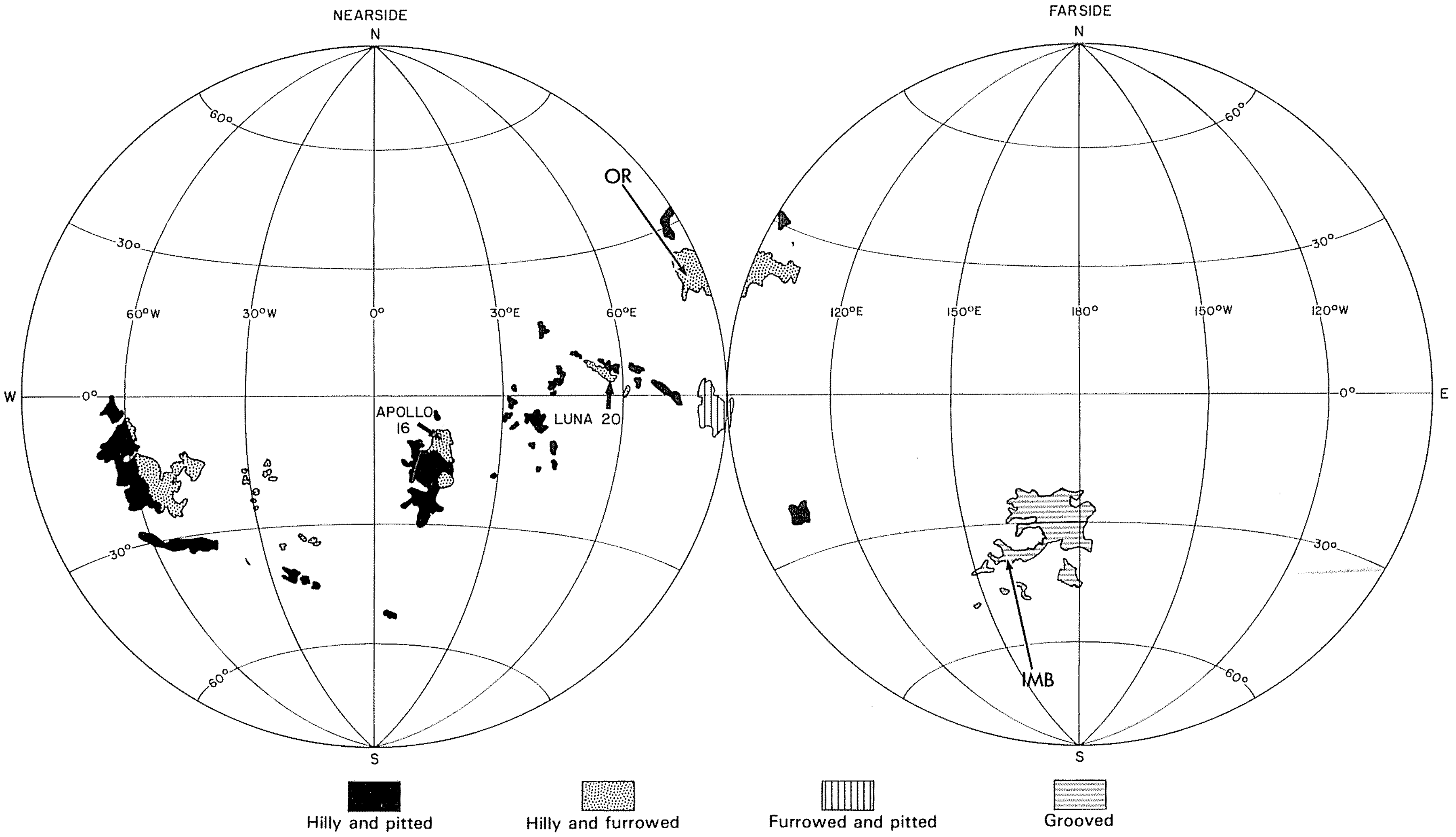

FIGURE 10.33.—Four types of lunar terrain with small negative features (after Howard and others, 1974, fig. 13). Original caption states that terrains are not clearly related to basins, but text offers basin-related, nonvolcanic interpretations. Antipodal effects may explain patches IMB (Imbrium) and OR (Orientale) (compare figures 4.7 and 10.32). Pitted and furrowed deposit at long 90° E. (in Smythii basin) may be related to Crisium basin.

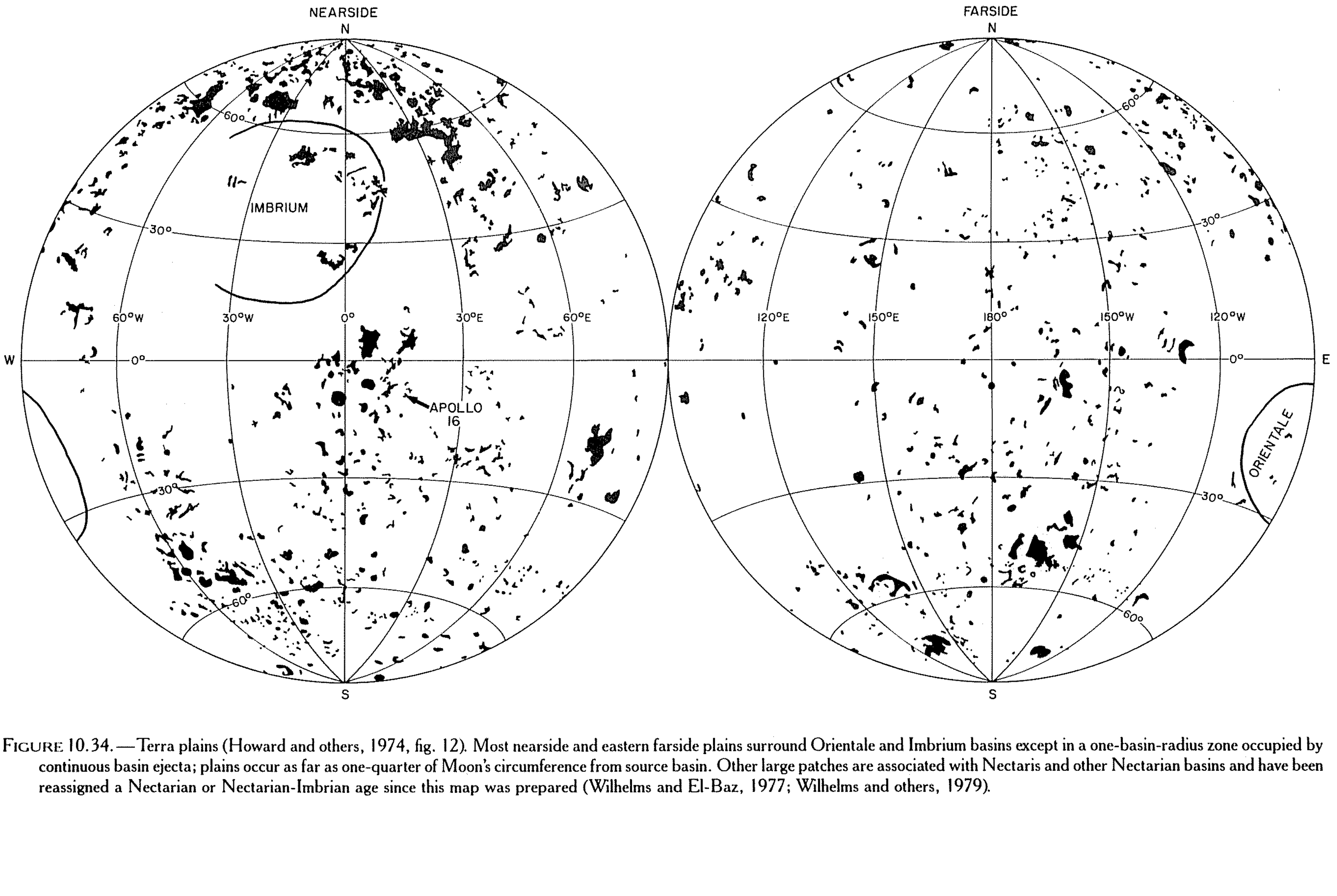

FIGURE 10.34.—Terra plains (Howard and others, 1974, fig. 12). Most nearside and eastern farside plains surround Orientale and Imbrium basins except in a one-basin-radius zone occupied by continuous basin ejecta; plains occur as far as one-quarter of Moon's circumference from source basin. Other large patches are associated with Nectaris and other Nectarian basins and have been reassigned a Nectarian or Nectarian-Imbrian age since this map was prepared (Wilhelms and El-Baz, 1977; Wilhelms and others, 1979).

seem to be somehow related to the Imbrium basin (Eggleton and Marshall, 1962); the grooves of the northern (Smoky Mountain) facies of the Descartes are closely radial to Imbrium.

These relations do not specify whether primary- or secondary-impact mechanisms were more important in the units' emplacement. Whereas gradation with the Hevelius Formation indicates that some of the Cayley-like Orientale plains deposits consist of pooled primary basin ejecta that segregated from the Hevelius (fig. 4.4*D*; Eggleton and Schaber, 1972), similar plains are distal to Orientale-secondary craters (fig. 4.4*G*). The Descartes Formation, though exceptionally conspicuous, is similar in general morphology to other circum-Imbrium hilly-and-furrowed units already interpreted as part of the secondary-crater retinue of the Imbrium basin (fig. 10.33). Many grooves and scarps of the southern (Stone Mountain) facies, however, are transverse to the Imbrium-radial direction (fig. 9.9) and are less like secondary craters than like the dunelike deposits of Orientale that originated by surface flow of basin ejecta (figs. 4.4*F–H*). Therefore, the major issue being debated, as was the case with the Apollo 14 materials, is the proportion of Imbrium ejecta to "local" material excavated by the Imbrium secondaries.

Diversion by the Kant Plateau of material flowing from Imbrium has been suggested as the cause of the transverse trend of the Stone Mountain facies (Hodges, 1972; Hodges and others, 1973; Moore and others, 1974; Hodges and Muehlberger, 1981). Hodges and Muehlberger proposed that a long trough radial to Imbrium (fig. 10.35) facilitated the flow. Flow elsewhere in the region is indicated by a thick deposit, evidently from Imbrium, in the crater Anděl M west of the Apollo 16 landing site (Moore and others, 1974). The Apollo 16 landing site and many plains-dunes associations around Orientale lie two-thirds of a basin diameter from the rims of their respective basins.

Most investigators, however, doubt that much primary ejecta could have reached the Apollo 16 landing site all the way from the Imbrium rim (Montes Apenninus) by surface flow. This viewpoint is supported by the abundant evidence for Imbrium secondaries in the region. Many pits and deeply etched grooves that seem clearly to be secondary to Imbrium are adjacent to the two sampled units (fig. 10.35). Clustering of a group of craters on the Kant Plateau immediately east of the landing site suggests an origin as Imbrium secondaries. Alignment of the nearly equant pair Dollond B and Dollond C northwest of the landing site is also typical of secondary fields, and these 32- to 37-km-diameter craters are similar in size to Imbrium secondaries in other regions. Any Imbrium material at the site may, therefore, have arrived in impacting Imbrium projectiles (Wilhelms, 1972c) or in a debris flow initiated by secondary impacts of the projectiles (Morrison and Oberbeck, 1975; Oberbeck, 1975; Oberbeck and others, 1975).

As for the Apollo 14 landing-site region, an intermediate view is more likely than an all-primary or all-secondary origin. A flow initiated by secondary impacts would contain mixed primary and secondary ejecta of Imbrium and could create the same morphologies and regional relations as a flow of purely primary material. Morrison and Oberbeck (1975) calculated that a deposit dislodged at the Apollo 16 landing site by Imbrium projectiles would contain only 13 to 18 percent of Imbrium-primary ejecta. At the landing site itself, however, whatever secondaries were formed are buried by the Cayley and Descartes deposits. Therefore, these deposits either are primary (like those at the Apollo 14 site) or originated from secondary craters northwest of the Apollo 16 site. Much more Imbrium material than 13 to 18 percent would be present if the deposit originated to the northwest (fig. 10.26).

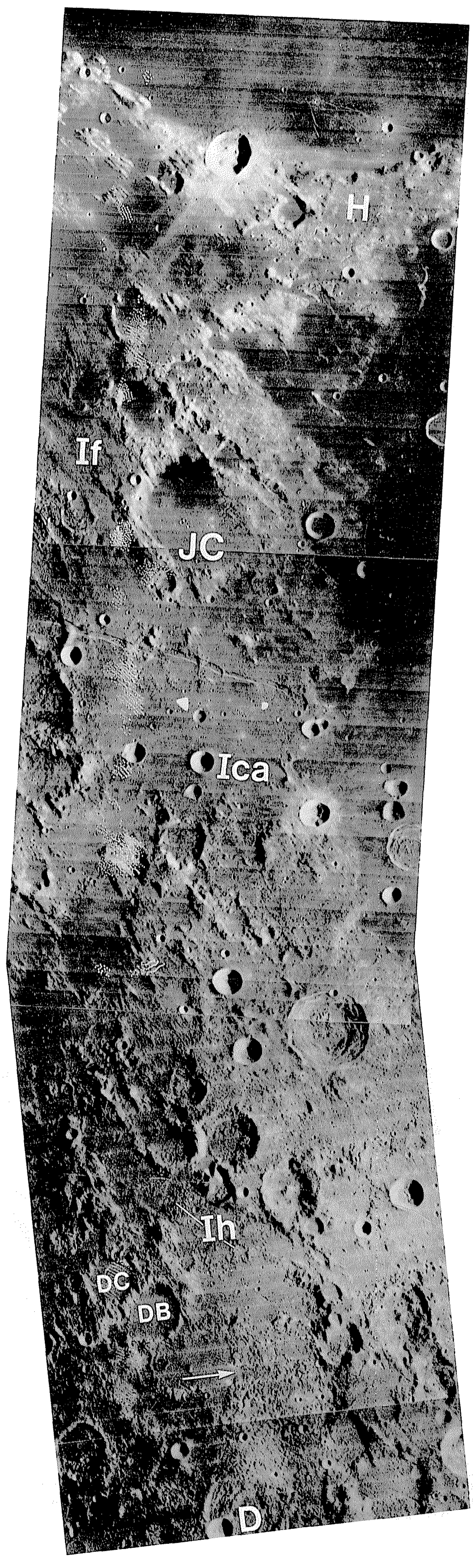

FIGURE 10.35.—Strip of eastern nearside terra, 900 km long, from Montes Haemus (H) to crater Descartes (D; 48 km, 12° S., 16° E.). Montes Haemus is 1,000 km from center of Imbrium basin, and Descartes 1,800 km. North half of photographed area is distinctly inundated by Imbrium-basin deposits (If, Fra Mauro Formation); formation has accumulated against southeast wall of Julius Caesar (JC). The Cayley Formation in its type area (Ica; compare fig. 10.38) is apparently gradational with the Fra Mauro Formation; other patches, as at Apollo 16 landing site (arrow), seem more isolated, yet are situated near Imbrium-radial lineations, as at Dollond B (DB; 37 km) and Dollond C (DC; 32 km). Hilly and furrowed material of the Descartes Mountains (around and south of Apollo 16 landing site to bottom of photograph), though also seemingly isolated, forms part of Imbrium-radial system north of Apollo 16 site and is similar to hilly material farther north (Ih). Mosaic of Orbiter 4 frames H–89 (below) and H–90 (above).

Any of the debris-flow mechanisms could emplace the Cayley and the Descartes Formations either simultaneously or sequentially (fig. 10.39). Simultaneous emplacement (fig. 10.39*A*) seems to be consistent with the Orientale relations because the Orientale plains and dunelike deposits appear to be gradational (figs. 4.4*F–H*). If simultaneously emplaced, the differing morphologies might arise either because (1) a higher melt content (chap. 9) caused the Cayley deposits to pool in depressions (Hodges and Muehlberger, 1981; Ulrich and Reed, 1981) or because (2) the Descartes material, but not the Cayley material, reached and was crumpled into dunelike topography by the Kant Plateau. Alternatively, an embankment of ejecta may have been emplaced by the Nectaris basin, followed at the beginning of the Imbrian Period by secondary impacts forming the Descartes furrows and a debris flow forming the Cayley (fig. 10.39*B*). The measured absolute ages and the apparent lithologic differences between the Cayley and the Descartes (see chap. 9; table 9.1) are consistent with this sequence.

Among the absolute ages of the sampled impact-melt fragments are some that are distinctly younger than the 3.92 ± 0.03-aeon age tentatively identified here with the Nectaris impact (table 9.1). A few of these ages might indicate an Imbrium-basin origin of materials in the units or, at least, in the melt-rich Cayley. Although the methodologic problems are severe (see chap. 9), these ages are at least consistent with an Imbrian age of the younger impact-melt rocks.

"Local" origin

In the Imbrium debris-flow models, strata of the Cayley and Descartes Formations would possess considerable lateral continuity, though also considerable lithologic diversity. In "local origin" models, in contrast, the units formed piecemeal and were derived from various relatively small deposits quite diverse in lithology, absolute age, and composition. Sample diversity is commonly cited as requiring such diverse "local" sources.

Local origin of the Cayley and of plains in general is commonly envisioned as dislodgement of debris from crater walls and redeposition in adjacent depressions (Morrison and Oberbeck, 1975; Oberbeck and others, 1974, 1975, 1977; Oberbeck, 1975; Oberbeck and Morrison, 1976). An early suggestion of this type was that the plains consist of accumulated secondary ejecta of craters (Oberbeck and others, 1974). The concentration of plains around Imbrium in many additional localities indicates, however, that if secondary impacts emplaced the Cayley, they were from Imbrium.

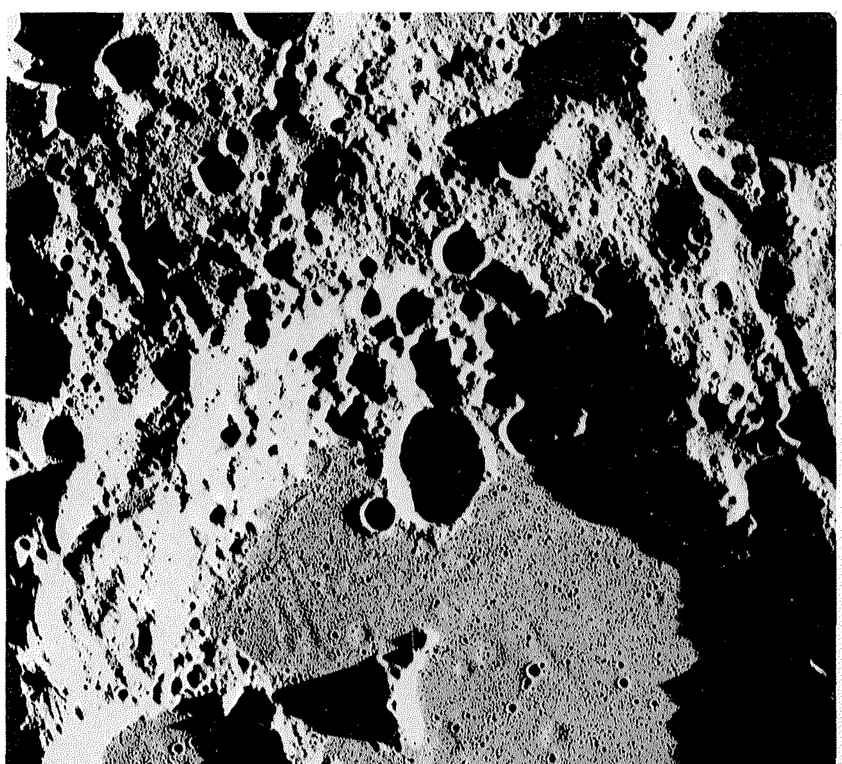

FIGURE 10.36.—Plains materials superposed on Imbrium-secondary craters, probably consisting of debris dislodged and ejected by secondary impacts (Oberbeck and others, 1974) superposed on north (near-Imbrium) wall of crater Albategnius (136 km). Visibility of secondary chains buried by plains on floor is enhanced by Sun elevation, only 5° above horizontal (from right). Neukum (1977) suggested that plains postdate Imbrium and Orientale basins and are volcanic. Apollo 16 frame M–449.

One of the most widely favored hypotheses has been that the deposits originated as material of pre-Imbrian "local" craters (Head, 1974d; Oberbeck and others, 1974, 1975). Head (1974d) suggested that an "unnamed crater B" dominates the landing site's geology and petrology (fig. 10.40). The Cayley is supposed to consist of melt rock from the fallback on this crater's floor, and melt-poor rocks are supposed to have come from the less highly shocked rim materials of unnamed crater B and other old craters. Head (1974d) thought that unnamed crater B transects the Stone Mountain facies (of Nectaris-basin origin) and is transected by the Smoky Mountain facies. Unnamed crater B, however, is a vague circular feature or coalescence of subcircular features that lacks the continuity, terraces, and other hallmarks of a crater young enough to affect the surface geology; it interrupts no furrows. If it exists at all, it is too deeply buried by both Descartes facies and the Cayley to have furnished much material to the bedrock-breccia deposits of either unit. Furthermore, no other craters older than the Cayley and the Descartes Formations are sufficiently near to have furnished much material to either bedrock deposit (pls. 6, 7). If "local" material constitutes these formations, it is Nectaris-basin primary ejecta.

Although a "local" origin in the sense generally meant seems to be refuted by the photogeologic relations, several processes that might be defined as local probably did contribute to the observed diversity of the samples. First, secondary impacts of Imbrium ejecta dislodged material, mostly Nectaris-basin primary ejecta but possibly including some crater material, that lay northwest of the landing site. Second, the reworked Nectaris-basin ejecta itself consists of materials that were derived from diverse small-scale deposits of craters and, possibly, of volcanic flows that were in the Nectaris target area before the Nectaris impact. Any later impact would have incorporated, shocked, melted, and reworked such earlier impact and volcanic materials. Most of the chemical, chronologic, and lithologic diversity of the Apollo 16 samples probably results from this pre-Nectarian diversity, which is a feature of all impact deposits.

The preceding discussion pertains to the bedrock deposits. All hypotheses acknowledge that several local processes contributed to

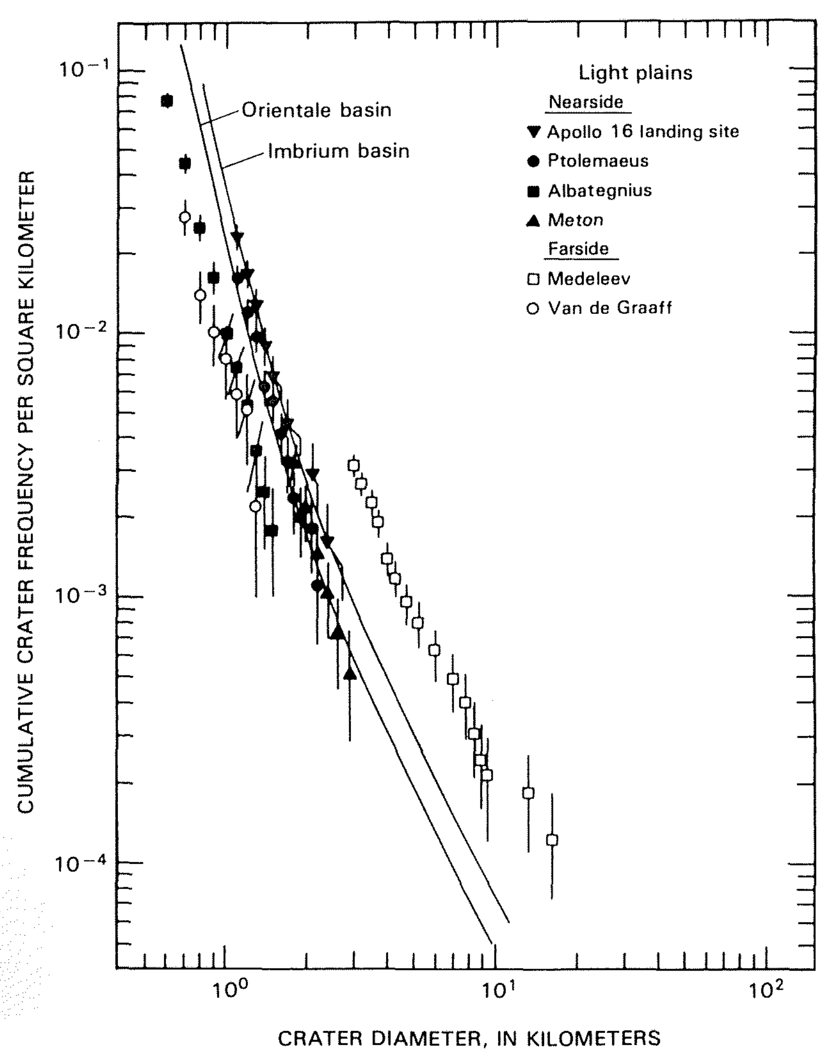

FIGURE 10.37.—Size-frequency distributions of craters superposed on terra plains of several ages (Neukum and others, 1975b; compare fig. 11.2). Curves represent, from oldest to youngest: plains in Mendeleev (compare fig. 9.29); Imbrium basin and plains at Apollo 16 landing site, indistinguishable; plains in Ptolemaeus; Orientale basin, similar to Ptolemaeus plains; plains in Albategnius, considerably younger than Orientale basin; and mare materials in Van de Graaff.

the diversity of the overlying relatively thin regolith at the landing site:

1. Large craters probably pierced the Cayley Formation and introduced some of the underlying material into the regolith. Seismic data indicate that the Cayley is about 200 m thick (Hodges and others, 1973; Cooper and others, 1974). Impacts on the order of North Ray Crater in size (1 km) could penetrate this thickness. Many subdued craters of this size are visible and probably "contaminated" the regolith during the Imbrian Period (fig. 9.9). The introduced material probably was mostly Nectaris ejecta but may also have included some crater materials.
2. The regolith developed on each formation contains some fragments derived from the other formation by post-Imbrium impacts. Origin as Orientale-basin ejecta seemed to be supported by three post-Imbrium Ar-Ar ages (table 9.1) and a precise Rb-Sr age of 3.76 ± 0.01 aeons (Papanastassiou and Wasserburg, 1972b) for Cayley sample 68415 (Chao and others, 1975). An alternative origin more in keeping with the regional relations is that this rock (samples 68415, 68416) was derived from impact melt of an Imbrian crater that formed nearby a few tens of millions of years after the Cayley and Descartes Formations. This origin is supported by the fact that its composition is similar to that of the station 11 regolith, which accumulated on the Descartes Formation (P.D. Spudis, oral commun., 1983).
3. Like all lunar regoliths, the Apollo 16 regolith undoubtedly contains some material derived by small post-Imbrium impacts from other nearby units. For example, fragments of mare basalt were probably introduced into Theophilus ejecta (see chap. 11; Delano, 1975).

Conclusions

1. The relation of surface morphologies to the Imbrium basin suggests that the Cayley Formation and at least part of the Descartes Formation are also genetically related to that basin (fig. 10.39).
2. I favor origin of the Cayley by some sort of Imbrium debris-flow emplacement, and origin of the Descartes by modification of Nectaris-basin deposits by the same debris flow or by Imbrium-secondary impacts (fig. 10.39).
3. Secondary impacts are more likely to have contributed to the deposits than at the Apollo 14 landing site because secondary craters are more evident and primary-ejecta features less evident than at that site. However, I consider neither the relative role of primary and secondary ejecta of the Imbrium basin nor the origin of the overall mountainous topography of the Descartes Formation to be established.
4. The absolute ages of certain samples support a Nectaris-basin origin for much of the Descartes material, and other absolute ages suggest addition of some Imbrium material (table 9.1). However, the relative amounts of Imbrium and Nectaris ejecta in the Descartes and Cayley Formations are unknown.
5. Pre-Imbrian "local" craters contributed little material to the site except as parts of the Nectaris ejecta, as minor parts of the Imbrium debris flow, and as regolith fragments.
6. Post-Imbrium craters melted some local materials.
7. Although this list of unsolved problems is unsatisfyingly long, at least the dominant role of basin deposits over "local" crater deposits appears to be well established.

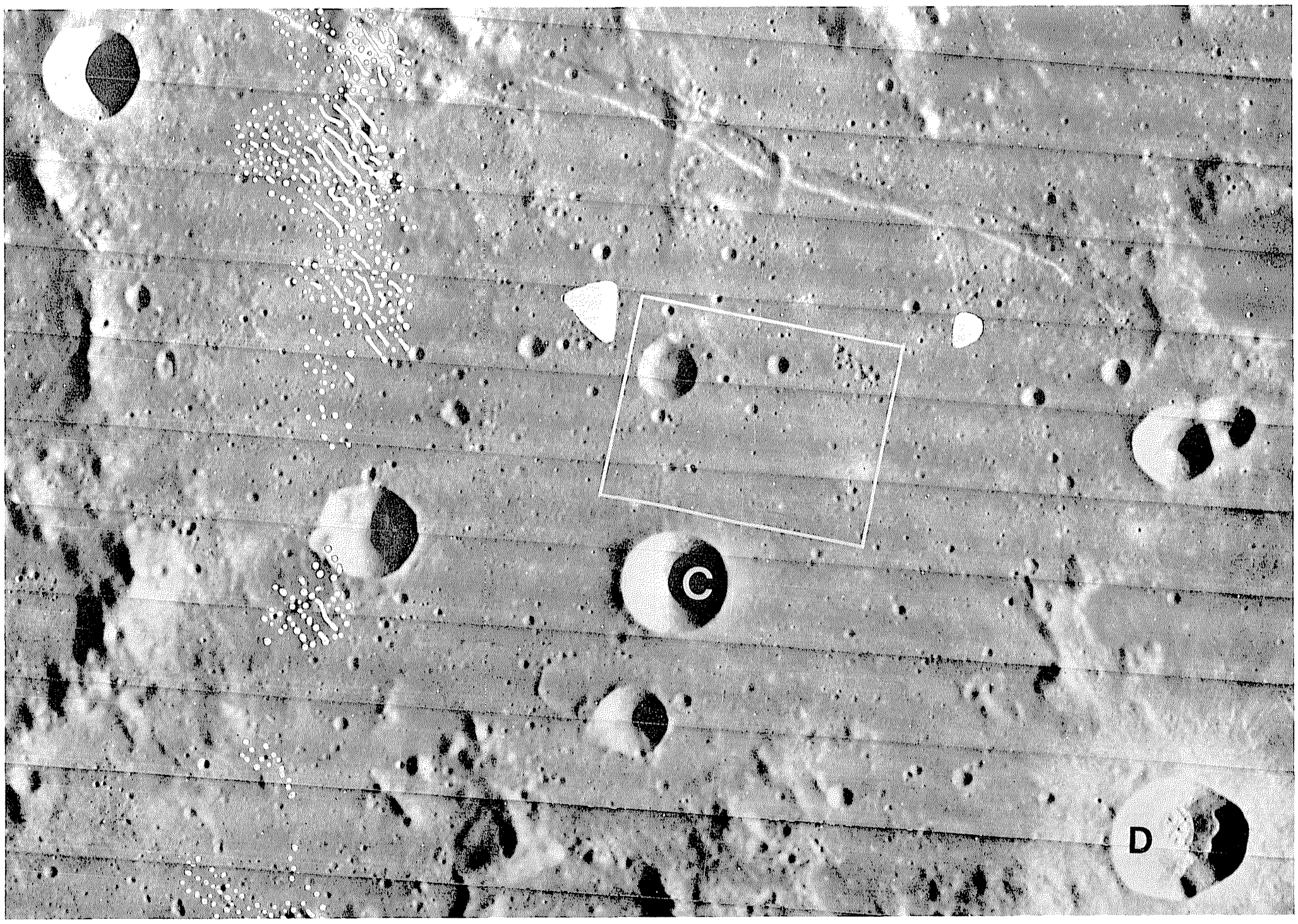

FIGURE 10.38.—Type area of the Cayley Formation (Morris and Wilhelms, 1967).

A. Regional view. Type area (3.5–4.5° N., 15.5–16.25° E.) is partly within and partly below rectangle outlining *B*. Crater Cayley (C; 14 km), moderately fresh, with lightly cratered ejecta, is probably Eratosthenian. Dionysius (D; 18 km), very fresh, is Copernican. More highly degraded and shallower craters above, below, and left of crater Cayley are probably Imbrian. Intercrater septum of pair near right edge of photograph indicates simultaneous (primary or secondary) impact (see chap. 3). Part of Rima Ariadaeus is at top (see chap. 6). Lineated, pre-Imbrian craters truncated by left edge of photograph are also truncated by right edge of figure 10.16. Orbiter 4 frame H–90.

OTHER BASIN AND CRATER MATERIALS

Recognition criteria

The units discussed heretofore in this chapter are parts of extensive deposits of the Imbrium basin, and the Orientale deposits described in chapter 4 constitute another widespread group of contemporaneous units. Like all other lunar time-stratigraphic units, the Lower Imbrian Series also contains randomly scattered primary-crater materials (table 10.2).

The regional units establish Imbrian ages of the scattered units over a large area of the Moon. Imbrian craters are sandwiched between deposits of the Imbrium basin and Upper Imbrian mare materials. Examples inside the Imbrium basin include Archimedes, Plato, the Iridum crater, and Cassini. Outlying craters, such as Lansberg, whose ejecta is superposed on Imbrium deposits but embayed by mare materials, are also Imbrian (fig. 10.41).

Furthermore, stratigraphic relations divide some craters into Lower and Upper Imbrian. Craters superposed on Imbrium deposits and overlain by Orientale deposits are Lower Imbrian (fig. 10.2). Other fresh-appearing craters buried by Orientale ejecta or secondaries are also likely to be Lower Imbrian (fig. 10.42), as are craters overlain by relatively old Upper Imbrian crater materials (fig. 10.43).

Counts of craters of the large sizes required to date pre-Nectarian and Nectarian surfaces (see chap. 7) are statistically valid for deposits of two Imbrian basins and marginally definitive for a third (fig. 10.4). I determined cumulative frequencies of 28 and 22 craters larger than 20 km in diameter per million square kilometers on Imbrium-basin and Orientale-basin deposits, respectively. The large statistical samples suggest that these are good values for the lowermost Imbrian and

TABLE 10.2.—*Possible Lower Imbrian craters*

[Cross rules divide diameter ranges mapped differently in plate 8: smaller than 30 km, unmapped; 30 to 59 km, interiors mapped; 60 km and larger, exterior deposits mapped where exposed. UI?, possibly Upper Imbrian]

Crater	Diameter (km)	Center (lat)	Center (long)	Figure	Remarks
Protagoras-----	22	56° N.	7° E.	10.15	---
Ukert----------	23	8° N.	2° E.	10.1	---
Inghirami A----	34	45° S.	65° W.	10.42	Covered by Orientale.
La Condamine---	37	53° N.	28° W.	3.8, 10.43	Covered by Iridum.
Crüger---------	46	17° S.	67° W.	4.4H, 7.8	---
Maupertuis-----	46	50° N.	27° W.	3.8, 10.43	Covered by Iridum.
Campanus-------	48	28° S.	28° W.	6.9	---
Cassini--------	57	40° N.	5° E.	1.6, 10.12	UI?
Macrobius-----	64	21° N.	46° E.	9.11	---
Lomonosov-----	93	27° N.	98° E.	1.2, 4.7, 8.13, 9.28	Typical; mare fill.
Arzachel------	97	18° S.	2° W.	1.8, 7.7	UI?
Letronne------	119	11° S.	42° W.	6.3, 12.3C	UI?, half-buried.
Compton-------	162	56° N.	105° E.	4.2B, 9.4, 9.23, 10.6	UI?, interior ring.
Keeler--------	169	10° S.	162° E.	1.4, 3.1, 8.7	---
Petavius------	177	25° S.	60° E.	4.2C, 9.5	Floor and rim faulted.

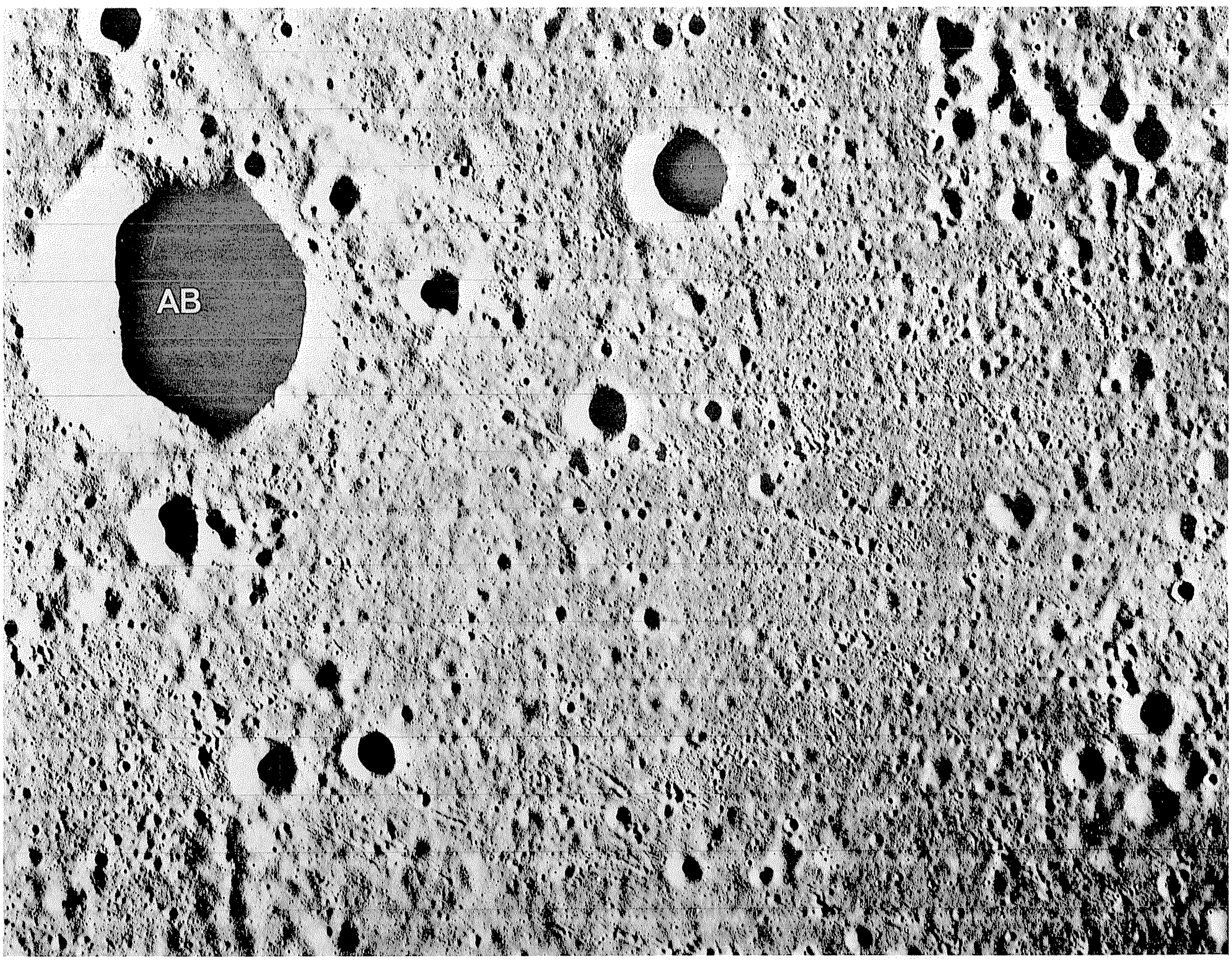

B. Area outlined in *A*. The Cayley Formation is more densely cratered than a mare surface and is saturated by small subdued craters, as expected on a Lower Imbrian surface. Many secondary clusters are also superposed—large in upper right, small and linear elsewhere (probable source, Dionysius). Relief is enhanced by low Sun illumination, 11° above horizon (from right). AB, crater Ariadaeus B (8 km), whose flat floor is visible in *A* but is obscured here; Imbrian age is confirmed by crater density similar to that on the Cayley Formation. Orbiter 2 frame M–61.

the boundary between the two Imbrian series, respectively. Sparse crater counts indicate that the Schrödinger basin is also Imbrian (fig. 10.4; density, 20 such craters). Schrödinger is the topographically freshest lunar basin of its size and thus appears to be relatively young (fig. 10.44). It had been considered Nectarian because of its moderately large density of small craters, although no definite Nectarian craters are known to be superposed (Wilhelms and others, 1979). If it is Imbrian, superposition of some probable Orientale secondaries (fig. 10.44) restricts its age to Early Imbrian.

Otherwise, counts of craters smaller than 20 km in diameter are required to date Imbrian surfaces not in contact with definite Imbrian deposits. Figure 10.4 plots the counts by Neukum and others (1975a) of craters as small as 1.4 km in diameter on Montes Apenninus, which fall on the projection of the curve determined here for craters larger than 20 km in diameter. Crater frequencies for the plains at the Apollo 16 landing site nearly coincide with those for the Apennines. The counts by Neukum and others (1975a) and myself indicate that the Orientale and Imbrium curves are approximately parallel for both small and large superposed craters.

Craters that are thought to be too fresh to be Nectarian and that are overlain by relatively old mare materials are likely to be Early Imbrian—for example, Lomonosov (fig. 9.28). Stratigraphically isolated Early Imbrian craters are difficult to distinguish from Nectarian and Late Imbrian craters, and so the compilation here (pl. 8; table 10.2) is based mostly on qualitative assessments of morphology and some sparse size-frequency counts.

The distinction between small craters of the Lower and Upper Imbrian Series is still less clear. Craters smaller than about 20 km in diameter in the terrae are hard to date by morphology (Wilhelms and others, 1978). Debris from the walls has filled Imbrian craters smaller than about 8 km in diameter more deeply than their younger counterparts, and commonly has created shallow bowl-shaped or flat-floored interiors from originally steeper more nearly conical profiles. However, detection of this distinction requires good photographic resolution and Sun illumination (figs. 10.38, 10.41). Fresh Imbrian-age primary craters may be indistinguishable from sharp Orientale- or Imbrium-basin secondary craters of similar sizes. Small flat-floored or otherwise subdued Imbrian primary craters may resemble some Nectarian primaries or partly buried secondaries of one of the Imbrian basins. Imbrian craters disappear at diameters of about 1 km on the Fra Mauro Formation (fig. 7.14; Trask, 1971).

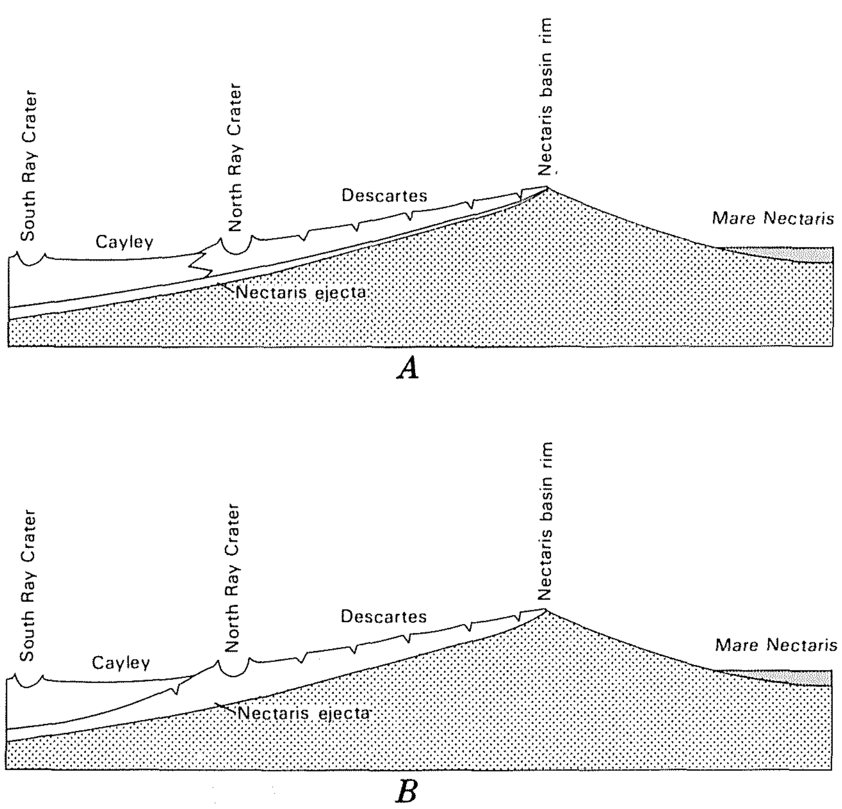

FIGURE 10.39.—Diagrammatic geologic cross sections drawn across region of Apollo 16 landing site, illustrating alternative interpretations.
A. The Descartes and Cayley Formations were both emplaced in an Imbrium debris surge.
B. The Descartes was emplaced as Nectaris ejecta and furrowed by impacts of Imbrium ejecta. The Cayley was emplaced in an Imbrium debris surge. The Cayley would consist mostly of Imbrium ejecta if the surge originated near Imbrium, and mostly of Nectaris ejecta if the surge originated nearer the Apollo 16 landing site.

Frequency

Despite the difficulties, Lower Imbrian craters are here distinguished from Nectarian and Upper Imbrian craters as well as possible and are mapped in plate 8. In a farside area of 14.2×10^6 km^2 that excludes the Orientale deposits which overlie all other materials of the series, 73 unburied craters at least 30 km in diameter are interpreted as Lower Imbrian. For this density (5.1 craters/10^6 km^2), 195 craters of this size were formed over the whole Moon.

OTHER TERRA MATERIALS

The discussions of the Orientale and Imbrium basins have offered basin-impact alternatives (Howard and others, 1974) to the volcanic origins previously considered or assumed for many terra landforms. However, volcanic origins for some terra plains (Neukum, 1977), as well as for a few isolated domelike structures, are still being entertained.

The "domes" have a volcanolike morphology in the form of summit or flank pits and unusually red spectra (fig. 10.45; Wilhelms and McCauley, 1971; McCauley, 1973; Scott and Eggleton, 1973; Malin, 1974; Head and McCord, 1978; Basaltic Volcanism Study Project, 1981, p. 762–763). The most densely concentrated are the Mairan and Gruithuisen domes near the Iridum crater, between Mare Imbrium and northern Oceanus Procellarum or Sinus Roris (Scott and Eggleton, 1973). They may represent rare differentiated volcanic materials akin to KREEP-rich material or certain still more highly

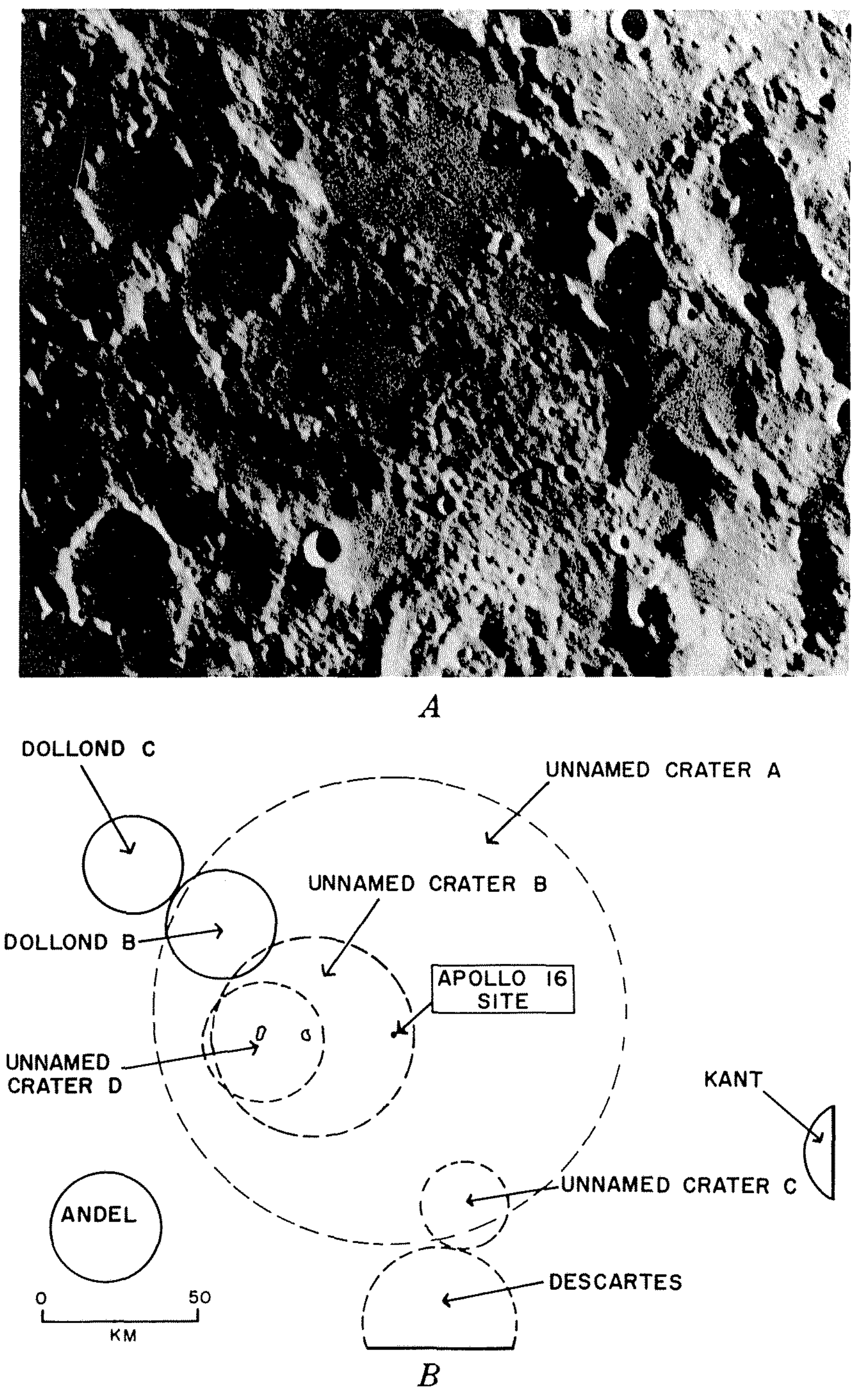

FIGURE 10.40.—Vicinity of Apollo 16 landing site.
A. Telescopic photograph.
B. "Unnamed" craters believed by Head (1974d) to constitute area of *A* and to have contributed materials to Apollo 16 samples.

differentiated "granitic" or "quartz-monzodioritic" compositions that appear in small amounts in lunar samples (Ryder and others, 1975a; Ryder, 1976). The craters atop some of these domes argue for volcanic origins (fig. 10.45*A*). Experience with other seemingly volcanic landforms, however, recommends a search for impact origins. Some "domes" may result from blanketing of Imbrium massifs and Iridum-secondary craters by Iridum ejecta (P.D. Spudis, oral commun., 1980).

MARE MATERIALS

Whether any Lower Imbrian mare materials are exposed is uncertain. None could remain exposed within reach of the Orientale ejecta. Judging from the mapped extent of the Orientale deposits and secondary craters on the west-limb and farside terrae, the nearside maria probably would have been heavily mantled or cratered if their surface units predated Orientale. Orientale and other large basins might even cover the whole Moon with debris (Moore and others, 1974; Chao and others, 1975). However, some outlying points may be spared a cover because outer impact ejecta is concentrated in raylike stringers (pl. 3; fig. 4.6).

Certain heavily cratered maria on the east limb may be of pre-Orientale, Early Imbrian age. One example is the patchily distributed planar material in the Australe basin (fig. 10.46). In albedo, these plains are intermediate between typical mare and typical circumbasin terra plains, and the superposed crater densities are similar to those of Orientale (J.M. Diaz and A.B. Watkins, written commun., 1976). These marelike materials are older than the Imbrian craters Humboldt and Jenner (Wilhelms and El-Baz, 1977). Dark-haloed craters are evident on the marelike plains (Schultz and Spudis, 1979). A thin dusting of mare basalt by Orientale ejecta may explain the plains' albedo. Other densely cratered materials with

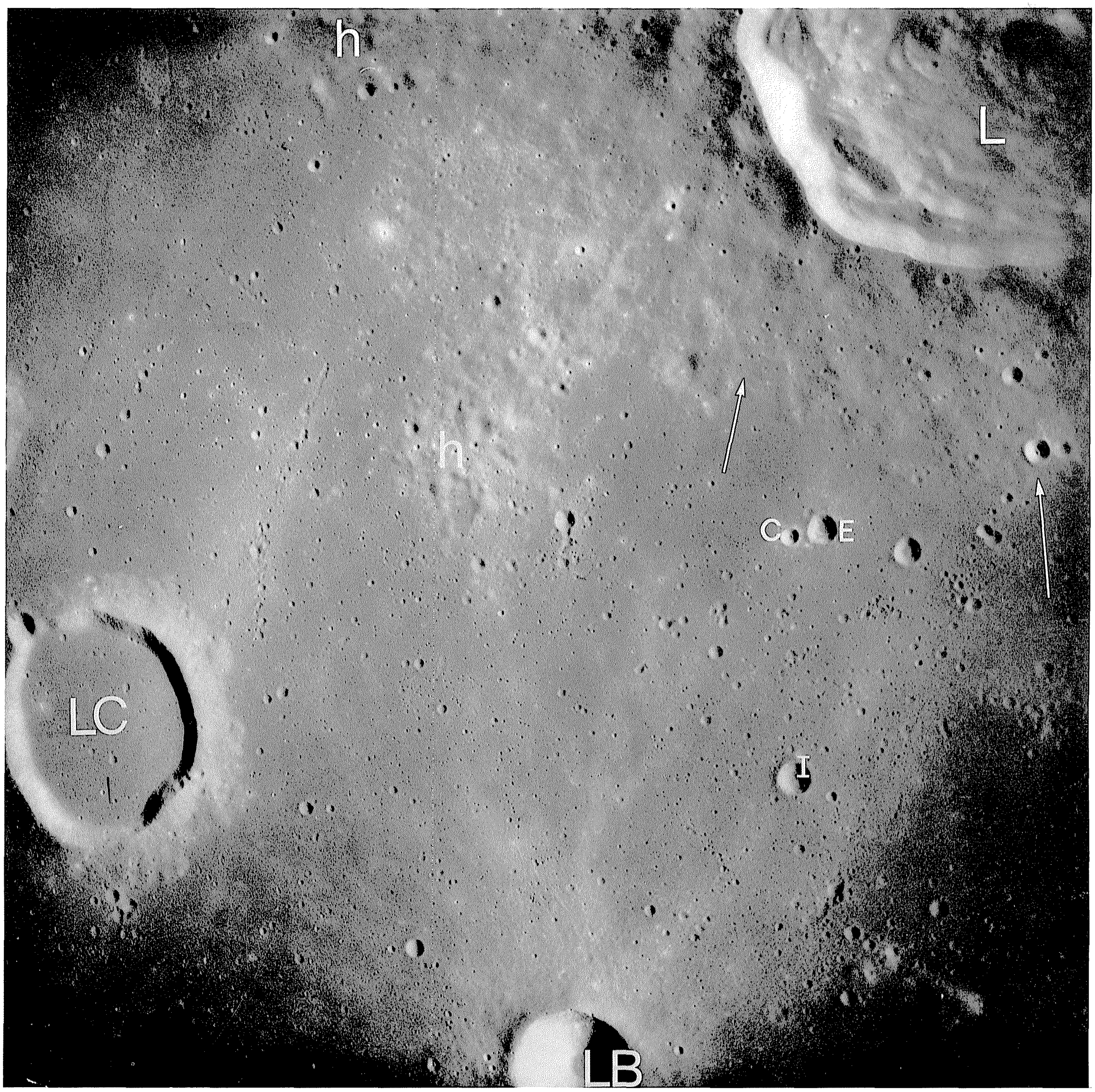

FIGURE 10.41.—Imbrian craters on periphery of Imbrium basin. Lansberg (L; 39 km, 0.3° S., 26.5° W.) is superposed on hummocky Imbrium ejecta (h) and embayed by mare materials (arrows). Interior and periphery of Lansberg C (LC; 17 km) are flooded more deeply. Rayed, probably Copernican, but somewhat degraded crater Lansberg B (LB; 9 km) is superposed on the mare. Craters in 1-km size range are probably Imbrian (I), Eratosthenian (E), and Copernican (C). Apollo 12 frame H–8095.

intermediate albedos lie in Mare Marginis (fig. 4.7) and at the distal margin of Mare Frigoris (Lucchitta, 1978).

Nevertheless, none of these criteria prove an Early Imbrian age. Even the obviously Late Imbrian materials near Orientale (fig. 10.3) are quite heavily cratered. All exposed mare materials may, therefore, be Upper Imbrian or younger and are so mapped here (pls. 9–11). They can be locally subdivided in considerable detail, as shown in the next two chapters.

CHRONOLOGY

Radiometric ages of Imbrium-basin materials are clustered within a short interval. The oldest are those of an older cluster of ages at the Apollo 14 landing site (3.87–3.96 aeons), but these ages pertain to pre-Imbrian rocks. The Apollo 15 KREEP basalt, 3.85 ± 0.04 aeons old, probably was derived from a deposit (Apennine Bench Formation) that is superposed on other basin materials. This basalt may be the best dated of the Apollo 14 and 15 terra materials (G. W. Lugmair, oral commun., 1982); it is contemporaneous with or younger than the Imbrium basin, depending on its origin. Black-and-white breccia believed to have been collected from the Imbrium massifs has been dated at 3.86 ± 0.04 aeons. A younger cluster of ages from the Fra Mauro Formation at the Apollo 14 landing site falls mostly between 3.82 and 3.84 aeons. The time of the Imbrium impact seems to be well constrained at from 3.82 to 3.87 aeons ago; the average and well-represented date of 3.85 aeons ago is tentatively adopted here.

One group of basalt samples from the Apollo 11 landing site yielded ages as old as 3.84 ± 0.03 aeons (table 11.1; Guggisberg and others, 1979). The source flows of these samples are not exposed (see chap. 11); they are probably Lower Imbrian.

No other Lower Imbrian units have been dated isotopically. The interpretation of ages reported for the Cayley Formation at the Apollo 16 landing site is highly uncertain, except that the Cayley materials are no more than 3.92 aeons old. Materials of the Descartes Formation, which may have been emplaced 3.92 ± 0.03 aeons ago, were modified and probably augmented by Imbrium-basin materials 3.85 aeons ago.

The upper age boundary of the series is limited by the ages of the oldest nearly exposed mare basalt. This material was recovered from the Apollo 17 landing site and is described in the next chapter; it is 3.72 aeons old. Therefore, the Orientale impact that ended the Early Imbrian Epoch occurred some time between 3.85 and 3.72 aeons ago. Relative crater frequencies (figs. 8.16, 10.4) suggest that it occurred about 3.8 aeons ago. Thus, the Early Imbrian Epoch spanned about 50 million years.

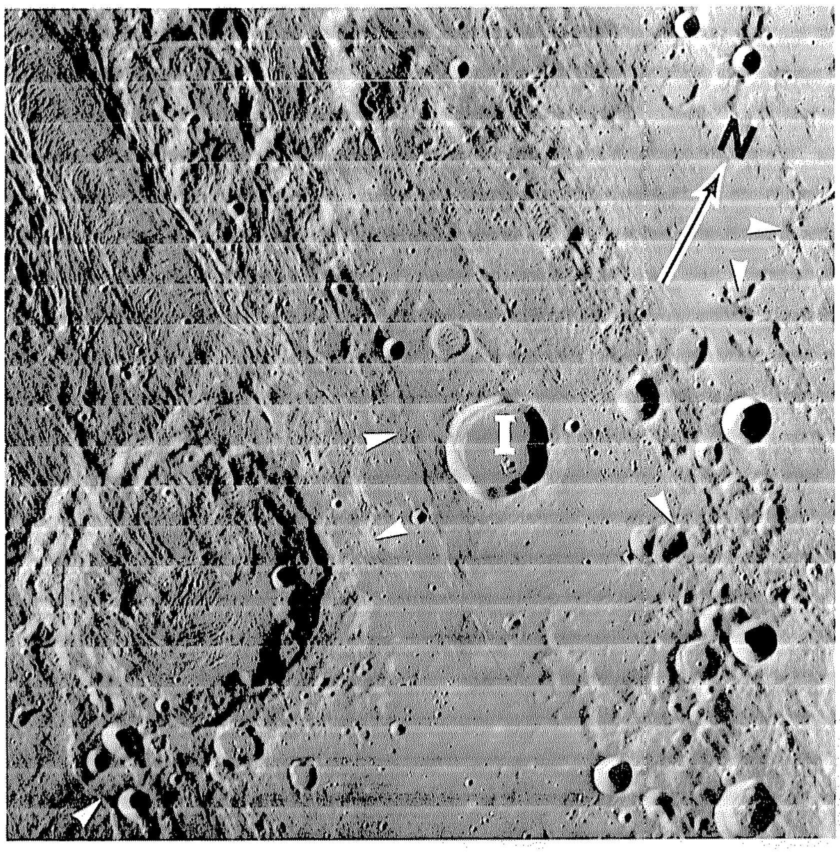

FIGURE 10.42.—Terrain centered 600 km southeast of Orientale-basin rim (Montes Cordillera). Largest crater is Inghirami (91 km, 48° S., 69° W.); other probable primary crater older than Orientale deposits is Inghirami A (I; 34 km). Relatively young ages for both craters are suggested by moderately sharp textural elements, especially smaller Inghirami A. If they are Imbrian and not Nectarian, these craters must be Early Imbrian because they are buried by Orientale deposits. Textured Hevelius Formation and plains intergrade. Arrowheads indicate embayment of Orientale-secondary craters by plains; most or all of clustered craters in lower right corner are Orientale secondaries. Orbiter 4 frame H–172.

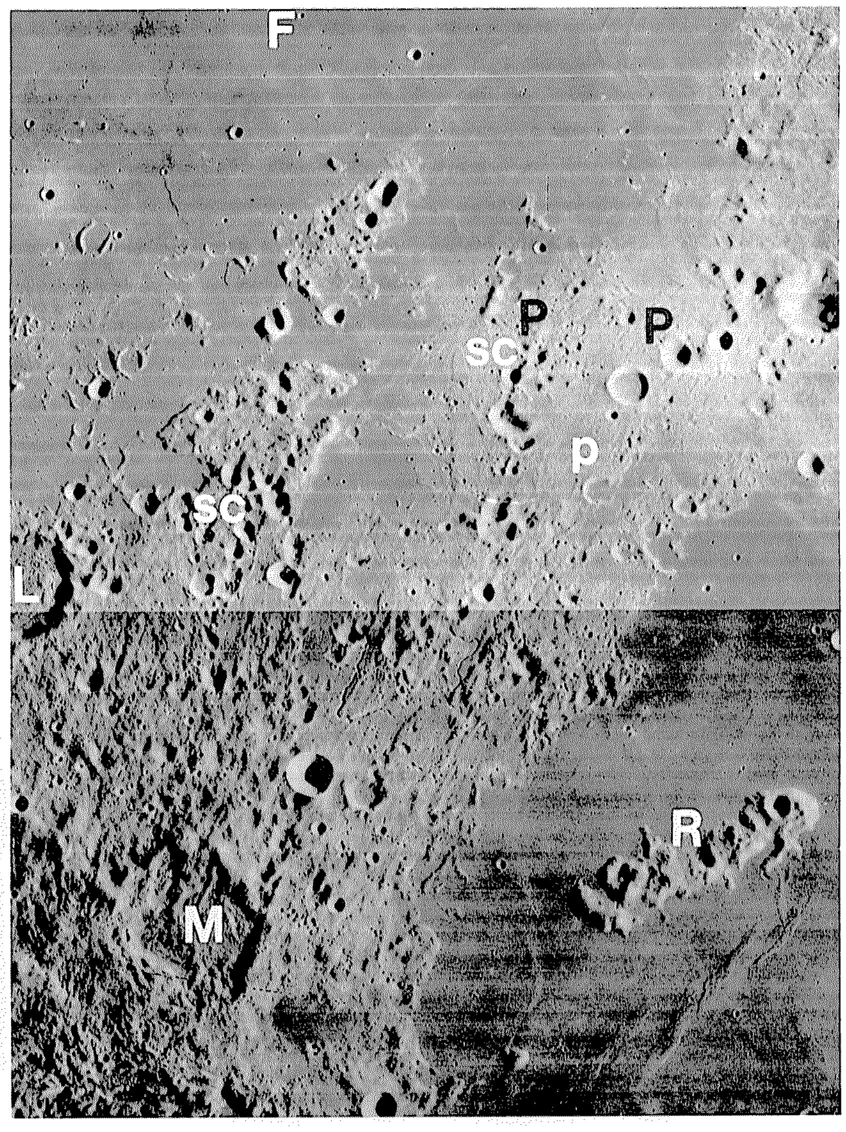

FIGURE 10.43.—Terra between Mare Frigoris (F) and Mare Imbrium, underlain by deposits of Imbrium basin. Lower Imbrian craters La Condamine (L; 37 km, 53° N., 28° W.) and Maupertuis (M; 46 km) are swamped by deposits of Iridum crater (Ulrich, 1969), which grade outward to conspicuous secondary craters (sc) and to light plains deposits (white p). Secondary craters of crater Plato (black P), centered outside right edge of picture, are superposed on Iridum-secondary craters. Iridum crater (centered outside lower left corner of photograph) is slightly younger than Orientale (fig. 10.4) but older than Plato, and so is probably early Late Imbrian. The Straight Range (Montes Recti, R) is part of Imbrium ring overlain by Iridum deposits. Orbiter 4 frame H–139.

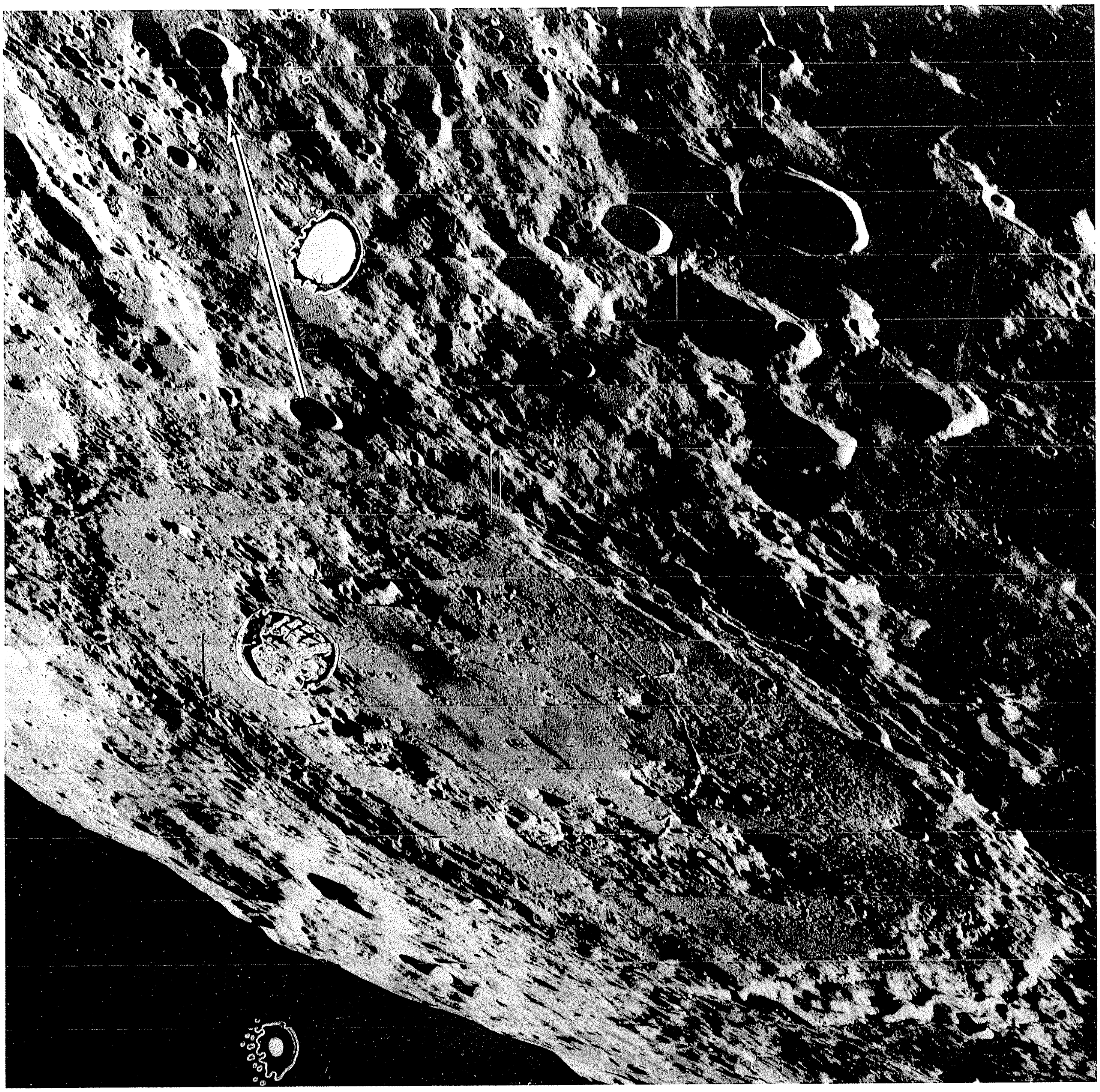

FIGURE 10.44.—Schrödinger basin (320 km). Arrow indicates probable secondary craters of Orientale, centered 2,150 km in direction of arrow; overlap and orientation of cluster are consistent with Orientale origin (Wilhelms and others, 1979). Large chain to left of arrow is secondary to Schrödinger. (White and black-and-white spots are blemishes.) Orbiter 5 frame H–21.

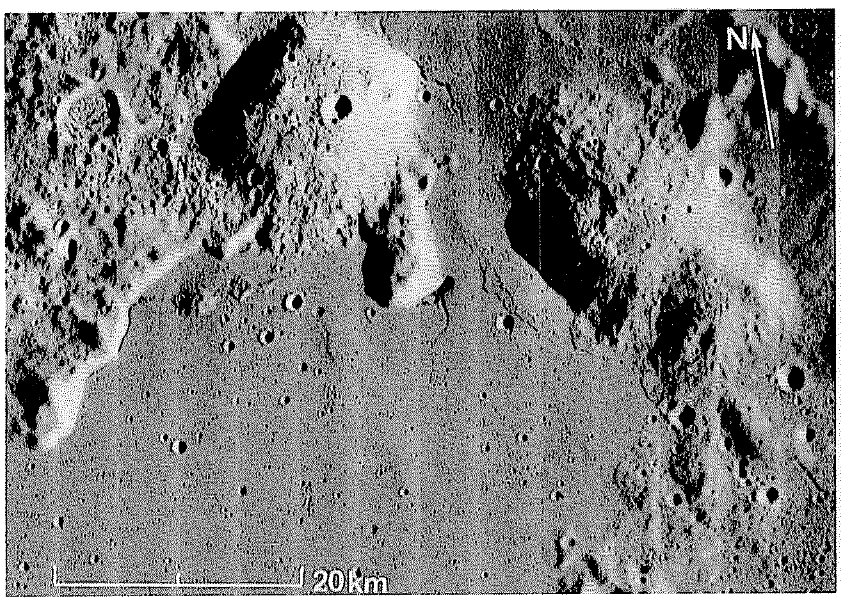

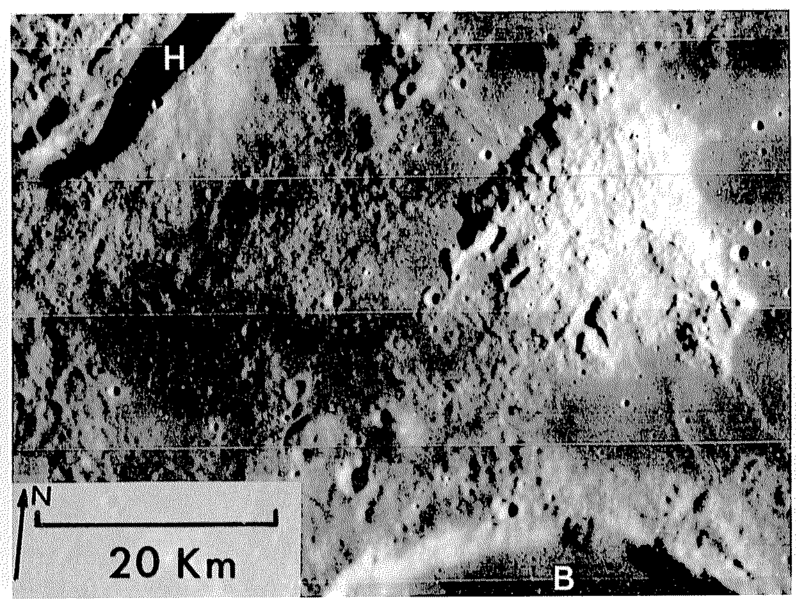

FIGURE 10.45.—Domical terra landforms of possible volcanic origin. *A*. Gruithuisen domes (36° N., 40° W.). Orbiter 5 frame M–182.

B. Hansteen alpha (12° S., 50° W.). B, crater Billy; H, crater Hansteen. Orbiter 4 frame H–149.

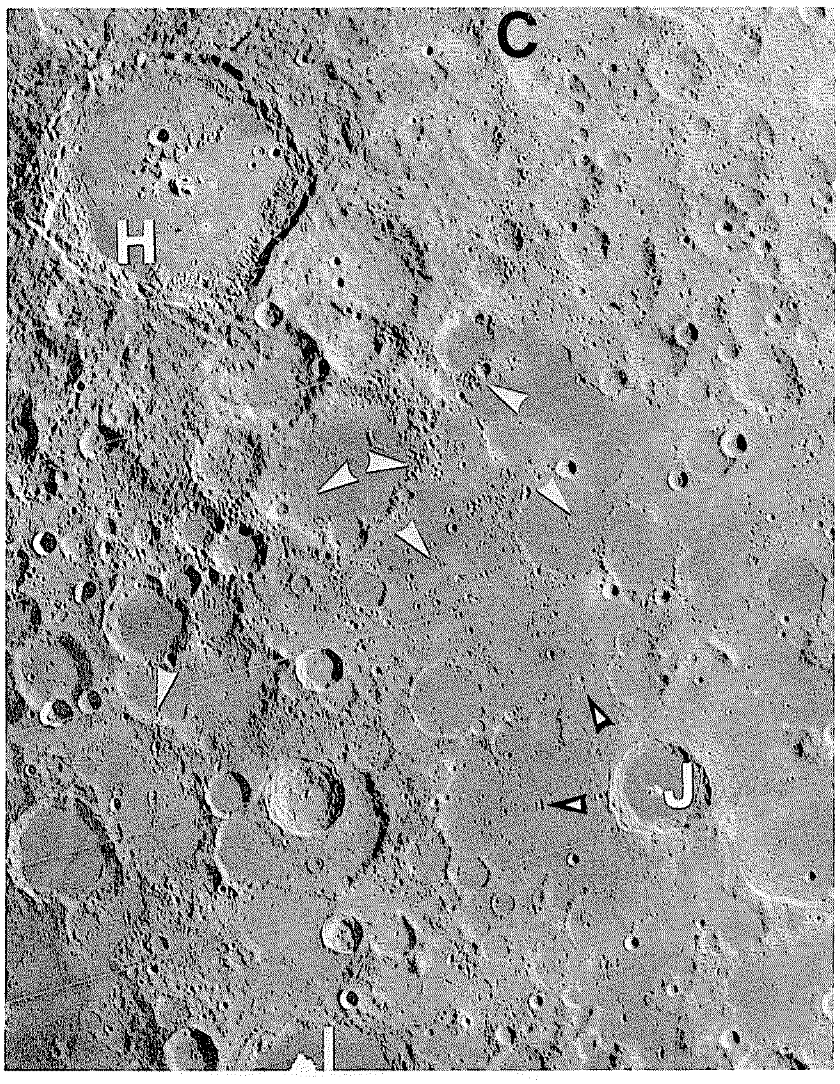

FIGURE 10.46.—Stratigraphic relations of mare and crater materials in Mare Australe.
A. Deposits of Jenner (J; 72 km, 42° S., 96° W.) and Humboldt (H; 207 km, 27° S., 81° E.), both Upper Imbrian, are superposed on mare basalt (white-on-black arrowheads), whereas a younger mare unit encroaches on Humboldt secondaries (white arrowheads). C, pre-Nectarian crater Curie (139 km, 23° S., 92° E.); L, pre-Nectarian crater Lyot. Orbiter 4 frame M–9.

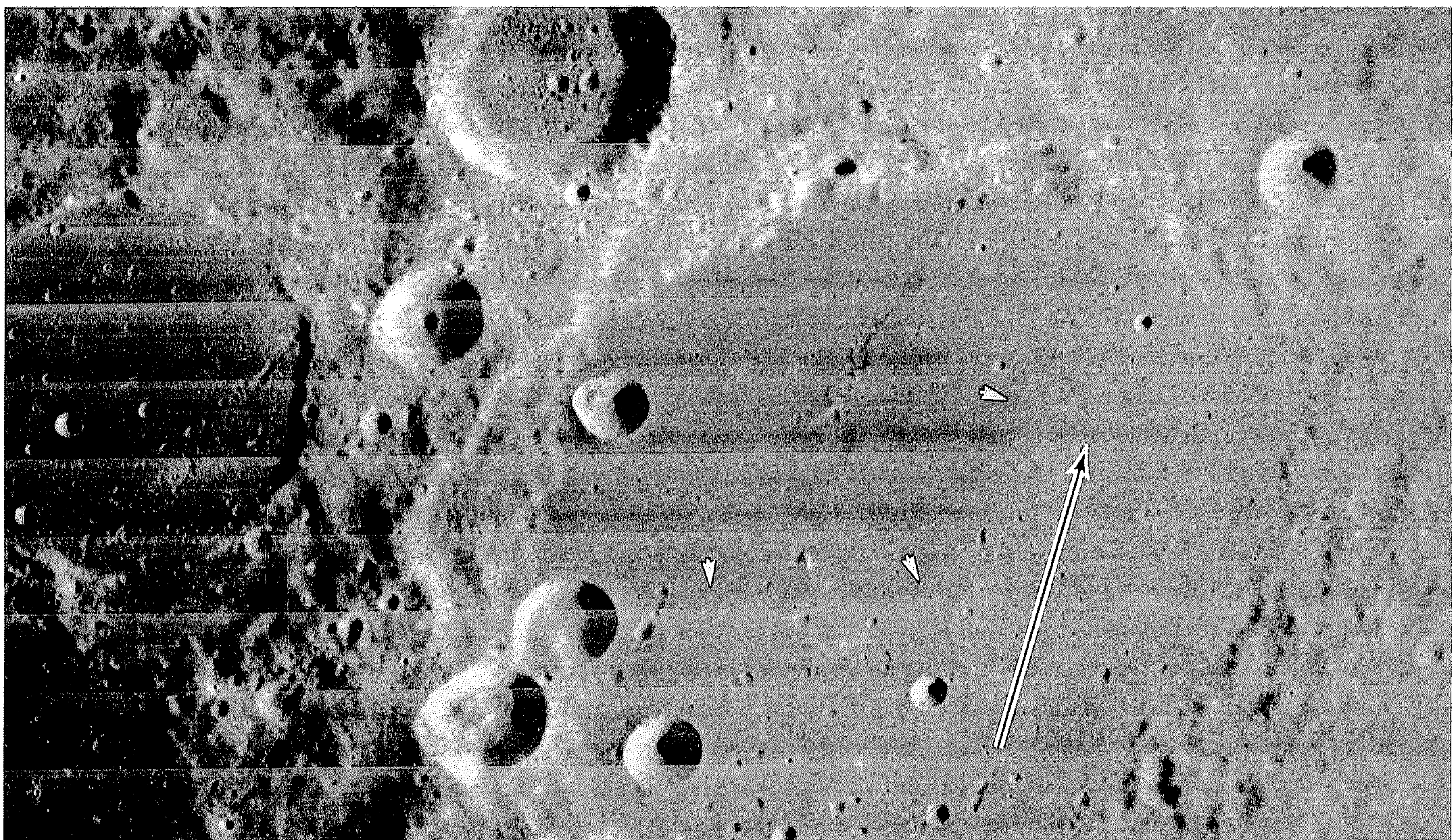

B. Two mare units in Lyot (141 km, 50° S., 84° W.). Younger unit encroaches on older (white arrowheads). Secondary craters of crater Humboldt are superposed on older unit, including at shaft end of black-and-white arrow, which points to Humboldt, 10° W. of N. Older unit may be Lower Imbrian; younger unit is Upper Imbrian. Orbiter 4 frame H–9.